Advances in Mechanical Engineering

Heat Transfer in Nanofluids

Guest Editors: Oronzio Manca, Yogesh Jaluria, and Dimos Poulikakos

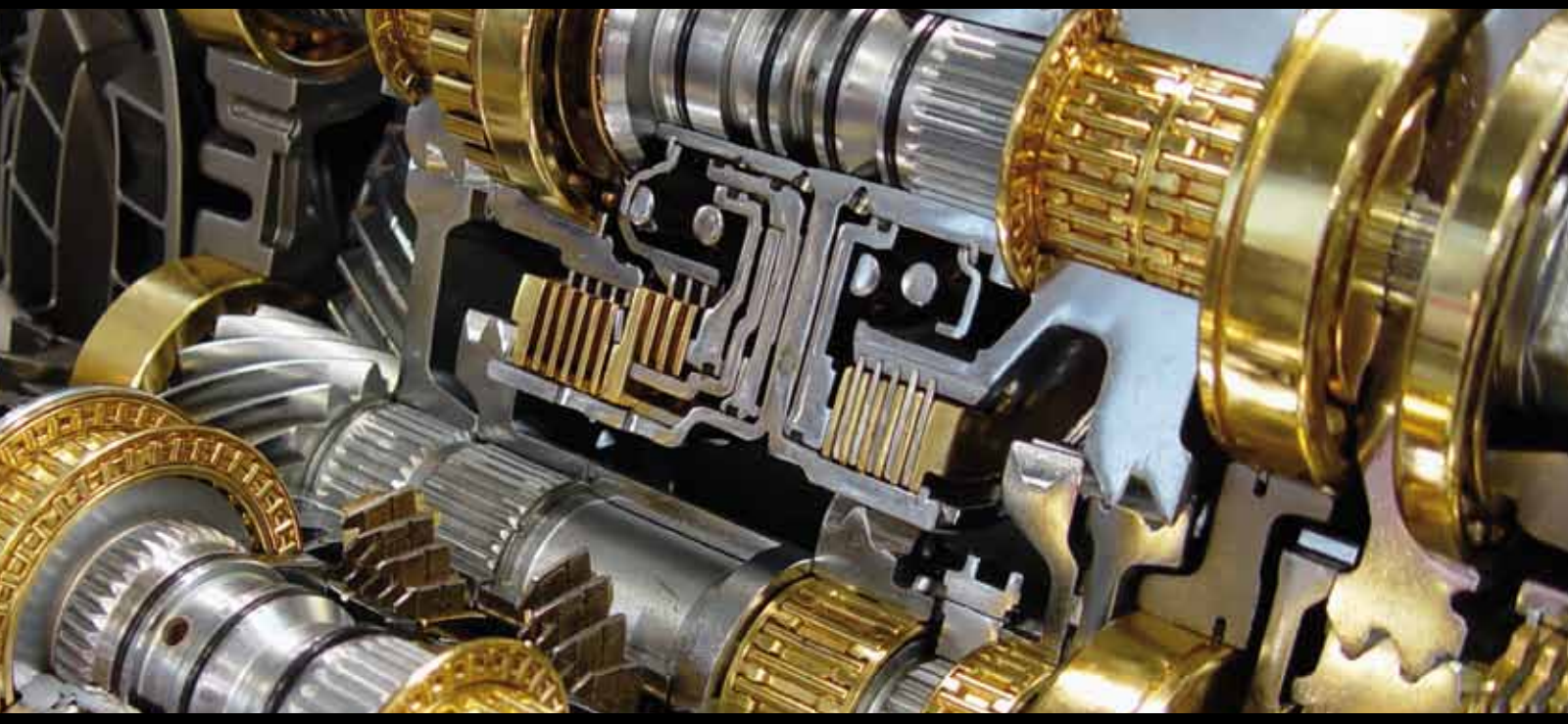

Heat Transfer in Nanofluids

Advances in Mechanical Engineering

Heat Transfer in Nanofluids

Guest Editors: Oronzio Manca, Yogesh Jaluria, and Dimos Poulikakos

Editorial Board

Contents

Hindawi Publishing Corporation
Advances in Mechanical Engineering
Volume 2010, Article ID 380826, 2 pages
doi:10.1155/2010/380826

Editorial

Heat Transfer in Nanofluids

Oronzio Manca,[1] Yogesh Jaluria,[2] and Dimos Poulikakos[3]

[1] *Dipartimento di Ingegneria Aerospaziale e Meccanica, Seconda Università degli Studi di Napoli, Via Roma 29, 81031 Aversa, Italy*
[2] *Department of Mechanical and Aerospace Engineering, Rutgers, The State University of New Jersey, Piscataway, New Brunswick, NJ 08901-8554, USA*
[3] *Laboratory of Thermodynamics in Emerging Technologies, Department of Mechanical and Process Engineering, ETH Zurich, 8092 Zurich, Switzerland*

Correspondence should be addressed to Oronzio Manca, oronzio.manca@unina2.it

Received 13 May 2010; Accepted 13 May 2010

Heat transfer can be enhanced by employing various techniques and methodologies, such as increasing either the heat transfer surface or the heat transfer coefficient between the fluid and the surface, that allow high heat transfer rates in a small volume. Cooling is one of the most important technical challenges facing many diverse industries, including microelectronics, transportation, solid-state lighting, and manufacturing.

There is, therefore, an urgent need for new and innovative coolants with improved performance. The addition of micrometer- or millimeter-sized solid metal or metal oxide particles to the base fluids shows an increment in the thermal conductivity of resultant fluids. But the presence of milli- or microsized particles in a fluid poses a number of problems. They do not form a stable solution and tend to settle down. Apart from the application in the field of heat transfer, nanofluids (nanometer particles in a fluid) can also be synthesized for unique magnetic, electrical, chemical, and biological applications. They also cause erosion and clogging of the heat transfer channels.

The novel concept of "nanofluids" has been proposed as a route to surpassing the performance of heat transfer fluids currently available. A very small amount of nanoparticles, when dispersed uniformly and suspended stably in base fluids, can provide impressive improvements in the thermal properties of base fluids. Nanofluids, which are a colloidal mixture of nanoparticles (1–100 nm) and a base liquid (nanoparticle fluid suspensions), is the term first coined by Choi in 1995 [1] at the Argonne National Laboratory to describe the new class of nanotechnology-based heat transfer fluids that exhibit thermal properties superior to those of their base fluids or conventional particle fluid suspensions.

Several investigations have revealed that the thermal conductivity of the fluid containing nanoparticles could be increased by more than 20% for the case of very low nanoparticles concentrations. Nowadays a fast growth of research activity in this heat transfer area has arisen. In fact, the exponential increase in the number of research articles dedicated to this subject thus far shows a noticeable growth and the importance of heat transfer enhancement technology in general. Just to give some data in table is given the number of papers from 1993 to 2010 (up to April) found in SCOPUS under "Nanofluids" and the other two columns are the papers found under "Nanofluids AND Heat Transfer" and "Nanofluids AND Properties". Moreover, in SCOPUS under "Nanofluids and Review" about 34 papers were given as that result. This indicates a the high interest in nanofluids activity research and the potential market for nanofluids for heat transfer applications is estimated by the CEA in 2007 to be over 2 billion dollars per year worldwide, with prospect of further growth in the next 5–10 years, as underlined in [2].

The aim of this special issue is to collect basic, application and review articles of the most recent developments and research efforts in this field, with the purpose to provide guidelines for future research directions. The order of the papers is given presenting a possible range of applications, a review on specific heat capacity, and an experimental study to evaluate the effects of particle species, surface charge, concentration, preparation technique, and base fluid on thermal transport capability of nanofluids. A survey

Table 1: Number of papers on "nanofluids", "nanofluids and heat transfer", and "nanofluids and properties" by SCOPUS database.

Year	Nanofluids	Nanofluids and heat transfer	Nanofluids and properties
1993	1	0	0
1995	1	1	0
1996	2	2	0
1997	2	1	1
1999	2	2	1
2000	4	3	3
2001	5	2	2
2002	5	2	2
2003	19	9	6
2004	35	23	8
2005	90	50	34
2006	124	62	32
2007	175	89	50
2008	225	107	91
2009	222	109	96
2010	95	54	25
total	1007	516	351

on heat transfer in nanofluids is summarized in order to analyze the theories regarding heat transfer mechanisms in nanofluids and to discuss the effects of clustering on thermal conductivity. After some considerations to address whether the heat transfer in nanofluids still satisfies the classical energy equation are theoretically examined by the macroscale manifestation of the microscale physics in nanofluids, an experimental investigation on natural convection heat transfer characteristics in nanofluids in an enclosure and a numerical study on turbulent forced convection flow of nanofluids in a circular tube subjected are presented in the last two papers.

Oronzio Manca
Yogesh Jaluria
Dimos Poulikakos

References

[1] S. U. S. Choi, "Enhancing thermal conductivity of fluids with nanoparticles," in *Developments and Applications of Nonnewtonian Flows*, D. A. Singer and H. P. Wang, Eds., vol. 231, pp. 99–105, American Society of Mechanical Engineers, New York, NY, USA, 1995.

[2] D. Wen, G. Lin, S. Vafaei, and K. Zhang, "Review of nanofluids for heat transfer applications," *Particuology*, vol. 7, no. 2, pp. 141–150, 2009.

Hindawi Publishing Corporation
Advances in Mechanical Engineering
Volume 2010, Article ID 519659, 11 pages
doi:10.1155/2010/519659

Review Article

Applications of Nanofluids: Current and Future

Kaufui V. Wong and Omar De Leon

Mechanical and Aerospace Engineering Department, University of Miami, Coral Gables, FL 33124, USA

Correspondence should be addressed to Kaufui V. Wong, kwong@miami.edu

Received 29 May 2009; Accepted 24 November 2009

Academic Editor: Yogesh Jaluria

Nanofluids are suspensions of nanoparticles in fluids that show significant enhancement of their properties at modest nanoparticle concentrations. Many of the publications on nanofluids are about understanding their behavior so that they can be utilized where straight heat transfer enhancement is paramount as in many industrial applications, nuclear reactors, transportation, electronics as well as biomedicine and food. Nanofluid as a smart fluid, where heat transfer can be reduced or enhanced at will, has also been reported. This paper focuses on presenting the broad range of current and future applications that involve nanofluids, emphasizing their improved heat transfer properties that are controllable and the specific characteristics that these nanofluids possess that make them suitable for such applications.

1. Introduction

Nanofluids are dilute liquid suspensions of nanoparticles with at least one of their principal dimensions smaller than 100 nm. From previous investigations, nanofluids have been found to possess enhanced thermophysical properties such as thermal conductivity, thermal diffusivity, viscosity and convective heat transfer coefficients compared to those of base fluids like oil or water [1–6]

From the current review, it can be seen that nanofluids clearly exhibit enhanced thermal conductivity, which goes up with increasing volumetric fraction of nanoparticles. The current review does concentrate on this relatively new class of fluids and not on colloids which are nanofluids because the latter have been used for a long time. Review of experimental studies clearly showed a lack of consistency in the reported results of different research groups regarding thermal properties [7, 8]. The effects of several important factors such as particle size and shapes, clustering of particles, temperature of the fluid, and dissociation of surfactant on the effective thermal conductivity of nanofluids have not been studied adequately. It is important to do more research so as to ascertain the effects of these factors on the thermal conductivity of wide range of nanofluids.

Classical models cannot be used to explain adequately the observed enhanced thermal conductivity of nanofluids. Recently most developed models only include one or two postulated mechanisms of nanofluids heat transfer. For instance, there has not been much fundamental work reported on the determination of the effective thermal diffusivity of nanofluids nor heat transfer coefficients for nanofluids in natural convection [9].

There is a growth is the use of colloids which are nanofluids in the biomedical industry for sensing and imaging purposes. This is directly related to the ability to design novel materials at the nanoscale level alongside recent innovations in analytical and imaging technologies for measuring and manipulating nanomaterials. This has led to the fast development of commercial applications which use a wide variety of manufactured nanoparticles. The production, use and disposal of manufactured nanoparticles will lead to discharges to air, soils and water systems. Negative effects are likely and quantification and minimization of these effects on environmental health is necessary. True knowledge of concentration and physicochemical properties of manufactured nanoparticles under realistic conditions is important to predicting their fate, behavior and toxicity in the natural aquatic environment. The aquatic colloid and atmospheric ultrafine particle literature both offer evidence as to the likely behavior and impacts of manufactured nanoparticles [10], and there is no pretense that a review duplicating similar literature about the use of colloids which are also nanofluids is attempted in the current review.

Owing to their enhanced properties as thermal transfer fluids for instance, nanofluids can be used in a plethora of engineering applications ranging from use in the automotive industry to the medical arena to use in power plant cooling systems as well as computers.

2. Heat Transfer Applications

2.1. Industrial Cooling Applications. Routbort et al. [11] started a project in 2008 that employed nanofluids for industrial cooling that could result in great energy savings and resulting emissions reductions. For U.S. industry, the replacement of cooling and heating water with nanofluids has the potential to conserve 1 trillion Btu of energy. For the U.S. electric power industry, using nanofluids in closed-loop cooling cycles could save about 10–30 trillion Btu per year (equivalent to the annual energy consumption of about 50,000–150,000 households). The associated emissions reductions would be approximately 5.6 million metric tons of carbon dioxide; 8,600 metric tons of nitrogen oxides; and 21,000 metric tons of sulfur dioxide.

For Michelin North America tire plants, the productivity of numerous industrial processes is constrained by the lack of facility to cool the rubber efficiently as it is being processed. This requires the use of over 2 million gallons of heat transfer fluids for Michelin's North American plants. It is Michelin's goal in this project to obtain a 10% productivity increase in its rubber processing plants if suitable water-based nanofluids can be developed and commercially produced in a cost-effective manner.

Han et al. [12] have used phase change materials as nanoparticles in nanofluids to simultaneously enhance the effective thermal conductivity and specific heat of the fluids. As an example, a suspension of indium nanoparticles (melting temperature, 157°C) in polyalphaolefin has been synthesized using a one-step, nanoemulsification method. The fluid's thermophysical properties, that is, thermal conductivity, viscosity, and specific heat, and their temperature dependence were measured experimentally. The observed melting-freezing phase transition of the indium nanoparticles significantly augmented the fluid's effective specific heat.

This work is one of the few to address thermal diffusivity; similar studies allow industrial cooling applications to continue without thorough understanding of all the heat transfer mechanisms in nanofluids.

2.2. Smart Fluids. In this new age of energy awareness, our lack of abundant sources of clean energy and the widespread dissemination of battery operated devices, such as cell-phones and laptops, have accented the necessity for a smart technological handling of energetic resources. Nanofluids have been demonstrated to be able to handle this role in some instances as a smart fluid.

In a recent paper published in the March 2009 issue of Physical Review Letters, Donzelli et al. [13] showed that a particular class of nanofluids can be used as a smart material working as a heat valve to control the flow of heat. The nanofluid can be readily configured either in a "low" state, where it conducts heat poorly, or in a "high" state, where the dissipation is more efficient. To leap the chasm to heating and cooling technologies, the researchers will have to show more evidence of a stable operating system that responds to a larger range of heat flux inputs.

2.3. Nuclear Reactors. Kim et al. [14, 15] at the Nuclear Science and Engineering Department of the Massachusetts Institute of Technology (MIT), performed a study to assess the feasibility of nanofluids in nuclear applications by improving the performance of any water-cooled nuclear system that is heat removal limited. Possible applications include pressurized water reactor (PWR) primary coolant, standby safety systems, accelerator targets, plasma divertors, and so forth, [16].

In a pressurized water reactor (PWR) nuclear power plant system, the limiting process in the generation of steam is critical heat flux (CHF) between the fuels rods and the water—when vapor bubbles that end up covering the surface of the fuel rods conduct very little heat as opposed to liquid water. Using nanofluids instead of water, the fuel rods become coated with nanoparticles such as alumina, which actually push newly formed bubbles away, preventing the formation of a layer of vapor around the rod and subsequently increasing the CHF significantly.

After testing in MIT's Nuclear Research Reactor, preliminary experiments have shown promising success where it is seen that PWR is significantly more productive. The use of nanofluids as a coolant could also be used in emergency cooling systems, where they could cool down overheat surfaces more quickly leading to an improvement in power plant safety.

Some issues regarding the use of nanofluids in a power plant system include the unpredictability of the amount of nanoparticles that are carried away by the boiling vapor. One other concern is what extra safety measures that have to be taken in the disposal of the nanofluid. The application of nanofluid coolant to boiling water reactors (BWR) is predicted to be minimal because nanoparticle carryover to the turbine and condenser would raise erosion and fouling concerns.

From Jackson's study [17], it was observed that considerable enhancement in the critical heat flux can be achieved by creating a structured surface from the deposition of nanofluids. If the deposition film characteristics such as the structure and thickness can be controlled it may be possible to increase the CHF with little decrease in the heat transfer. Whereas the nanoparticles themselves cause no significant difference in the pool-boiling characteristics of water, the boiling of nanofluids shows promise as a simple way to create an enhanced surface.

The use of nanofluids in nuclear power plants seems like a potential future application [16]. Several significant gaps in knowledge are evident at this time, including, demonstration of the nanofluid thermal-hydraulic performance at prototypical reactor conditions and the compatibility of the nanofluid chemistry with the reactor materials.

Another possible application of nanofluids in nuclear systems is the alleviation of postulated severe accidents during which the core melts and relocates to the bottom

of the reactor vessel. If such accidents were to occur, it is desirable to retain the molten fuel within the vessel by removing the decay heat through the vessel wall. This process is limited by the occurrence of CHF on the vessel outer surface, but analysis indicates that the use of nanofluid can increase the in-vessel retention capabilities of nuclear reactors by as much as 40% [18].

Many water-cooled nuclear power systems are CHF-limited, but the application of nanofluid can greatly improve the CHF of the coolant so that there is a bottom-line economic benefit while also raising the safety standard of the power plant system.

2.4. Extraction of Geothermal Power and Other Energy Sources. The world's total geothermal energy resources were calculated to be over 13000 ZJ in a report from MIT (2007) [19]. Currently only 200 ZJ would be extractable, however, with technological improvements, over 2,000 ZJ could be extracted and supply the world's energy needs for several millennia. When extracting energy from the earth's crust that varies in length between 5 to 10 km and temperature between 500°C and 1000°C, nanofluids can be employed to cool the pipes exposed to such high temperatures. When drilling, nanofluids can serve in cooling the machinery and equipment working in high friction and high temperature environment. As a "fluid superconductor," nanofluids could be used as a working fluid to extract energy from the earth core and processed in a PWR power plant system producing large amounts of work energy.

In the sub-area of drilling technology, so fundamental to geothermal power, improved sensors and electronics cooled by nanofluids capable of operating at higher temperature in downhole tools, and revolutionary improvements utilizing new methods of rock penetration cooled and lubricated by nanofluids will lower production costs. Such improvements will enable access to deeper, hotter regions in high grade formations or to economically acceptable temperatures in lower-grade formations.

In the sub-area of power conversion technology, improving heat-transfer performance for lower-temperature nanofluids, and developing plant designs for higher resource temperatures to the supercritical water region would lead to an order of magnitude (or more) gain in both reservoir performance and heat-to power conversion efficiency.

Tran et al. [20], funded by the United States Department of Energy (USDOE), performed research targeted at developing a new class of highly specialized drilling fluids that may have superior performance in high temperature drilling. This research is applicable to high pressure high temperature drilling, which may be pivotal in opening up large quantities of previously unrecoverable domestic fuel resources. Commercialization would be the bottleneck of progress in this sub-area.

3. Automotive Applications

Engine oils, automatic transmission fluids, coolants, lubricants, and other synthetic high-temperature heat transfer fluids found in conventional truck thermal systems—radiators, engines, heating, ventilation and air-conditioning (HVAC)—have inherently poor heat transfer properties. These could benefit from the high thermal conductivity offered by nanofluids that resulted from addition of nanoparticles [2, 21].

3.1. Nanofluid Coolant. In looking for ways to improve the aerodynamic designs of vehicles, and subsequently the fuel economy, manufacturers must reduce the amount of energy needed to overcome wind resistance on the road. At high speeds, approximately 65% of the total energy output from a truck is expended in overcoming the aerodynamic drag. This fact is partly due to the large radiator in front of the engine positioned to maximize the cooling effect of oncoming air.

The use of nanofluids as coolants would allow for smaller size and better positioning of the radiators. Owing to the fact that there would be less fluid due to the higher efficiency, coolant pumps could be shrunk and truck engines could be operated at higher temperatures allowing for more horsepower while still meeting stringent emission standards.

Argonne researchers, Singh et al. [22], have determined that the use of high-thermal conductive nanofluids in radiators can lead to a reduction in the frontal area of the radiator by up to 10%. This reduction in aerodynamic drag can lead to a fuel savings of up to 5%. The application of nanofluid also contributed to a reduction of friction and wear, reducing parasitic losses, operation of components such as pumps and compressors, and subsequently leading to more than 6% fuel savings. It is conceivable that greater improvement of savings could be obtained in the future.

In order to determine whether nanofluids degrade radiator material, they have built and calibrated an apparatus that can emulate the coolant flow in a radiator and are currently testing and measuring material loss of typical radiator materials by various nanofluids. Erosion of radiator material is determined by weight loss-measurements as a function of fluid velocity and impact angle.

In their tests, they observed no erosion using nanofluids made from base fluids ethylene and tri-cloroethylene gycols with velocities as high as 9 m/s and at 90°–30° impact angles. There was erosion observed with copper nanofluid at a velocity of 9.6 m/s and impact angle of 90°. The corresponding recession rate was calculated to be 0.065 mils/yr of vehicle operation.

Through preliminary investigation, it was determined that copper nanofluid produces a higher wear rate than the base fluid and this is possibly due to oxidation of copper nanoparticles. A lower wear and friction rate was seen for alumina nanofluids in comparison to the base fluid. Some interesting erosion test results from Singh et al. [22] are shown in Tables 1 and 2.

Shen et al. [23] researched the wheel wear and tribological characteristics in wet, dry and minimum quantity lubrication (MQL) grinding of cast iron. Water-based alumina and diamond nanofluids were applied in the MQL grinding process and the grinding results were compared with those of pure water. Nanofluids demonstrated the benefits of reducing grinding forces, improving surface roughness, and preventing burning of the workpiece. Contrasted to

Table 1: Erosion Test Results for 50% Ethlyene Glycol, 50% H2O Aluminum 3003 - 50°C Rig [22].

Impact Angle (*)	Velocity (m/s)	Time (hrs)	Weight Loss (mg)
90	8.0	236	0 ± 0.2
90	10.5	211	0 ± 0.2
50	6.0	264	0 ± 0.2
50	10.0	244	0 ± 0.2
30	8.0	283	0 ± 0.2
30	10.5	293	0 ± 0.2

Table 2: Erosion Test Results for Cu Nanoparticles in Trichloroethylene Glycol on Al 3003 - 50°C Rig [22].

Impact Angle (*)	Velocity (m/s)	Time (hrs)	Weight Loss (mg)
90	4.0	217	0 ± 0.2
30	4.0	311	0 ± 0.2
90	7.6	341	0 ± 0.2
30	7.6	335	0 ± 0.2
30	9.6	336	0 ± 0.2

dry grinding, MQL grinding could considerably lower the grinding temperature.

More research must be conducted on the tribological properties using nanofluids of a wider range of particle loadings as well as on the erosion rate of radiator material in order to help develop predictive models for nanofluid wear and erosion in engine systems. Future research initiatives involve nanoparticles materials containing aluminum and oxide-coated metal nanoparticles. Additional research and testing in this area will assist in the design of engine cooling and other thermal management systems that involve nanofluids.

Future engines that are designed using nanofluids' cooling properties would be able to run at more optimal temperatures allowing for increased power output. With a nanofluids engine, components would be smaller and weigh less allowing for better gas mileage, saving consumers money and resulting in fewer emissions for a cleaner environment.

3.2. Nanofluid in Fuel. The aluminum nanoparticles, produced using a plasma arc system, are covered with thin layers of aluminum oxide, owing to the high oxidation activity of pure aluminum, thus creating a larger contact surface area with water and allowing for increased decomposition of hydrogen from water during the combustion process. During this combustion process, the alumina acts as a catalyst and the aluminum nanoparticles then serve to decompose the water to yield more hydrogen. It was shown that the combustion of diesel fuel mixed with aqueous aluminum nanofluid increased the total combustion heat while decreasing the concentration of smoke and nitrous oxide in the exhaust emission from the diesel engine [24, 25].

3.3. Brake and Other Vehicular Nanofluids. As vehicle aerodynamics is improved and drag forces are reduced, there is a higher demand for braking systems with higher and more efficient heat dissipation mechanisms and properties such as brake nanofluid.

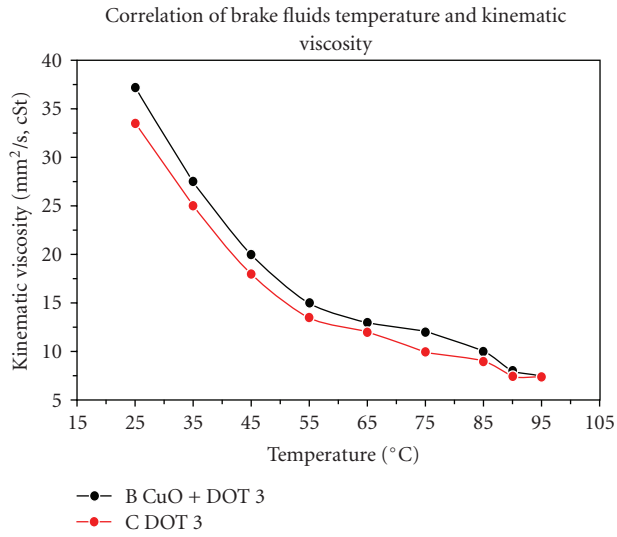

Figure 1: CBN Temperature and Viscosity Fluctuations [24, 25].

A vehicle's kinetic energy is dispersed through the heat produced during the process of braking and this is transmitted throughout the brake fluid in the hydraulic braking system. If the heat causes the brake fluid to reach its boiling point, a vapor-lock is created that retards the hydraulic system from dispersing the heat caused from braking. Such an occurrence will in turn will cause a brake malfunction and poses a safety hazard in vehicles. Since brake oil is easily affected by the heat generated from braking, nanofluids with enhanced characteristics maximize performance in heat transfer as well as remove any safety concerns.

Copper-oxide brake nanofluid (CBN) is manufactured using the method of arc-submerged nanoparticle synthesis system (ASNSS). Essentially this is done by melting bulk copper metal used as the electrode which is submerged in dielectric liquid within a vacuum-operating environment and the vaporized metals are condensed in the dielectric liquid [24, 25].

Aluminum-oxide brake nanofluid (AOBN) is made using the plasma charging arc system. This is performed in a very similar fashion to that of the ASNSS method. The aluminum metal is vaporized by the plasma electric arc at a high temperature and mixed thoroughly with the dielectric liquid [24, 25].

CBN has a thermal conductivity 1.6 times higher than that of the brake fluid designated DOT3, while AOBN's thermal conductivity is only 1.5 times higher than DOT3. This enhanced thermal conductivity optimizes heat transmission and lubrication.

CBN and AOBN both have enhanced properties such as a higher boiling point, higher viscosity and a higher conductivity than that of traditional brake fluid (DOT3). By yielding a higher boiling point, conductivity and viscosity, CBN and AOBN reduce the occurrence of vapor-lock and offer increased safety while driving. Important findings of Kao et al. [24, 25] are shown in Figure 1 and Table 3.

Table 3: CBN and AOBN Boiling Point and Thermal Conductivity Fluctuations [24, 25].

	DOT3*	CBN 2 wt% (CuO + DOT3)	DOT3*	AOBN 2 wt% (Al_2O_3+ DOT3)
Boiling Point	270°C	278°C	240°C	248°C
Conductivity (25°C)	0.03 W/m°C	0.05 W/m°C	0.13 W/m°C	- 0.19 W/m°C

* Different DOT3 brake fluids were used.

In the nanofluid research applied to the cooling of automatic transmissions, Tzeng et al. [26] dispersed CuO and Al_2O_3 nanoparticles into engine transmission oil. The experimental setup was the transmission of a four-wheel-drive vehicle. The transmission had an advanced rotary blade coupling, where high local temperatures occurred at high rotating speeds. Temperature measurements were taken on the exterior of the rotary-blade-coupling transmission at four engine operating speeds (range from 400 to 1600 rpm), and the optimum composition of nanofluids with regard to heat transfer performance was studied. The results indicated that CuO nanofluids resulted in the lowest transmission temperatures both at high and low rotating speeds. Therefore, the use of nanofluid in the transmission has a clear advantage from the thermal performance viewpoint. As in all nanofluid applications, however, consideration must be given to such factors as particle settling, particle agglomeration, and surface erosion.

In automotive lubrication applications, Zhang [27] reported that surface-modified nanoparticles stably dispersed in mineral oils are effective in reducing wear and enhancing load-carrying capacity. Results from a research project involving industry and academia points to the use of nanoparticles in lubricants to enhance tribological properties such as load-carrying capacity, wear resistance, and friction reduction between moving mechanical components. Such results are promising for enhancing heat transfer rates in automotive systems through the use of nanofluids.

4. Electronic Applications

Nanofluids are used for cooling of microchips in computers and elsewhere. They are also used in other electronic applications which use microfluidic applications.

4.1. Cooling of Microchips. A principal limitation on developing smaller microchips is the rapid heat dissipation. However, nanofluids can be used for liquid cooling of computer processors due to their high thermal conductivity. It is predicted that the next generation of computer chips will produce localized heat flux over 10 MW/m^2, with the total power exceeding 300 W. In combination with thin film evaporation, the nanofluid oscillating heat pipe (OHP) cooling system will be able to remove heat fluxes over 10 MW/m^2 and serve as the next generation cooling device that will be able to handle the heat dissipation coming from new technology [28, 29].

In order to observe the oscillation, researchers had to modify the metal pipe system of the OHP to use glass or plastic for visibility. However, since OHP systems are usually made of copper, the use of glass or plastic changes the thermal transfer properties of the system and subsequently altering the performance of the system and the legitimacy of the experimental data [28, 29].

So as to obtain experimental data while maintaining the integrity of the OHP system, Arif [30] employed neutron imaging to study the liquid flow in a 12-turn nanofluid OHP. As a consequence of the high intensity neutron beam from an amorphous silicon imaging system, they were able to capture dynamic images at 1/30th of a second. The nanofluid used was composed of diamond nanoparticles suspended in water.

Even though nanofluids and OHPs are not new discoveries, combining their unique features allows for the nanoparticles to be completely suspended in the base liquid increasing their heat transport capability. Since nanofluids have a strong temperature-dependent thermal conductivity and they show a nonlinear relationship between thermal conductivity and concentration, they are high performance conductors with an increased CHF. The OHP takes intense heat from a high-power device and converts it into kinetic energy of fluids while not allowing the liquid and vapor phases to interfere with each other since they flow in the same direction.

In their experiment, Ma et al. [28, 29] introduced diamond nanoparticles into high performance liquid chromatography (HPLC) water. The movement of the OHP keeps the nanoparticles from settling and thus improving the efficiency of the cooling device. At an input power of 80 W, the diamond nanofluid decreased the temperature difference between the evaporator and the condenser from 40.9°C to 24.3°C.

However, as the heat input increases, the oscillating motion increases and the resultant temperature difference between the evaporator and condenser does not continue to increase after a certain power input. This phenonmenon inhibits the effective thermal conductivity of the nanofluid from continuously increasing. However, at its maximum power level of 336 W, the temperature difference for the nanofluid OHP was still less than that for the OHP with pure water, Figure 2. Hence, it has been shown that the nanofluid can significantly increase the heat transport capability of the OHP.

Lin et al. [31] investigated nanofluids in pulsating heat pipes by using silver nanoparticles, and discovered encouraging results. The silver nanofluid improved heat transfer characteristics of the heat pipes.

Nguyen et al. [32] investigated the heat transfer enhancement and behavior of Al_2O_3-water nanofluid with the

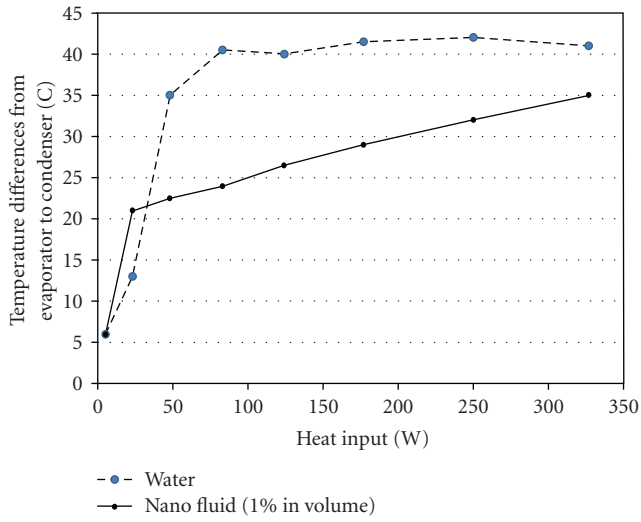

Figure 2: Effect of nanofluid on heat transport capability in an OHP [28, 29].

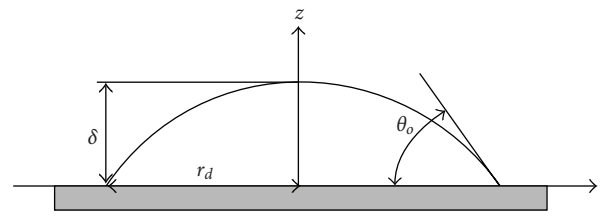

Figure 3: Schematic diagram of droplet shape.

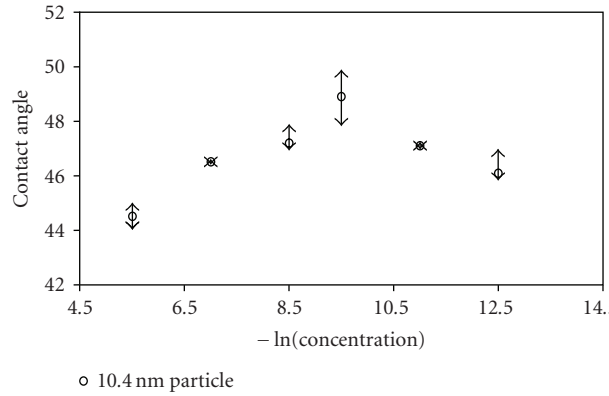

Figure 4: Variation of contact angle for 10 nm bismuth telluride nanoparticles concentration on a glass substrate [34].

intention of using it in a closed cooling system designed for microprocessors or other electronic devices. The experimental data supports that the inclusion of nanoparticles into distilled water produces a significant increase of the cooling convective heat transfer coefficient. At a given particle concentration of 6.8%, the heat transfer coefficient increased as much as 40% compared to the base fluid of water. Smaller Al_2O_3 nanoparticles also showed higher convective heat transfer coefficients than the larger ones.

Further research of nanofluids in electronic cooling applications will lead to the development of the next generation of cooling devices that incorporate nanofluids for ultrahigh-heat-flux electronic systems.

4.2. Microscale Fluidic Applications. The manipulation of small volumes of liquid is necessary in fluidic digital display devices, optical devices, and microelectromechanical systems (MEMS) such as lab-on-chip analysis systems. This can be done by electrowetting, or reducing the contact angle by an applied voltage, the small volumes of liquid. Electrowetting on dielectric (EWOD) actuation is one very useful method of microscale liquid manipulation.

Vafaei et al. [33] discovered that nanofluids are effective in engineering the wettability of the surface and possibly of surface tension. Using a goniometer, it was observed that even the addition of a very low concentration of bismuth telluride nanofluid dramatically changed the wetting characteristics of the surface. Concentrations as low as 3×10^{-6} increased the contact angle to over 40°, distinctly indicating that the nanoparticles change the force balance in the vicinity of the triple line. The contact angle, θ°, Figure 3 rises with the concentration of the nanofluid, reaches a maximum, and then decreases, Figure 4 [34].

The droplet contact angle was observed to change depending on the size of the nanoparticles as well. Smaller nanoparticles are more effective in increasing the contact angle. The reason for this effect is that smaller particles would provide more surface-to-volume area, for the same concentration.

Dash et al. used the EWOD effect to demonstrate that nanofluids display increased performance and stability when exposed to electric fields, Figure 5. The experiment consisted of placing droplets of water-based solutions containing bismuth telluride nanoparticles onto a Teflon-coated silicon wafer. A strong change in the angle at with the droplet contacted the wafer was observed when an electric field was applied to the droplet. The change noticed with the nanofluids was significantly greater than when not using nanofluids. The bismuth telluride nanofluid also displayed enhanced droplet stability and absence of the contact angle saturation effect compared to solutions of 0.01 N Na_2SO_4 and thioglycolic acid in deionized water.

That the contact angle of droplets of nanofluids can be changed has potential applications for efficiently moving liquids in microsystems, allowing for new methods for focusing lenses in miniature cameras as well as for cooling computer chips.

5. Biomedical Applications.

5.1. Nanodrug Delivery. Most bio-MEMS studies were done in academia in the 1990s, while recently commercialization of such devices have started. Examples include an electronically activated drug delivery microchip [35]; a controlled delivery system via integration of silicon and electroactive polymer technologies; a MEMS-based DNA sequencer developed by Cepheid [36]; and arrays of in-plane and out-of-plane hollow micro-needles for dermal/transdermal drug

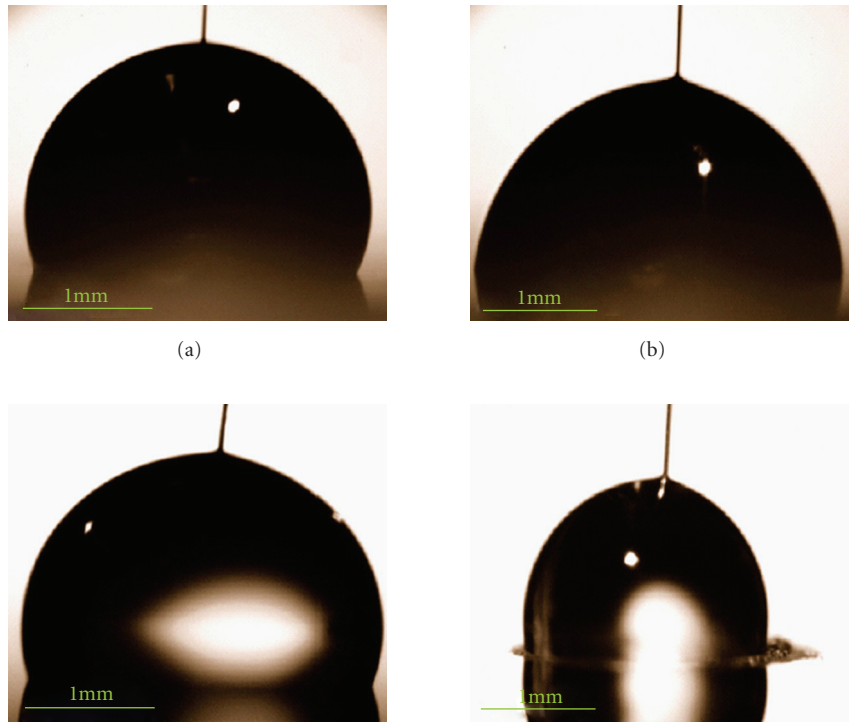

Figure 5: Nanofluid droplet with applied voltage (a) 0 V and (b) 64.5 V 0.01 M Na_2SO_4 droplet under (c) 0 V and (d) 40 V. The Na_2SO_4 droplet becomes unstable at approximately 40 V seen by the gas bubbles forming in the contact line, [34].

delivery [37, 38] as well as nanomedicine applications of nanogels or gold-coated nanoparticles [39]. An objective of the advanced endeavors in developing integrated micro- or nano-drug delivery systems is the interest in easily monitoring and controlling target-cell responses to pharmaceutical stimuli, to understand biological cell activities, or to enable drug development processes.

While conventional drug delivery is characterized by the "high-and-low" phenomenon, microdevices facilitate precise drug delivery by both implanted and transdermal techniques. This means that when a drug is dispensed conventionally, drug concentration in the blood will increase, peak and then drop as the drug is metabolized, and the cycle is repeated for each drug dose. Employing nano-drug delivery (ND) systems, controlled drug release takes place over an extended period of time. Thus, the desired drug concentration will be sustained within the therapeutic window as required.

A nanodrug-supply system, that is, a bio-MEMS, was introduced by Kleinstreuer et al. [40]. Their principal concern were the conditions for delivering uniform concentrations at the microchannel exit of the supplied nano-drugs. A heat flux which depends on the levels of nano-fluid and purging fluid velocity was added to ascertain that drug delivery to the living cells occurs at an optimal temperature, that is, 37°C. The added wall heat flux had also a positive influence on drug-concentration uniformity. In general, the nano-drug concentration uniformity is affected by channel length, particle diameter and the Reynolds number of both the nanofluid supply and main microchannels. Since the transport mechanisms are dependent on convection—diffusion, longer channels, smaller particle diameters as well as lower Reynolds numbers are desirable for best, that is, uniform drug delivery.

5.2. Cancer Theraupetics. There is a new initiative which takes advantage of several properties of certain nanofluids to use in cancer imaging and drug delivery. This initiative involves the use of iron-based nanoparticles as delivery vehicles for drugs or radiation in cancer patients. Magnetic nanofluids are to be used to guide the particles up the bloodstream to a tumor with magnets. It will allow doctors to deliver high local doses of drugs or radiation without damaging nearby healthy tissue, which is a significant side effect of traditional cancer treatment methods. In addition, magnetic nanoparticles are more adhesive to tumor cells than non-malignant cells and they absorb much more power than microparticles in alternating current magnetic fields tolerable in humans; they make excellent candidates for cancer therapy.

Magnetic nanoparticles are used because as compared to other metal-type nanoparticles, these provide a characteristic for handling and manipulation of the nanofluid by magnetic force [41]. This combination of targeted delivery and controlled release will also decrease the likelihood of systemic toxicity since the drug is encapsulated and biologically unavailable during transit in systemic circulation. The nanofluid containing magnetic nanoparticles also acts

as a super-paramagnetic fluid which in an alternating electromagnetic field absorbs energy producing a controllable hyperthermia. By enhancing the chemotherapeutic efficacy, the hyperthermia is able to produce a preferential radiation effect on malignant cells [42].

There are numerous biomedical applications that involve nanofluids such as magnetic cell separation, drug delivery, hyperthermia, and contrast enhancement in magnetic resonance imaging. Depending on the specific application, there are different chemical syntheses developed for various types of magnetic nanofluids that allow for the careful tailoring of their properties for different requirements in applications. Surface coating of nanoparticles and the colloidal stability of biocompatible water-based magnetic fluids are the two particularly important factors that affect successful application [43, 44].

Nanofluids could be applied to almost any disease treatment techniques by reengineering the nanoparticles' properties. In their study, the nanoparticles were laced with the drug docetaxel to be dissolved in the cells' internal fluids, releasing the anticancer drug at a predetermined rate. The nanoparticles contain targeting molecules called aptamers which recognize the surface molecules on cancer cells preventing the nanoparticles from attacking other cells. In order to prevent the nanoparticles from being destroyed by macrophages—cells that guard against foreign substances entering our bodies—the nanoparticles also have polyethylene glycol molecules. The nanoparticles are excellent drug-delivery vehicles because they are so small that living cells absorb them when they arrive at the cells' surface.

For most biomedical uses the magnetic nanoparticles should be below 15 nm in size and stably dispersed in water. A potential magnetic nanofluid that could be used for biomedical applications is one composed of FePt nanoparticles. This FePt nanofluid possesses an intrinsic chemical stability and a higher saturation magnetization making it ideal for biomedical applications. However, before magnetic nanofluids can be used as drug delivery systems, more research must be conducted on the nanoparticles containing the actual drugs and the release mechanism.

5.3. Cryopreservation. Conventional cryopreservation protocols for slow-freezing or vitrification involve cell injury due to ice formation/cell dehydration or toxicity of high cryoprotectant (CPA) concentrations, respectively. In the study by X. He et al. [45], they developed a novel cryopreservation technique to achieve ultra-fast cooling rates using a quartz micro-capillary (QMC). The QMC enabled vitrification of murine embryonic stem (ES) cells using an intracellular cryoprotectant concentration in the range used for slowing freezing (1–2 M). More than 70% of the murine ES cells post-vitrification attached with respect to non-frozen control cells, and the proliferation rates of the two groups were alike. Preservation of undifferentiated properties of the pluripotent murine ES cells post-vitrification cryopreservation was verified using three different types of assays. These results indicate that vitrification at a low concentration (2 M) of intracellular cryoprotectants is a viable and effective approach for the cryopreservation of murine embryonic stem cells.

5.4. Nanocryosurgery. Cryosurgery is a procedure that uses freezing to destroy undesired tissues. This therapy is becoming popular because of its important clinical advantages. Although it still cannot be regarded as a routine method of cancer treatment, cryosurgery is quickly becoming as an alternative to traditional therapies.

Simulations were performed by Yan and Liu [46] on the combined phase change bioheat transfer problems in a single cell level and its surrounding tissues, to explicate the difference of transient temperature response between conventional cyrosugery and nanocyrosurgery. According to theoretical interpretation and existing experimental measurements, intentional loading of nanoparticles with high thermal conductivity into the target tissues can reduce the final temperature, increase the maximum freezing rate, and enlarge the ice volume obtained in the absence of nanoparticles. Additionally, introduction of nanoparticle enhanced freezing could also make conventional cyrosurgery more flexible in many aspects such as artificially interfering in the size, shape, image and direction of iceball formation. The concepts of nanocyrosurgery may offer new opportunities for future tumor treatment.

With respect to the choice of particle for enhancing freezing, magnetite (Fe_3O_4) and diamond are perhaps the most popular and appropriate because of their good biological compatibility. Particle sizes less than 10 μm are sufficiently small to start permitting effective delivery to the site of the tumor, either via encapsulation in a larger moiety or suspension in a carrier fluid. Introduction of nanoparticles into the target via a nanofluid would effectively increase the nucleation rate at a high temperature threshold.

5.5. Sensing and Imaging. Colloidal gold has been used for several centuries now, be it as colorant of glass ("Purple of Cassius") and silk, in medieval medicine for the diagnosis of syphilis or, more recently, in chemical catalysis, non-linear optics, supramolecular chemistry, molecular recognition and the biosciences. Colloidal gold is often referred to as the most stable of all colloids. Its history, properties and applications have been reviewed extensively. For a thorough and up-to-date overview the paper by Daniel and Astruc [48] and the references cited therein may be consulted. As stated in the introduction, no attempt is made here to review the use of colloids which are also nanofluids. An increase of colloids which are nanofluids is expected in this category.

6. Other Applications

6.1. Nanofluid Detergent. Nanofluids do not behave in the same manner as simple liquids with classical concepts of spreading and adhesion on solid surfaces [7, 49, 50]. This fact opens up the possibility of nanofluids being excellent candidates in the processes of soil remediation, lubrication, oil recovery and detergency. Future engineering applications could abound in such processes.

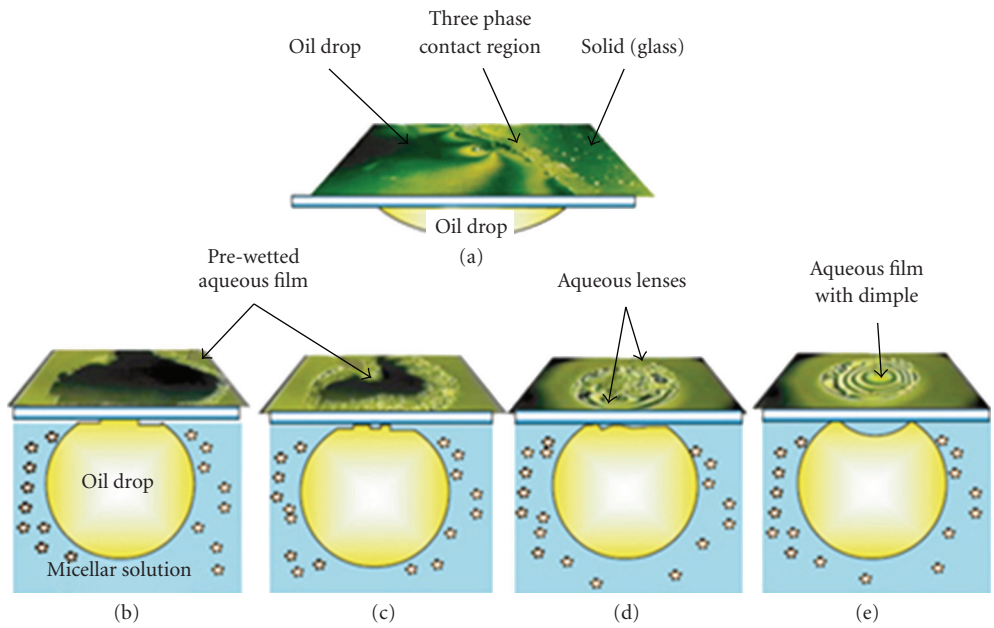

Figure 6: (a) Photomicrograph showing the oil drop placed on a glass surface and differential interference patterns formed at the three-phase contact region [47]. (b), Photomicrographs taken after addition of the nanofluid at (b), 30 s; 2 minutes; (d), 4 minutes; (e), 6 minutes region [47].

Wasan and Nikolov [47] of Illinois Institute of Technology in Chicago were able to use reflected-light digital video microscopy to determine the mechanism of spreading dynamics in liquid containing nanosized polystyrene particles, Figure 6. They were able to demonstrate the two-dimensional crystal-like formation of the polystyrene spheres in water and how this enhances the spreading dynamics of a micellar fluid at the three-phase region [47].

When encountering an oil drop, the polystyrene nanoparticles concentrate and rearrange around the drop creating a wedge-like region between the surface and the oil drop. The nanoparticles then diffuse into the wedge film and cause an increase in concentration and subsequently an increase in disjoining pressure around the film region. Owing to the increase in pressure, the oil-solution interface moves forward allowing the polystyrene nanoparticles to spread along the surface. It is this mechanism that causes the oil drop to detach completely from the surface.

Wasan and Nikolov [47] performed an additional experiment where they introduced an electrolyte into the process in order to decrease the interfacial tension at the interface of the oil and the nanofluid, but found that the drop did not become detached from the surface. They actually observed a diminished disjoining pressure contrary to the logical prediction. Additional work must be done in this area to determine such behavior of the nanofluid.

Overall, this phenomenon which involves the increased spreading of the detergent surfactants, which are not only limited to polystyrene nanoparticles, and enhanced oil removal process offers a new way of removing stains and grease from surfaces. This type of nanofluid also has potential in the commercial extraction of oil from the ground as well as the remediation of oil spills.

7. Conclusion

Nanofluids are important because they can be used in numerous applications involving heat transfer, and other applications such as in detergency. Colloids which are also nanofluids have been used in the biomedical field for a long time, and their use will continue to grow. Nanofluids have also been demonstrated for use as smart fluids. Problems of nanoparticle agglomeration, settling, and erosion potential all need to be examined in detail in the applications. Nanofluids employed in experimental research have to be well characterized with respect to particle size, size distribution, shape and clustering so as to render the results most widely applicable. Once the science and engineering of nanofluids are fully understood and their full potential researched, they can be reproduced on a large scale and used in many applications. Colloids which are also nanofluids will see an increase in use in biomedical engineering and the biosciences.

Further research still has to be done on the synthesis and applications of nanofluids so that they may be applied as predicted. Nevertheless, there have been many discoveries and improvements identified about the characteristics of nanofluids in the surveyed applications and we are a step closer to developing systems that are more efficient and smaller, thus rendering the environment cleaner and healthier.

References

[1] S. U. S. Choi, "Nanofluids: from vision to reality through research," *Journal of Heat Transfer*, vol. 131, no. 3, pp. 1–9, 2009.

[2] W. Yu, D. M. France, J. L. Routbort, and S. U. S. Choi, "Review and comparison of nanofluid thermal conductivity and heat transfer enhancements," *Heat Transfer Engineering*, vol. 29, no. 5, pp. 432–460, 2008.

[3] T. Tyler, O. Shenderova, G. Cunningham, J. Walsh, J. Drobnik, and G. McGuire, "Thermal transport properties of diamond-based nanofluids and nanocomposites," *Diamond and Related Materials*, vol. 15, no. 11-12, pp. 2078–2081, 2006.

[4] S. K. Das, S. U. S. Choi, and H. E. Patel, "Heat transfer in nanofluids—a review," *Heat Transfer Engineering*, vol. 27, no. 10, pp. 3–19, 2006.

[5] M.-S. Liu, M. C.-C. Lin, I.-T. Huang, and C.-C. Wang, "Enhancement of thermal conductivity with carbon nanotube for nanofluids," *International Communications in Heat and Mass Transfer*, vol. 32, no. 9, pp. 1202–1210, 2005.

[6] S. U. S. Choi, Z. G. Zhang, and P. Keblinski, "Nanofluids," in *Encyclopedia of Nanoscience and Nanotechnology*, H. S. Nalwa, Ed., vol. 6, pp. 757–737, American Scientific, Los Angeles, Calif, USA, 2004.

[7] S. M. S. Murshed, S.-H. Tan, and N.-T. Nguyen, "Temperature dependence of interfacial properties and viscosity of nanofluids for droplet-based microfluidics," *Journal of Physics D*, vol. 41, no. 8, Article ID 085502, 5 pages, 2008.

[8] K.-F. V. Wong and T. Kurma, "Transport properties of alumina nanofluids," *Nanotechnology*, vol. 19, no. 34, Article ID 345702, 8 pages, 2008.

[9] K.-F. V. Wong, B. L. Bon, S. Vu, and S. Samedi, "Study of nanofluid natural convection phenomena in rectangular enclosures," in *Proceedings of the ASME International Mechanical Engineering Congress and Exposition (IMECE '07)*, vol. 6, pp. 3–13, Seattle, Wash, USA, November 2007.

[10] Y. Ju-Nam and J. R. Lead, "Manufactured nanoparticles: an overview of their chemistry, interactions and potential environmental implications," *Science of the Total Environment*, vol. 400, no. 1–3, pp. 396–414, 2008.

[11] J. Routbort, et al., Argonne National Lab, Michellin North America, St. Gobain Corp., 2009, http://www1.eere.energy.gov/industry/nanomanufacturing/pdfs/nanofluids_industrial_cooling.pdf.

[12] Z. H. Han, F. Y. Cao, and B. Yang, "Synthesis and thermal characterization of phase-changeable indium/polyalphaolefin nanofluids," *Applied Physics Letters*, vol. 92, no. 24, Article ID 243104, 3 pages, 2008.

[13] G. Donzelli, R. Cerbino, and A. Vailati, "Bistable heat transfer in a nanofluid," *Physical Review Letters*, vol. 102, no. 10, Article ID 104503, 4 pages, 2009.

[14] S. J. Kim, I. C. Bang, J. Buongiorno, and L. W. Hu, "Study of pool boiling and critical heat flux enhancement in nanofluids," *Bulletin of the Polish Academy of Sciences—Technical Sciences*, vol. 55, no. 2, pp. 211–216, 2007.

[15] S. J. Kim, I. C. Bang, J. Buongiorno, and L. W. Hu, "Surface wettability change during pool boiling of nanofluids and its effect on critical heat flux," *International Journal of Heat and Mass Transfer*, vol. 50, no. 19-20, pp. 4105–4116, 2007.

[16] J. Boungiorno, L.-W. Hu, S. J. Kim, R. Hannink, B. Truong, and E. Forrest, "Nanofluids for enhanced economics and safety of nuclear reactors: an evaluation of the potential features issues, and research gaps," *Nuclear Technology*, vol. 162, no. 1, pp. 80–91, 2008.

[17] E. Jackson, *Investigation into the pool-boiling characteristics of gold nanofluids*, M.S. thesis, University of Missouri-Columbia, Columbia, Mo, USA, 2007.

[18] J. Buongiorno, L. W. Hu, G. Apostolakis, R. Hannink, T. Lucas, and A. Chupin, "A feasibility assessment of the use of nanofluids to enhance the in-vessel retention capability in light-water reactors," *Nuclear Engineering and Design*, vol. 239, no. 5, pp. 941–948, 2009.

[19] "The Future of Geothermal Energy," MIT, Cambridge, Mass, USA, 2007.

[20] P. X. Tran, D. K. lyons, et al., "Nanofluids for Use as Ultra-Deep Drilling Fluids," U.S.D.O.E., 2007, http://www.netl.doe.gov/publications/factsheets/rd/R&D108.pdf.

[21] M. Chopkar, P. K. Das, and I. Manna, "Synthesis and characterization of nanofluid for advanced heat transfer applications," *Scripta Materialia*, vol. 55, no. 6, pp. 549–552, 2006.

[22] D. Singh, J. Toutbort, G. Chen, et al., "Heavy vehicle systems optimization merit review and peer evaluation," Annual Report, Argonne National Laboratory, 2006.

[23] B. Shen, A. J. Shih, S. C. Tung, and M. Hunter, "Application of nanofluids in minimum quantity lubrication grinding," *Tribology and Lubrication Technology*.

[24] M. J. Kao, C. H. Lo, T. T. Tsung, Y. Y. Wu, C. S. Jwo, and H. M. Lin, "Copper-oxide brake nanofluid manufactured using arc-submerged nanoparticle synthesis system," *Journal of Alloys and Compounds*, vol. 434-435, pp. 672–674, 2007.

[25] M. J. Kao, H. Chang, Y. Y. Wu, T. T. Tsung, and H. M. Lin, "Producing aluminum-oxide brake nanofluids using plasma charging system," *Journal of the Chinese Society of Mechanical Engineers*, vol. 28, no. 2, pp. 123–131, 2007.

[26] S.-C. Tzeng, C.-W. Lin, and K. D. Huang, "Heat transfer enhancement of nanofluids in rotary blade coupling of four-wheel-drive vehicles," *Acta Mechanica*, vol. 179, no. 1-2, pp. 11–23, 2005.

[27] Q. Xue, J. Zhang, and Z. Zhang, "Synthesis, structure and lubricating properties of dialkyldithiophosphate-modified Mo-S compound nanoclusters," *Wear*, vol. 209, no. 1-2, pp. 8–12, 1997.

[28] H. B. Ma, C. Wilson, B. Borgmeyer, et al., "Effect of nanofluid on the heat transport capability in an oscillating heat pipe," *Applied Physics Letters*, vol. 88, no. 14, Article ID 143116, 3 pages, 2006.

[29] H. B. Ma, C. Wilson, Q. Yu, K. Park, U. S. Choi, and M. Tirumala, "An experimental investigation of heat transport capability in a nanofluid oscillating heat pipe," *Journal of Heat Transfer*, vol. 128, no. 11, pp. 1213–1216, 2006.

[30] M. Arif, "Neutron imaging for fuel cell research," in *Proceedings of the Imaging and Neutron Workshop*, Oak Ridge, Tenn, USA, October 2006.

[31] Y.-H. Lin, S.-W. Kang, and H.-L. Chen, "Effect of silver nanofluid on pulsating heat pipe thermal performance," *Applied Thermal Engineering*, vol. 28, no. 11-12, pp. 1312–1317, 2008.

[32] C. T. Nguyen, G. Roy, C. Gauthier, and N. Galanis, "Heat transfer enhancement using Al_2O_3-water nanofluid for an electronic liquid cooling system," *Applied Thermal Engineering*, vol. 27, no. 8-9, pp. 1501–1506, 2007.

[33] S. Vafaei, T. Borca-Tasciuc, M. Z. Podowski, A. Purkayastha, G. Ramanath, and P. M. Ajayan, "Effect of nanoparticles on sessile droplet contact angle," *Nanotechnology*, vol. 17, no. 10, pp. 2523–2527, 2006.

[34] R. K. Dash, T. Borca-Tasciuc, A. Purkayastha, and G. Ramanath, "Electrowetting on dielectric-actuation of microdroplets of aqueous bismuth telluride nanoparticle suspensions," *Nanotechnology*, vol. 18, no. 47, Article ID 475711, 6 pages, 2007.

[35] R. S. Shawgo, A. C. R. Grayson, Y. Li, and M. J. Cima, "BioMEMS for drug delivery," *Current Opinion in Solid State and Materials Science*, vol. 6, no. 4, pp. 329–334, 2002.

[36] Cepheid, 2009, http://www.Cepheid.Com.
[37] A. Ovsianikov, B. Chichkov, P. Mente, N. A. Monteiro-Riviere, A. Doraiswamy, and R. J. Narayan, "Two photon polymerization of polymer-ceramic hybrid materials for transdermal drug delivery," *International Journal of Applied Ceramic Technology*, vol. 4, no. 1, pp. 22–29, 2007.
[38] K. Kim and J.-B. Lee, "High aspect ratio tapered hollow metallic microneedle arrays with microfluidic interconnector," *Microsystem Technologies*, vol. 13, no. 3-4, pp. 231–235, 2007.
[39] V. Labhasetwar and D. L. Leslie-Pelecky, *Biomedical Applications of Nanotechnology*, John Wiley & Sons, New York, NY, USA, 2007.
[40] C. Kleinstreuer, J. Li, and J. Koo, "Microfluidics of nano-drug delivery," *International Journal of Heat and Mass Transfer*, vol. 51, no. 23-24, pp. 5590–5597, 2008.
[41] D. Bica, L. Vékás, M. V. Avdeev, et al., "Sterically stabilized water based magnetic fluids: synthesis, structure and properties," *Journal of Magnetism and Magnetic Materials*, vol. 311, no. 1, pp. 17–21, 2007.
[42] P.-C. Chiang, D.-S. Hung, J.-W. Wang, C.-S. Ho, and Y.-D. Yao, "Engineering water-dispersible FePt nanoparticles for biomedical applications," *IEEE Transactions on Magnetics*, vol. 43, no. 6, pp. 2445–2447, 2007.
[43] L. Vékás, D. Bica, and M. V. Avdeev, "Magnetic nanoparticles and concentrated magnetic nanofluids: synthesis, properties and some applications," *China Particuology*, vol. 5, no. 1-2, pp. 43–49, 2007.
[44] L. Vékás, D. Bica, and O. Marinica, "Magnetic nanofluids stabilized with various chain length surfactants," *Romanian Reports in Physics*, vol. 58, no. 3, pp. 257–267, 2006.
[45] X. He, E. Y. H. Park, A. Fowler, M. L. Yarmush, and M. Toner, "Vitrification by ultra-fast cooling at a low concentration of cryoprotectants in a quartz micro-capillary: a study using murine embryonic stem cells," *Cryobiology*, vol. 56, no. 3, pp. 223–232, 2008.
[46] J.-F. Yan and J. Liu, "Nanocryosurgery and its mechanisms for enhancing freezing efficiency of tumor tissues," *Nanomedicine*, vol. 4, no. 1, pp. 79–87, 2008.
[47] D. T. Wasan and A. D. Nikolov, "Spreading of nanofluids on solids," *Nature*, vol. 423, no. 6936, pp. 156–159, 2003.
[48] M.-C. Daniel and D. Astruc, "Gold nanoparticles: assembly, supramolecular chemistry, quantum-size-related properties, and applications toward biology, catalysis, and nanotechnology," *Chemical Reviews*, vol. 104, no. 1, pp. 293–346, 2004.
[49] K. Sefiane, J. Skilling, and J. MacGillivray, "Contact line motion and dynamic wetting of nanofluid solutions," *Advances in Colloid and Interface Science*, vol. 138, no. 2, pp. 101–120, 2008.
[50] Y. H. Jeong, W. J. Chang, and S. H. Chang, "Wettability of heated surfaces under pool boiling using surfactant solutions and nano-fluids," *International Journal of Heat and Mass Transfer*, vol. 51, no. 11-12, pp. 3025–3031, 2008.

Hindawi Publishing Corporation
Advances in Mechanical Engineering
Volume 2010, Article ID 172085, 4 pages
doi:10.1155/2010/172085

Research Article

On the Specific Heat Capacity of CuO Nanofluid

Le-Ping Zhou,[1] Bu-Xuan Wang,[2] Xiao-Feng Peng,[2] Xiao-Ze Du,[1] and Yong-Ping Yang[1]

[1] *School of Energy and Power, Key Laboratory of Condition Monitoring and Control for Power Plant Equipment of Ministry of Education, North China Electric Power University, Beijing 102206, China*
[2] *Thermal Engineering Department, Tsinghua University, Beijing 100084, China*

Correspondence should be addressed to Bu-Xuan Wang, bxwang@mail.tsinghua.edu.cn

Received 14 April 2009; Revised 28 June 2009; Accepted 29 August 2009

Academic Editor: Oronzio Manca

This paper reviews briefly the definition of heat capacity and clarifies the defined specific heat capacity and volumetric heat capacity. The specific heat capacity and volumetric heat capacity, with our measured experimental data for CuO nanofluids, are discussed as an illustrating example. The result indicates that the specific heat capacity of CuO nanofluid decreases gradually with increasing volume concentration of nanoparticles. The measurement and the prediction from the thermal equilibrium model exhibit good agreement. The other simple mixing model fails to predict the specific heat capacity of CuO nanofluid. The nanoparticle size effect and solid-liquid interface effect on the specific heat capacity of nanofluid are discussed.

1. Introduction

Nanofluids, that is, liquids with nanometer-sized particles suspensions, have attracted a substantial amount of attention since Masuda et al. reported firstly, in 1993, their precursory observations on the thermal conductivity enhancement in liquid dispersions of nanoparticles [1]. To meet potentially the increasing demand for high thermal conductive working fluids, many researches are focused on the basic thermophysical properties of nanofluids, for example, effective thermal conductivity, effective viscosity, thermal diffusivity, specific heat capacity, Prandtl number, and so forth, with which researchers investigate the convective heat transfer and flow characteristics of nanofluids. However, only effective thermal conductivity and effective viscosity are extensively covered in relevant studies [2]. As a thermodynamic property, the specific heat capacity of a nanofluid is important to dictate the nanoparticle and fluid temperature changes, which affect the temperature field of the nanofluid and hence the heat transfer and flow status. Other thermophysical properties, such as thermal diffusivity and Prandtl number need the knowledge of specific heat capacity, too.

Only several researches involve in experiments of the specific heat capacities of nanofluids. For example, Sinha et al. [3] measured the specific heat capacity of a nanotube solution (nanofluid) by an AC calorimeter. He et al. [4] measured the specific heat capacity of $BaCl_2$-water-based TiO_2 nanofluid with a heat-flux differential scanning calorimeter. Peng et al. [5] measured the specific heat capacity of water-based Cu, Al, Al_2O_3, and CuO nanofluids, and propylene glycol- (PG-) based Al_2O_3 nanofluid, with a special designed comparison calorimeter. Recently, Zhou and Ni [2] measured the specific heat capacity of water-based Al_2O_3 nanofluid with a power-compensated differential scanning calorimeter. These experiments show that the specific heat capacities of nanofluids are different from that of base fluid and vary with the size and volume concentration of nanoparticles. In most of the cases, however, there are no experimental data available for specific heat capacity, such that two kinds of models have been generally adopted to deduce it from the value of base fluid and nanoparticles. One is macroscopic, that the specific heat capacity of a nanofluid is equal to the volume average of the specific heat capacities of base fluid and nanoparticles. The other is mesoscopic, which assumes the base fluid and the nanoparticles are in their thermal equilibrium, respectively. Using the volumetric heat capacity instead, the volumetric heat capacity of a nanofluid can be expressed as the sum of the volumetric heat capacities for base fluid and nanoparticles, using their respective volume concentrations. These models are equivalent for small concentrations, but for large concentrations the models are obviously divergent. Zhou and Ni [2] also

summarized the models mentioned earlier and compared them with their experimental results, concluding that their experiments are in good agreement with the second model, while the first one fails to predict the specific heat capacity of nanofluid. The divergence arises from the misunderstanding for the definition of specific heat capacity and volumetric heat capacity. However, the misunderstanding remains in many articles, so that it is necessary to further explain the controversy among models and experiments.

In this study, we will first review briefly the definition of heat capacity and clarify the relation between specific heat capacity and volumetric heat capacity. We will measure the specific heat capacity of nanofluid made by EG (ethylene glycol) with inclusion of CuO nanoparticles at room temperature using the quasisteady-state principle [6], to compare with the mentioned models. We will also consider the particle size effect and particle-liquid interface effect on the specific heat capacity of nanofluid, and then compare them with our analytical results, to attempt to find the rule of specific heat capacity variation when increasing the volume concentration of nanoparticles and to apply it in the experimental and numerical investigations of nanofluid.

2. On the Definition of Heat Capacity

To avoid misunderstanding of the specific heat capacity of nanofluid and misemploying in experimental and numerical researches, we review here briefly the definition of heat capacity, together with the relation between specific heat capacity and volumetric heat capacity.

The heat capacity C of a substance, sometimes also called total heat capacity, is the amount of heat required to change its temperature by one Kelvin, and has units of joule per Kelvin (J/K) in the SI system [7, 8]. The equation relating thermal energy to heat capacity is $\Delta Q = C\Delta T$, where ΔQ is the thermal energy put into or taken out of the substance, and ΔT is the temperature differential. The heat capacity is therefore an extensive variable and depends simply on the amount of substance. The heat capacity for a mixture of different substances is the sum of the individual heat capacities:

$$C = C_1 + C_2 + \cdots . \tag{1}$$

The specific heat capacity c of a substance, also named mass-specific heat capacity in science and engineering, is the amount of the heat required to change its temperature of unit mass (one kilogram) of the substance by one Kelvin. The unit of specific heat capacity c in the SI system is the Joule per kilogram-Kelvin, J/(kg·K) [7, 8]. The equation relating heat energy to specific heat capacity is $\Delta Q = cm\Delta T$. The specific heat capacity corresponds to the quotient of heat capacity and mass, or $c = C/m$, where m is the total mass. The specific heat capacity of a mixture of substances is equal to the sum of the individual heat capacities divided by the total mass:

$$c = \frac{C}{m} = \frac{(c_1 m_1 + c_2 m_2 + \cdots)}{(m_1 + m_2 + \cdots)} = \omega_1 c_1 + \omega_2 c_2 + \cdots , \tag{2}$$

where $\omega_i = m_i/m$ is the mass concentration of the ith substance.

In the measurement of physical properties, the term "specific" means the measure is an intensive property, wherein the quantity of substance must be specified. For specific heat capacity, mass is the specified quantity (unit quantity). In some books on thermodynamics, the noted specific heat capacity is used for the molar heat capacity. Furthermore, the specific heat capacity is sometimes simply denoted as specific heat. These may cause confusion. In chemistry, the term molar heat capacity c_{mol} of a substance may be used to more explicitly describe the measure of the amount of the heat required to change its temperature of unit quantity of substance (one mole) by one Kelvin. The unit of molar heat capacity c_{mol} in the SI system is the joule per mole-Kelvin, J/(mol·K) [7, 8]. The equation relating heat energy to molar heat capacity is $\Delta Q = c_{\text{mol}} n\Delta T$, where n is the number of moles. The molar heat capacity is related to the heat capacity by $c_{\text{mol}} = C/n$, and is related to the specific heat capacity by $c_{\text{mol}} = cM$, where M is the molar mass. The molar heat capacity of a mixture of substances is equal to the sum of the individual heat capacities divided by the total number of moles:

$$\begin{aligned} c = \frac{C}{n} &= \frac{(c_{\text{mol1}} n_1 + c_{\text{mol2}} n_2 + \cdots)}{(n_1 + n_2 + \cdots)} \\ &= x_1 c_{\text{mol1}} + x_2 c_{\text{mol2}} + \cdots , \end{aligned} \tag{3}$$

where $x_i = n_i/n$ is the molar concentration of the ith substance. While the "specific heat, γ", of a substance is the ratio of the amount of heat required to raise the temperature of a given mass of the substance through a given range of temperature to the heat required to raise the temperature of an equal mass of water through the same range: $\gamma = c/c_0$, where c_0 is the specific heat capacity of water.

The specific volumetric heat capacity, ρc, of a substance is the amount of the heat required to change its temperature of unit volume of the substance by one Kelvin [7, 8], and ρ being the density or mass per unit volume. The volumetric heat capacity describes the ability of a given volume of a substance to store internal energy while undergoing a given temperature change, but without undergoing a phase change. The unit of volumetric heat capacity ρc in SI system is the Joule per square meter-Kelvin, J/(m^3·K). The equation relating thermal energy to volumetric heat capacity is $\Delta Q = \rho c V \Delta T$, where V is the total volume. The specific heat capacity corresponds to the quotient of heat capacity and volume, or C/V. The volumetric heat capacity of a mixture of substances is equal to the sum of the individual heat capacities divided by the total volume:

$$\rho c = \phi_1 \rho_1 c_1 + \phi_2 \rho_2 c_2 + \cdots , \tag{4}$$

where $\phi_i = V_i/V$ is the volume concentration of the ith substance, and $\rho = (\phi_1 \rho_1 + \phi_2 \rho_2)$, is the density of the mixture.

In the case of nanofluid, the specific heat capacity at constant pressure c_p can be derived from (6), which becomes

$$c_{p,nf} = \frac{\left[(1-\phi)\rho_f c_{p,f} + \phi \rho_{np} c_{p,np}\right]}{\left[\phi_f \rho_f + (1-\phi)\rho_{np}\right]}, \tag{5}$$

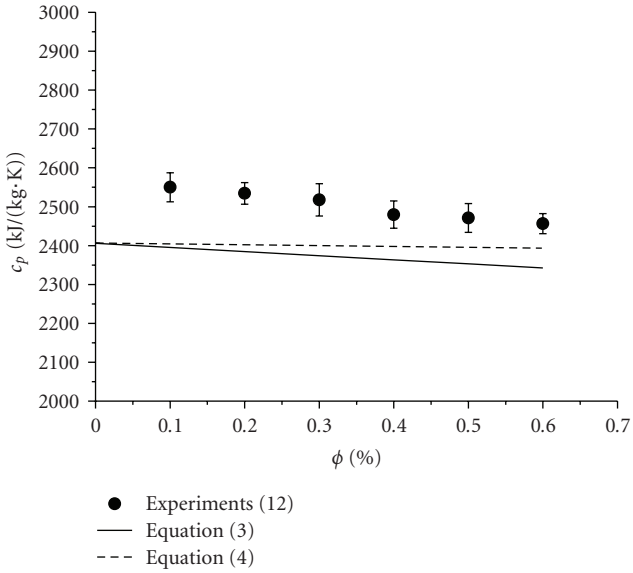

Figure 1: Specific heat capacity of CuO/EG nanofluid.

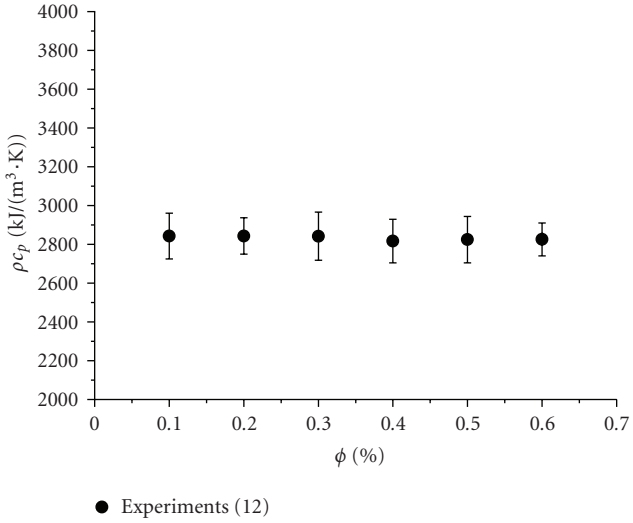

Figure 2: Volumetric heat capacity of CuO/EG nanofluid.

where ϕ is the volume concentration of nanoparticle, and the subscripts nf, f, and np represent for nanofluid, base fluid, and nanoparticle, respectively. The following equation is proposed for determining specific heat capacity of nanofluid and assessing heat transfer performance of nanofluids [9–11]:

$$c_{p,nf} = (1-\phi)c_{p,f} + \phi c_{p,np}. \quad (6)$$

However, it is approximately correct only for dilute suspensions when small density difference exists between base fluid and nanoparticle. For water-based Al_2O_3 nanofluid, for example, the deviation cannot be ignored, as the density ratio between nanoparticle and base fluid is large ($\rho_{np} = 3600\,\text{kg/m}^3$ for Al_2O_3, while $\rho_f = 994.7\,\text{kg/m}^3$ for water), so that large discrepancy occurs when increasing the volume concentration of nanoparticle [11].

3. Data Correlated with Discussions

Now, we will discuss, as an example, on the specific heat capacity and volumetric heat capacity with our measured experimental data for CuO nanofluids [12]. We use CuO nanoparticles (produced by chemical vapor-synthesis method) and EG as base fluid to prepare nanofluid for experiments. The nanoparticles are in form of loose agglomerates under atmospheric condition and can be dispersed in EG successfully through ultrasonic vibration for about three hours. The nanoparticles show a lognormal size distribution with nominal diameter of 50 nm. The quasisteady-state method is adopted to measure the specific heat capacity of nanofluid [6].

Figure 1 shows the specific heat capacity of CuO/EG nanofluid, of which the volume concentration of nanoparticle varying from 0.1% to 0.6% by interval of 0.1%. An obvious increase of specific heat capacity can be observed for these nanofluids, comparing with the value calculated from (5) and (6). The discrepancy between them indicates that neither of the two equations can be used to predict the tendency for fluid with nanoparticle inclusions. The experiments also present a slight decrease of specific heat capacity for CuO nanofluid when increasing the volume concentration of CuO nanoparticle, while it coincides with (5) for nearly the same linear tendency.

The volumetric heat capacity of nanofluid is important to dictate the temperature change of nanofluid. This is clear for analyzing the heat transfer between nanoparticle and base fluid, with energy conservation either in thermal equilibrium form or in nonequilibrium one. Figure 2 shows the corresponding volumetric heat capacity of CuO/EG nanofluid. The variation of volumetric heat capacity is small for dilute CuO/EG nanofluid. One can conclude that the volumetric heat capacity ratio of CuO/EG nanofluid versus deionized water will be approximately a constant, which may be helpful to analyze the energy conservation in a dimensionless form.

As shown in Figure 1, the discrepancy between the experimental results and (5) and (6) may arouse from the surface and size effects on the specific heat capacity of nanoparticle [12], and hence, decreased with increasing ϕ due to agglomeration of nanofluid (clustering). We adopt model I (6) and II (5), respectively, to show the nanoparticle size effect on the specific heat capacity of nanofluid, as shown in Figure 3. The specific heat capacities of nanoparticles correspond to the bulk, 50 nm and 25 nm CuO, respectively [12]. As shown, the specific heat capacity of nanofluid is underestimated using the specific heat capacity of bulk CuO. While the prediction can be improved with the specific heat capacity of CuO nanoparticle obtained from either theoretical analysis or experiments. The results from our previous calculation show that the discrepancy between nanoparticles with different sizes is small when increasing the nanoparticle volume concentration, due to the large specific heat capacity of base fluid.

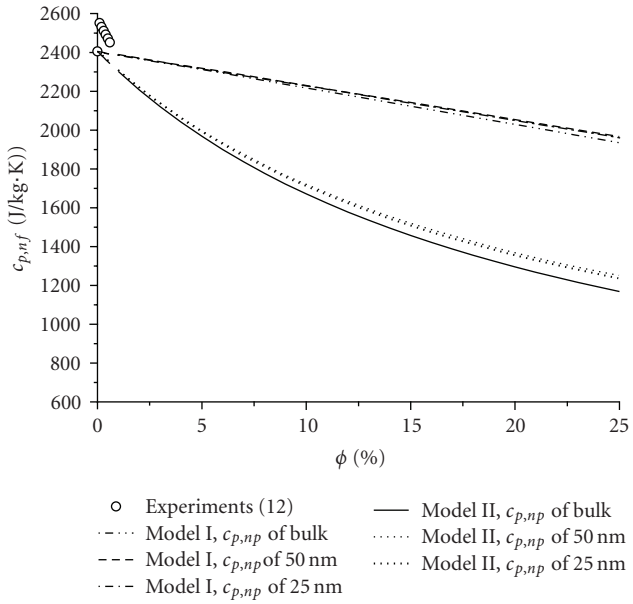

Figure 3: Specific heat capacity of CuO/EG nanofluid compared with model I and II.

Qualitatively, the solid-liquid interface may change the phonon vibration mode near the surface area of a nanoparticle and thus change the specific heat capacity of nanofluid. The high specific interfacial area of nanoparticle can adsorb liquid molecules to its surface and form liquid layers, which will reversely constrain nanoparticle and turns its free-boundary surface atoms to be nonfree interior atoms [12]. The varied Gibbs free energy of nanoparticle and liquid layers will further change the specific heat capacity of nanofluid.

4. Conclusion

This paper reviews briefly the definition of heat capacity and clarifies the defined specific heat capacity and volumetric heat capacity. For illustration, the specific heat capacity of nanofluid made by ethylene glycol and copper dioxide nanoparticle inclusions, measured at room temperature, were compared with two kinds of models for determination of the specific heat capacity of nanofluid, which are frequently used in researches on convective heat transfer experiments and simulations. The particle size effect and particle-liquid interface effect on the specific heat capacity of nanofluid are also discussed briefly. The effect of liquid adsorption on suspended nanoparticles' surface will also increase the specific heat capacity of nanofluid to some extent with increasing nanoparticles' volume concentration, which may be worthy to be investigated further for nanofluids.

Acknowledgment

The work was financially supported by the National Natural Science Foundation of China with Grant Number 50906024.

References

[1] H. Masuda, A. Ebata, K. Teramae, and N. Hishinuma, "Alternation of thermal conductivity and viscosity of liquid by dispersing ultra-fine particles (dispersion of γ-Al_2O_3, SiO_2 and TiO_2 ultra-fine particles)," *Netsu Bussei*, vol. 4, pp. 227–233, 1993 (Japanese).

[2] S. Q. Zhou and R. Ni, "Measurement of the specific heat capacity of water-based Al_2O_3 nanofluid," *Applied Physics Letters*, vol. 92, Article ID 093123, 3 pages, 2008.

[3] S. Sinha, S. Barjami, G. Iannacchione, and S. Sinha, "Thermal properties of carbon nanotube based fluids," in *Proceedings of the Memphis-Area Engineering and Sciences Conference (MAESC '04)*, 2004.

[4] Q. B. He, M. W. Tong, and Y. D. Liu, "Measurement of specific heat of TiO_2-$BaCl_2$-H_2O nano-fluids with DSC," *Refrigeration & Air-Conditioning*, vol. 7, no. 4, pp. 19–22, 2007 (Chinese).

[5] X. F. Peng, X. L. Yu, and F. Q. Yu, "Experimental study on the specific heat of nanofluids," *Journal of Materials Science & Engineering*, vol. 25, no. 5, pp. 719–722, 2007 (Chinese).

[6] B.-X. Wang, L.-P. Zhou, and X.-F. Peng, "A fractal model for predicting the effective thermal conductivity of liquid with suspension of nanoparticles," *International Journal of Heat and Mass Transfer*, vol. 46, no. 14, pp. 2665–2672, 2003.

[7] W. Benenson, J. W. Harris, H. Stocker, and H. Lutz, *Handbook of Physics*, Springer, New York, NY, USA, 2002.

[8] Y. Cengel and M. Boles, *Thermodynamics—An Engineering Approach*, McGraw-Hill, New York, NY, USA, 5th edition, 2005.

[9] J. Buongiorno, "Convective transport in nanofluids," *Journal of Heat Transfer*, vol. 128, no. 3, pp. 240–250, 2006.

[10] S. J. Palm, G. Roy, and C. T. Nguyen, "Heat transfer enhancement with the use of nanofluids in radial flow cooling systems considering temperature-dependent properties," *Applied Thermal Engineering*, vol. 26, no. 17-18, pp. 2209–2218, 2006.

[11] R. B. Mansour, N. Galanis, and C. T. Nguyen, "Effect of uncertainties in physical properties on forced convection heat transfer with nanofluids," *Applied Thermal Engineering*, vol. 27, no. 1, pp. 240–249, 2007.

[12] B.-X. Wang, L.-P. Zhou, and X.-F. Peng, "Surface and size effects on the specific heat capacity of nanoparticles," *International Journal of Thermophysics*, vol. 27, no. 1, pp. 139–151, 2006.

Hindawi Publishing Corporation
Advances in Mechanical Engineering
Volume 2010, Article ID 807610, 10 pages
doi:10.1155/2010/807610

Research Article

Effects of Particle Surface Charge, Species, Concentration, and Dispersion Method on the Thermal Conductivity of Nanofluids

Raghu Gowda,[1] Hongwei Sun,[1] Pengtao Wang,[1] Majid Charmchi,[1] Fan Gao,[2] Zhiyong Gu,[2] and Bridgette Budhlall[3]

[1] *Department of Mechanical Engineering, University of Massachusetts Lowell, Lowell, MA 01854, USA*
[2] *Department of Chemical Engineering, University of Massachusetts Lowell, Lowell, MA 01854, USA*
[3] *Department of Plastic Engineering, University of Massachusetts Lowell, Lowell, MA 01854, USA*

Correspondence should be addressed to Hongwei Sun, hongwei_sun@uml.edu

Received 1 July 2009; Revised 18 September 2009; Accepted 14 October 2009

Academic Editor: Oronzio Manca

The purpose of this experimental study is to evaluate the effects of particle species, surface charge, concentration, preparation technique, and base fluid on thermal transport capability of nanoparticle suspensions (nanofluids). The surface charge was varied by changing the pH value of the fluids. The alumina (Al_2O_3) and copper oxide (CuO) nanoparticles were dispersed in deionized (DI) water and ethylene glycol (EG), respectively. The nanofluids were prepared using both bath-type and probe sonicator under different power inputs. The experimental results were compared with the available experimental data as well as the predicted values obtained from Maxwell effective medium theory. It was found that ethylene glycol is more suitable for nanofluids applications than DI water in terms of thermal conductivity improvement and stability of nanofluids. Surface charge can effectively improve the dispersion of nanoparticles by reducing the (aggregated) particle size in base fluids. A nanofluid with high surface charge (low pH) has a higher thermal conductivity for a similar particle concentration. The sonication also has a significant impact on thermal conductivity enhancement. All these results suggest that the key to the improvement of thermal conductivity of nanofluids is a uniform and stable dispersion of nanoscale particles in a fluid.

1. Introduction

Due to the low thermal conductivities of most common liquids used in heat exchangers, such as water and ethylene glycol, it has become urgent to look into other advanced alternatives. A new type of fluids called nanofluids (suspensions of nanometer-sized particles in various fluids) has been extensively investigated to enhance the heat carrying capacity of fluids although the mechanism behind exceptionally enhanced thermal conductivity of nanofluids is still not well understood. Different mechanisms have been put forth to explain thermal transport enhancement such as interfacial resistance, nanoparticle motion, liquid layering at particle-liquid interface, and nanoparticle clustering [1]. Among them, nanoparticle motion (Brownian motion) [2–9] and nanoparticle clustering [10–15] have attracted most attention. The initial experiments show preferred thermal properties of nanofluids [16–20], such as an order of magnitude higher thermal conductivity than that predicted by conventional theory on heterogeneous two-component mixture. A very small concentration of copper nanoparticle (less than 0.3% volume fraction of 10 nm nanoparticles) can enhance the thermal conductivity of base fluid (ethylene glycol) by up to 40% [21]. On the other hand, the Hamilton and Crosser (HC) model predicts a less than 1.5% improvement in thermal conductivity [22]. In another study [16] where metallic multiwalled carbon nanotubes (MWCNTs) were dispersed in synthetic oil (α-olefin), an astonishing improvement of 160% in thermal conductivity was observed with only a 1.0% volume fraction of MWNT. The authors argue that the three-dimensional network formed by CNTs is responsible for significant thermal conductivity improvement. A recent study shows that the enhancement of thermal conductivity of nanofluids heavily depends on fluid temperature [9, 23] and particle sizes [24, 25]. Herein a two- to fourfold increase in thermal conductivity was observed when

the fluid temperature increased from 21°C to 51°C [23]. However, the hypothesis of thermal transport enhancement due to Brownian motion is being challenged [26–28]. The recent experimental and theoretical investigation strongly suggests that the nanoparticle aggregation (clusters) plays a significant role in the thermal transport in nanofluids. A light scattering method shows that the cluster size (due to aggregation) in a Fe-ethylene glycol nanofluids increases from 1 micron to 2.4 microns during a 50-minute waiting time after sonication [11]. The thermal conductivity can be enhanced due to percolation effect in the aggregates/clusters, especially for highly conducting particles. But sedimentation will increasingly take place when the size of aggregates exceeds a threshold value. The small particle size and short distance between particles increase the probability of aggregation. On the other hand, a low pH value actually means a high surface potential, and in turns a high repulsive energy and less aggregation [14, 29].

This research is focused on a systematic investigation of key parameters that affect the thermal conductivity of nanofluids. These parameters include surface charge, nanoparticle composition and concentration, base fluids, and preparation techniques. The paper starts with nanofluid preparation and the measurement system, followed with comparisons of the obtained results with those published in open literature and predicted by theory, and then the effects of key parameters are discussed and summarized in detail in the end of the paper.

2. Nanofluids Preparation and Experimental Apparatus

2.1. Nanofluid Preparation. Preparation of nanofluids through which nanoparticles should be uniformly dispersed in base fluids is the first step for improvement in thermal conductivity, but its importance is often ignored. The nanofluid does not simply refer to a liquid-solid mixture. Some special requirements are necessary, such as uniform, stable, and durable suspension, low or no aggregation of particles, and no chemical reaction. There are three primary methods being used to prepare nanofluids [29]: (i) direct dispersion of powder form nanoparticles in the base fluids; (ii) nanoparticle synthesized by chemical precipitation and then dispersed in base fluids; (iii) direct nanoparticle synthesis in the base fluid by organic reduction. Stability of the dispersion is ensured by controlling the surface charge of the nanoparticles through the control of the pH value of fluids. This is very effective for oxide nanoparticles such as alumina and copper oxide used in this research.

The nanofluids under current investigation can be divided into two groups based on the base fluids including DI water and ethylene glycol (EG). Both alumina (Al_2O_3) powder (nominal particle size provided by the manufacturer: 40–50 nm) and copper oxide (nominal particle size: 23–37 nm) were purchased from Alfa Aesar for this experiment. These nanoparticles were dispersed in DI water and/or EG (99%, source: Alfa Aesar) using three sonication methods. They are (1) sonication of nanofluids with a probe sonicator (Branson Digital Sonifier 450) at 80% magnitude (maximum power: 450 W) for 2 minutes; (2) another probe sonicator (Omni-Ruptor 250) at 80% magnitude (maximum power: 150 W) for 2 minutes, and (3) a bath sonicator (Model: 75D VWR) for 4.5 hours at maximum power setting (maximum power: 75 W). The alumina and copper oxide nanoparticles were imaged under a Philips EM400 transmission electron microscope (TEM) to obtain information about nanoparticle size and shape (Figure 1). As can be seen in Figure 1, the alumina nanoparticles are roughly spherical in shape but copper oxide nanoparticles show some deviations from spherical shapes. The size of alumna nanoparticles spans a wide range (from a few nm to 55 nm) but copper oxide nanoparticles do not have very small size particles.

The smaller sized alumina particles (nominal size: 10 nm) from a different source (NanoAmor Inc.) were also considered. But it was found that the dispersion of these alumina nanoparticles in DI water is very difficult even after adding various surfactants such as sodium dodecyl sulfate (SDS), cetyltrimethyl ammonium bromide (CTAB), Pluronic P105 and applying long time ultra sonication. No thermal conductivity measurement was conducted for these alumina nanoparticle solutions.

Temperature rise is minimized by utilizing multiple short sonications (instead of a long sonication) and the evaporation of base fluids is avoided by sealing the container with caps during sonication. The power and time settings of the ultra sonicators were chosen in such a way that a better dispersion is achieved with minimum increase in nanofluids temperature. For example, the DI water-based nanofluids reach 50°C after two-minute sonication. The nanofluids temperature returns back to room temperature (24°C) after around 1.5 hours waiting period. Before each measurement, both the pH and temperature of nanofluids are obtained by a pH probe (Mettler Toledo S-47). The temperature of nanofluids is maintained at room temperature during the measurement. Hydrochloric acid (HCl) (36%, VWR Scientific) or sodium hydroxide (NaOH) (99.99%, ACROS Organics)) is used to adjust the pH value of the nanofluids. An in-house equipment (Zetasizer Nano, Malvern Instruments Ltd) was used for zeta potential and size measurements of nanoparticles after dispersion.

2.2. Thermal Conductivity Measurement Apparatus. Transient hot wire method (THW) was adapted by many researchers to determine the thermal conductivity of the nanofluid suspensions [21, 30–35]. The THW method is a simple but effective transient method for measuring thermal conductivity of materials. This method determines the thermal conductivity by observing the rate at which the temperature of a very thin wire increases with time after an abrupt electrical pulse. It can eliminate the error from natural convection since the measurement is completed in a very short time (less than one second). Figure 2 presents the temperature rise of the wire during the thermal conductivity measurement for DI water.

In this research, an isonel coated platinum (source: A-M systems) with 25 μm in diameter and 15 cm in length

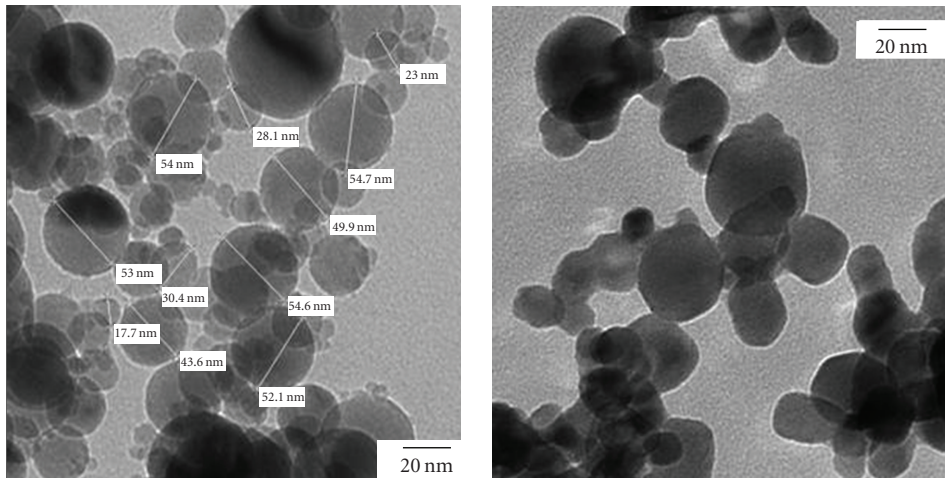

(a) (b)

Figure 1: TEM images of alumina (a) and copper oxide (b) nanoparticles.

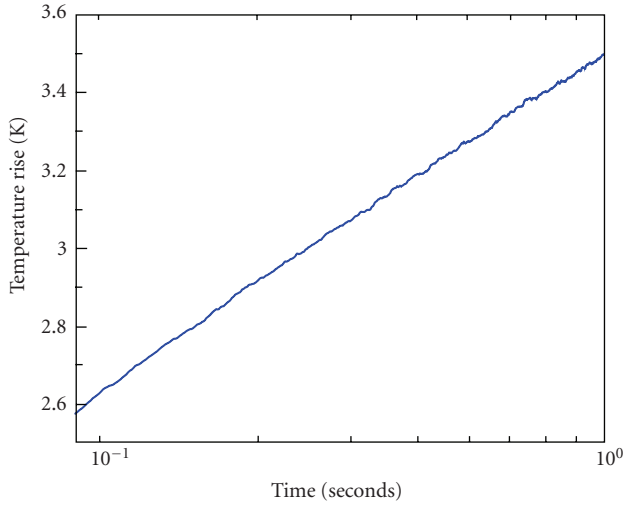

Figure 2: Temperature rise of the hotwire in DI water versus time (with time plotted on log scale).

was immersed horizontally in a plexiglass cell ($17 \times 2 \times 2.5$ cm) containing nanofluid (see Figure 3(b)). During the experiment, the wire serves as a heat source, a thermometer, as well as one of the legs of a Wheatstone bridge (Figure 3(a)). The temperature rise of the wire is calculated from the change in the resistance of the platinum wire with time, obtained by measuring the voltage offset using a data acquisition system (DAQ) (NI SCXI-1303). The R_1, R_2, and R_3 represent temperature compensated precision resistors (40 kΩ) in Figure 3(a). R_W and R_P denote the hot wire and the variable resistor to balance the Wheatstone bridge circuit, respectively. Before connecting platinum wire in the experimental system, the platinum wire was calibrated in a constant temperature bath and the measured temperature coefficient of resistance was 0.0033524 Ω/ΩK. The derivation of Fourier's equation for an infinite line heat source in an infinite heat medium gives us the following equation:

$$k = \frac{q}{4\pi L}\left(\frac{\ln(t)}{\Delta T}\right), \tag{1}$$

where k is the thermal conductivity of the fluid, q is the heat dissipation rate. L is the length of the wire and t the time (from start of heating), and ΔT is the temperature rise of the wire. Therefore, the temperature rise (ΔT) versus natural log of time (t) data were plotted and the slope was then used to calculate the thermal conductivity (Figure 2) and a linear relationship implies that conduction is the primary mode of heat transfer during the measurement [32]. The experiment lasts for around 5 seconds. The slope of the straight line in the curve ($\ln(t)/\Delta T$) between 0.1 and 1 second was used for the calculation of thermal conductivity (Figure 2).

The calibration of the apparatus was performed by comparing the measured thermal conductivities of DI water and EG with those from literature values at room temperature [36]. Deviation for DI water and EG is 0.66% and 2.36%, respectively. The uncertainty analysis of measured thermal conductivity was attached in the appendix. Each thermal conductivity value was obtained from an average of 20 measurements with an estimated accuracy of ± 0.0015 and ± 0.0013, respectively [37]. These results demonstrate that the experimental setup used in the present work can produce a reliable thermal-conductivity data. Additional details of the apparatus and technique are available elsewhere [32].

3. Results and Discussion

3.1. Comparison with Published Literature. The thermal conductivities of alumina/DI water, alumina/EG, and copper oxide/EG are compared with available published results [38–42]. The nanofluids were dispersed using the bath sonicator and the results are presented in Figures 4, 5, and 6. The experimental results are consistent with other published

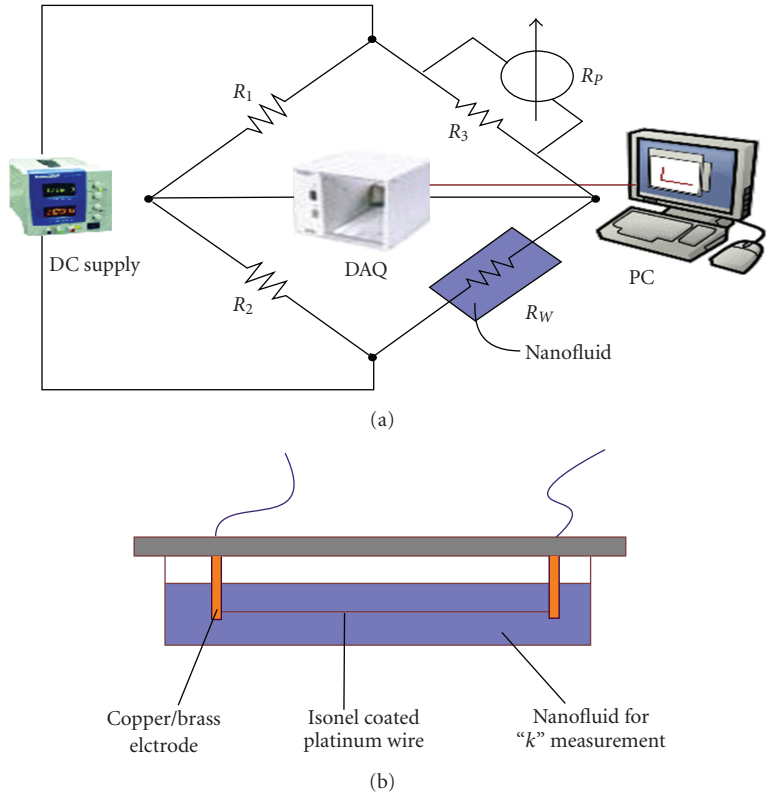

Figure 3: (a) Schematic of transient hot wire (THW) system and (b) test cell containing platinum wire and nanofluids.

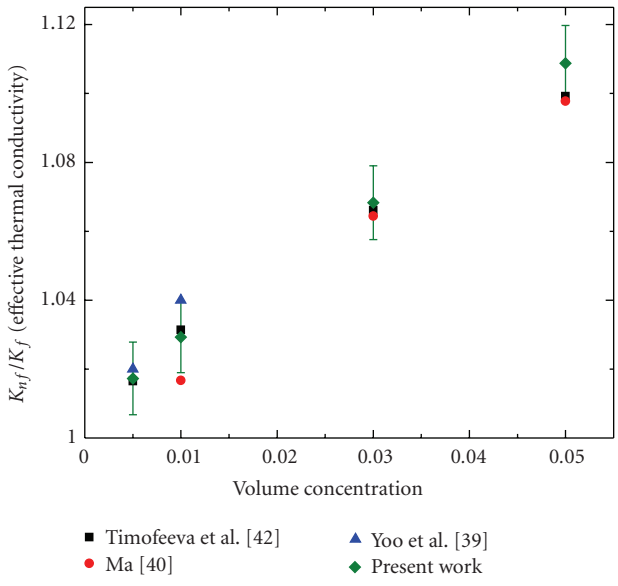

Figure 4: Comparison of experimental data of DI water-based alumina nanofluids with literature data [39, 40, 42].

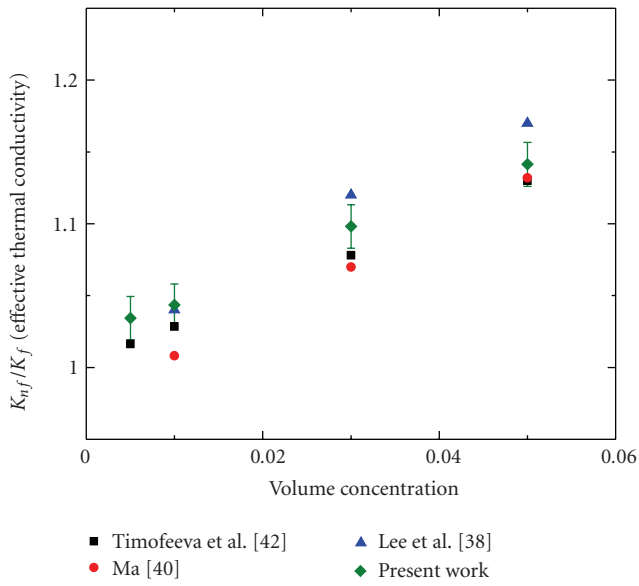

Figure 5: Comparison of experimental data of EG-based alumina nanofluids with literature data [38, 40, 42].

results within the experimental uncertainty. The thermal conductivity increases with the increase of volumetric fraction of nanofluids. Apparent density values for alumina (4.0 g/cm^3) and copper oxide (6.4 g/cm^3) were used for volume fraction calculations.

3.2. Effect of pH Value on Thermal Conductivity. Surface charge is critical for the stabilization of colloidal solutions. The effect of pH value on thermal conductivity of DI water-based alumina nanofluids was examined in this work. The pH values of alumina/DI water were changed from 7.0 to

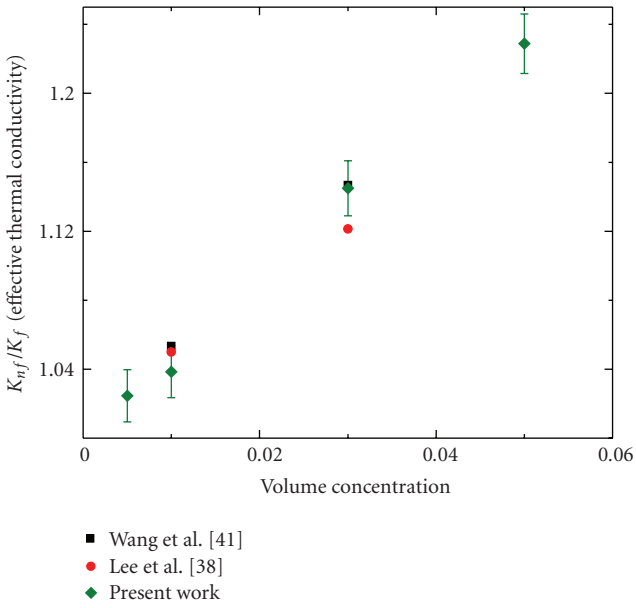

Figure 6: Comparison of experimental data for EG-based copper oxide nanofluids with literature data [38, 41].

2.0 by adding HCl solution into the nanofluids. By adding NaOH solutions, the values of 7.0 to 11.0 were obtained. The nanoparticles were dispersed using bath sonicator with parameters mentioned above. The corresponding thermal conductivities were measured using THW apparatus and plotted in Figure 7(a). As a comparison, the prediction from effective medium theory (EMT) is also plotted (solid line) [42]. The EMT gives a relationship between particle volume fraction and thermal conductivity improvement solely based on particle volume concentration (ϕ) as described below

$$\frac{K_{nf}}{K_F} = 1 + 3\phi. \tag{2}$$

The EMT theory is conventionally employed when (1) the particles are assumed to be static; (2) thermal conductivity of the particles is much higher than that of base fluid; (3) the volume fraction of particles is small; (4) the shape of particles is spherical. Compared with abnormal improvement in thermal conductivity reported by published results, overall the present thermal conductivity results of alumina nanofluids are lower than the values from the prediction from EMT theory. Our finding is consistent with published results by Timofeeva et al. [42]. The conclusion was made that the low thermal conductivity is mainly caused by aggregation of nanoparticles. One consequence of the aggregation is the reduction of particle numbers in solution and size increase (clustered structures) of particles. The impact of these mechanisms on thermal conductivity enhancement is complicated depending on the primary mechanism for heat transport. On one hand, the size increase of particles in nanofluids forms fractal/clustered structures in fluids which will shorten the heat conduction path in medium, so the thermal conductivity should be

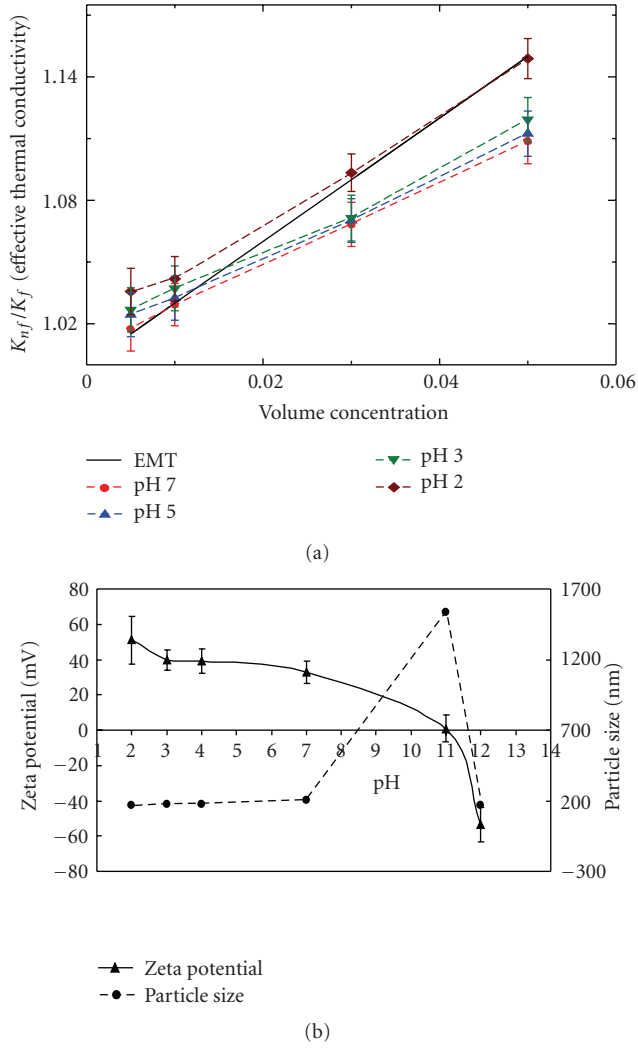

Figure 7: Effect of pH value on (a) thermal conductivity of DI water-based alumina nanofluids and (b) particle size.

increased. On the other hand, the size increase of particles reduces the particle motions which have been proposed to entrain the motion of the fluid for promoting more heat transfer. As a result, the enhancement in thermal conductivity will be reduced. The competition between these two heat transfer mechanisms decides the thermal conductivity enhancement.

To prove this hypothesis, the particle sizes in nanofluids were measured by a Zetasizer machine (Malvern Instruments Ltd), which is based on dynamic light scattering (DLS) technique. In DLS, particles are illuminated with a laser. The intensity of the scattered light fluctuates at a rate that is dependent upon the size of the particles as smaller particles are moved further by the solvent molecules and move more rapidly. Analysis of these intensity fluctuations yields the velocity of the Brownian motion and the particles hydrodynamic size is calculated using the Stokes-Einstein relationship. The results indicate that the average size of particles in the fluids is reduced from 207 nm to around

160 nm when the pH value changes from 7 to 2 (Figure 7(b)). It is also worth noting that the average particle size increases up to 1500 nm when the zeta potential of particle is around zero (pH = 11). It is apparent that a large aggregation occurs when the interparticle repulsion force between particles is small or the surface charge of nanoparticles is small. As the nanofluids become more acidic (lower pH value), more charges are accumulated on the particle surface. Less aggregation occurs and the dispersion is improved. As the result, the effective thermal conductivity increases. For instance, at volumetric fraction of 5%, the thermal conductivity ratio (nanofluids to base fluid) increases from 1.06 to 1.14 (within the error limit). The value of 1.14 is consistent with effective medium theory (EMT) prediction. But the EMT theory fails in taking into consideration the effect of nanoparticle size increase (due to aggregates/clusters formation) on thermal conductivity.

3.3. Effect of Base Fluids on Thermal Conductivity. To study the effect of base fluid property on thermal conductivity in nanofluids, DI water and EG-based alumina nanofluids were measured after they were dispersed using probe type sonicator. Figure 8 shows the trend of thermal conductivity of alumina nanoparticles in different base fluids at different volume concentrations. Apparently, the effective thermal conductivity (ratio of thermal conductivity of nanofluids to that of base fluid) of EG-based alumina nanofluids is higher than that of the DI water-based alumina nanofluids at same concentrations. Unlike DI water-based nanofluids, the thermal conductivity of EG-based alumina nanofluids accurately follows the trend predicted by EMT. One possibility is that in a colloidal system (nanofluids) consisting of a large number of small particles, particles will collide with each other in the course of their Brownian motion. In such a collision, the particles may be so attracted to one another that they stick together to form aggregates. The aggregation rate depends on both the viscosity of base fluid and surface charge of the nanoparticles [43]. A further study on the effect of base fluids on nanofluids thermal conductivity is underway.

3.4. Effect of Nanoparticle Species on Thermal Conductivity. To evaluate the effect of nanoparticle species on thermal conductivity, alumina, copper oxide, and a 1 : 1 mixture of alumina and copper oxide nanoparticles are dispersed in ethylene glycol. The thermal conductivities were measured and presented in Figure 9. The thermal conductivities of alumina (polycrystalline) and copper oxide are reported to be 18 W/m K and 20 W/m K, respectively [36]. The results clearly show that the thermal conductivity of copper oxide nanofluids is higher than that of alumina, which has lower thermal conductivity. But this seems to be not enough to explain the significant difference of thermal conductivities of two nanofluids. In addition, the thermal conductivity of 1 : 1 mixture of alumina and copper Oxide in EG lies in between these two nanofluids (alumina nanofluids and copper oxide nanofluids) at higher concentrations. We hypothesize that a lower interfacial thermal resistance of copper oxide-EG results in a higher thermal conductivity enhancement compared to alumina-EG fluids. This proposed explanation needs a direct measurement of interfacial thermal resistance at the liquid-solid interface, which cannot be conducted in our lab at the current time. The EMT theory, which only takes into account volumetric fraction effect, actually fails in predicting the effects of particle thermal conductivity and interfacial thermal resistance on thermal conductivity.

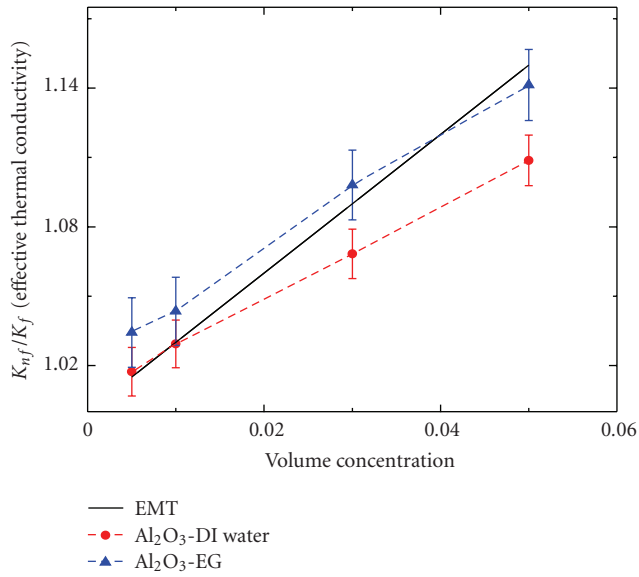

Figure 8: Effect of base fluids (DI water and EG) on thermal conductivity of alumina nanofluids.

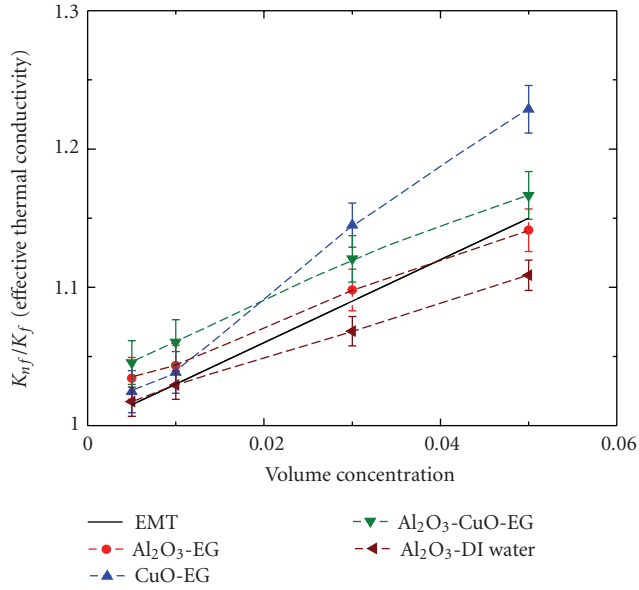

Figure 9: Effect of particle species on thermal conductivities of EG-based alumina, copper oxide, and 1 : 1 mixture of alumina and copper oxide nanofluids.

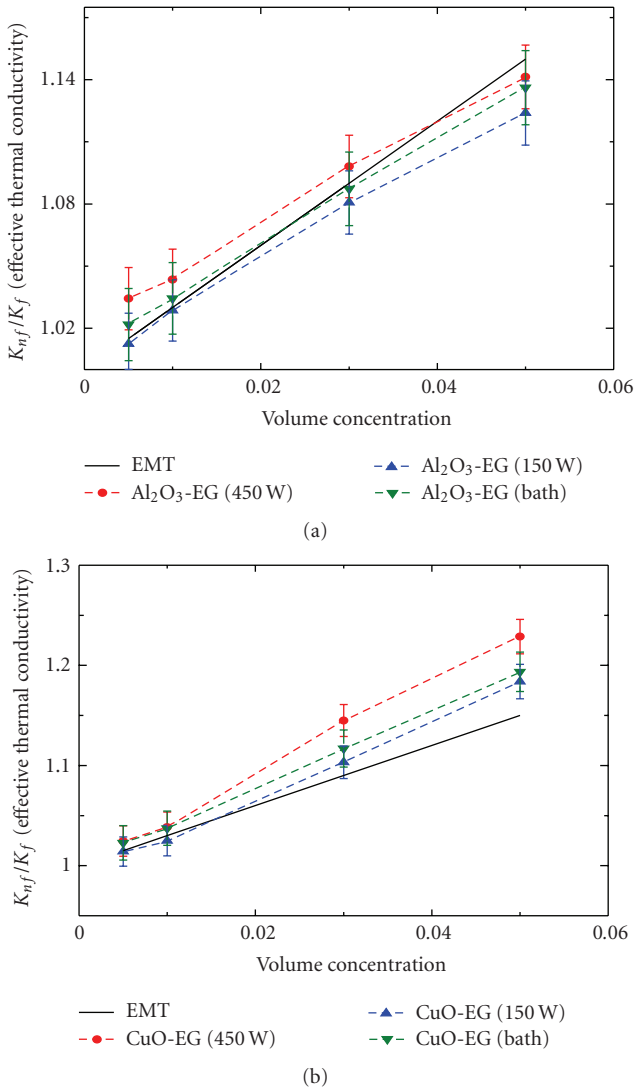

Figure 10: Effect of sonication power on thermal conductivities of EG-based (a) alumina and (b) copper oxide nanofluids.

3.5. Effect of Sonication Methods on Thermal Conductivity. Another important parameter to determine thermal conductivity of nanofluids is preparation method. Three sonication methods are used to study the effect of sonication techniques on effective thermal conductivity of nanofluids. All nanoparticles (alumina and copper oxide) are dispersed in EG. The three sonication techniques include: (1) sonication of nanofluids with a probe sonicator (Branson Digital Sonifier 450) at 80% magnitude (maximum power: 450 W) for 2 minutes; (2) another probe sonicator (Omni-Ruptor 250) at 80% magnitude (maximum power: 150 W) for 2 minutes, and (3) a bath sonicator (Model: 75D VWR) for 4.5 hours at maximum power setting (maxium power: 90 W). The measured thermal conductivities are plotted in Figure 10. For both alumina and copper oxide nanofluids, the 450 W probe sonication gave the highest effective thermal conductivity enhancement, followed by bath sonication, and lastly, 150 W probe sonication. Even at lower concentrations (<2%) the trend is still the same but EG-based alumina nanofluids have better effective thermal conductivities compared to EG-based copper oxide nanofluids. The sizes of particles in fluids versus the sonication methods are presented in Figure 11. As we expected, the 450 W probe sonication produces the smallest size (140 nm) of (agglomerated) particles in both DI water and EG-based nanofluids, and the 150 W probe yields larger particle size. Another important observation is that the particle size reduces from 175 nm to 140 nm for EG-based nanofluids compared to a reduction from 155 nm to 140 nm for DI water-based nanofluids. Therefore, sonication technique is more effective for EG-based nanofluids than DI water-based nanofluids. The effective thermal conductivity of nanofluids is directly linked to ultra-sonication power which influences the particle dispersion and average size in the nanofluids. An accurate theory which can incorporate sonication/dispersion criteria is needed to predict thermal conductivities of nanofluids.

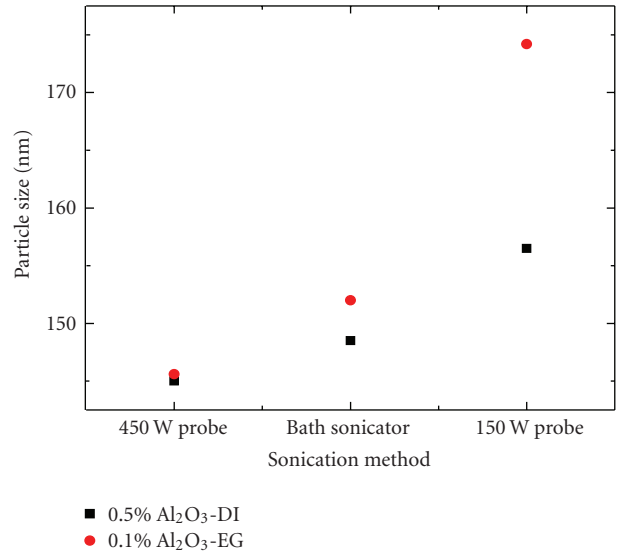

Figure 11: Effect of sonication power on (agglomerated) alumina particle size of DI water and EG-based nanofluids.

4. Conclusions

The effect of surface charge (pH value), base fluid, particle species, and dispersion method on thermal conductivity of alumina and copper oxide nanofluids are addressed in a systematic way. The high surface charge (low pH value) of nanofluids improves dispersion of nanoparticles in base fluids. The viscosity of base fluid reduces the Brownian velocity of nanoparticles so that the sedimentation/agglomeration of particles in nanofluids is decreased. All these lead to a higher thermal conductivity. Therefore, the thermal conductivity of nanofluids can be effectively improved by changing pH of fluids and by using more viscous fluids. Another important parameter is dispersion technique. The results demonstrate that high power sonication can significantly improve thermal conductivity of nanofluids and also stability of nanofluids.

Appendix

Uncertainty analysis is given as follows:

$$k = \frac{q}{4\pi L}\left(\frac{Ln(t)}{\Delta T}\right),$$
$$k = f(q, L, t, \Delta T). \tag{A.1}$$

Best estimate for the uncertainty [37] is given as follows:

$$\Delta k = \left[\left(\frac{\partial k}{\partial q}\Delta q\right)^2 + \left(\frac{\partial k}{\partial L}\Delta L\right)^2 + \left(\frac{\partial k}{\partial t}\Delta t\right)^2 + \left(\frac{\partial k}{\partial(\Delta T)}\Delta(\Delta T)\right)^2\right]^{1/2}. \tag{A.2}$$

(1) For $((\partial k/\partial q)\Delta q)$,we have

$$\frac{\partial k}{\partial q} = \frac{1}{4\pi L}\left(\frac{Ln(t)}{\Delta T}\right),$$

$$\Delta q = \left[\left(\frac{\partial q}{\partial V_{\text{in}}}\Delta V_{\text{in}}\right)^2 + \left(\frac{\partial q}{\partial R_w}R_{werr}\right)^2 + \left(\frac{\partial q}{\partial(\Delta R_w)}\Delta(\Delta R_w)\right)^2\right]^{1/2},$$

$$q = \frac{V_{\text{in}}^2(R_w + \Delta R_w)}{(2R_w + \Delta R_w)^2},$$

$$\frac{\partial q}{\partial V_{\text{in}}} = \frac{2V_{\text{in}}(R_w + \Delta R_w)}{(2R_w + \Delta R_w)^2},$$

$$\frac{\partial q}{\partial R_w} = \frac{V_{\text{in}}^2}{(2R_w + \Delta R_w)^2} - \frac{4V_{\text{in}}^2(R_w + \Delta R_w)}{(2R_w + \Delta R_w)^3},$$

$$\frac{\partial q}{\partial(\Delta R_w)} = \frac{V_{\text{in}}^2}{(2R_w + \Delta R_w)^2} - \frac{2V_{\text{in}}^2(R_w + \Delta R_w)}{(2R_w + \Delta R_w)^3},$$

$$\Delta R_w = \frac{4R_w\Delta V}{V_{\text{in}} - 2\Delta V},$$

$$\Delta(\Delta R_w) = \left[\left(\frac{\partial(\Delta R_w)}{\partial R_w}R_{werr}\right)^2 + \left(\frac{\partial(\Delta R_w)}{\partial(\Delta V)}\Delta(\Delta V)\right)^2 + \left(\frac{\partial(\Delta R_w)}{\partial V_{\text{in}}}\Delta V_{\text{in}}\right)^2\right]^{1/2},$$

$$\frac{\partial(\Delta R_w)}{\partial R_w} = \frac{4\Delta V}{V_{\text{in}} - 2\Delta V},$$

$R_{werr} = \pm 0.001\,\Omega$ (DMM multimeter),

$$\frac{\partial(\Delta R_w)}{\partial(\Delta V)} = \frac{4R_w}{(V_{\text{in}} - 2\Delta V)}\left[1 + \frac{2\Delta V}{(V_{\text{in}} - 2\Delta V)}\right],$$

$\Delta(\Delta V) = \pm 0.0018\,\text{V}$ (National Instruments SCXI-1303),

$$\frac{\partial(\Delta R_w)}{\partial V_{\text{in}}} = -\frac{4R_w\Delta V}{(V_{\text{in}} - 2\Delta V)^2},$$

$\Delta V_{\text{in}} = \pm 0.01\%$ Re ading

$+ 3\,\text{mV}$, (National Instruments SCXI-1303),

$\Delta V_{\text{in}} = \pm 0.0038V.$ (A.3)

(2) For $((\partial k/\partial L)\Delta L)$,we have

$$\frac{\partial k}{\partial L} = -\frac{q}{4\pi L^2}\left(\frac{Ln(t)}{\Delta T}\right),$$

$\Delta L = \pm 0.001\,\text{m}$ (ruler or scale). (A.4)

(3) For $((\partial k/\partial t)\Delta t)$,we have

$$\frac{\partial k}{\partial t} = \frac{q}{4\pi L}\left(\frac{1}{\Delta T}\right),$$

$\Delta t = \pm 0.001\,\text{sec}$ (National Instruments SCXI-1303). (A.5)

(4) For $((\partial k/\partial(\Delta T))\Delta(\Delta T))$,we have

$$\frac{\partial k}{\partial(\Delta T)} = -\frac{q}{4\pi L}\left(\frac{Ln(t)}{\Delta T^2}\right),$$

$$\Delta(\Delta T) = \left[\left(\frac{\partial(\Delta T)}{\partial R_w}R_{werr}\right)^2 + \left(\frac{\partial(\Delta T)}{\partial(\alpha)}\Delta\alpha\right)^2 + \left(\frac{\partial(\Delta T)}{\partial(\Delta R_w)}\Delta(\Delta R_w)\right)^2\right]^{1/2},$$

$$\Delta T = \frac{\Delta R_w}{\alpha R_w},$$

$$\frac{\partial(\Delta T)}{\partial(\Delta R_w)} = \frac{1}{\alpha R_w},$$

$$\frac{\partial(\Delta T)}{\partial(\alpha)} = -\frac{\Delta R_w}{\alpha^2 R_w},$$

$$\frac{\partial(\Delta T)}{\partial R_w} = -\frac{\Delta R_w}{\alpha R_w^2},$$

$$\alpha = \frac{dR}{dT},$$

$$\Delta(\alpha) = \left[\left(\frac{\partial\alpha}{\partial(dR)}\Delta(dR)\right)^2 + \left(\frac{\partial\alpha}{\partial(dT)}\Delta(dT)\right)^2\right]^{1/2},$$

$$\frac{\partial\alpha}{\partial(dR)} = \frac{1}{dT},$$

$$\Delta(dR) = R_{werr} = \pm 0.001\,\Omega \text{ (DMM multimeter)},$$

$$\frac{\partial\alpha}{\partial(dT)} = -\frac{dR}{(dT)^2},$$

$$\Delta(dT) = \pm 0.2^{\circ}\text{C (Thermometer)}. \tag{A.6}$$

Nomenclature

K_B: The Boltzmann constant
k_{nf}: Thermal conductivity of the nanoparticle suspension (nanofluids)
k_f: Thermal conductivity of the base fluid
L: Length of the platinum wire
q: Heat generated in the platinum wire
R_w: Resistance of platinum wire at room temperature
t: Time
T: Temperature
V_{in}: Voltage applied to the Wheatstone bridge of the transient hot wire apparatus
α: Temperature coefficient of resistance of the platinum wire
ϕ: Volume fraction of the nanoparticle suspension (nanofluids)
μ: The base fluid dynamic viscosity.

Acknowledgment

The authors would like to acknowledge the support of Nanomanufacturing Center of Excellence (NCOE) Strategic Seed Grant from the State of Massachusetts.

References

[1] J. A. Eastman, S. R. Phillpot, S. U. S. Choi, and P. Keblinski, "Thermal transport in nanofluids," *Annual Review of Materials Research*, vol. 34, pp. 219–246, 2004.

[2] S. Krishnamurthy, P. Bhattacharya, P. E. Phelan, and R. S. Prasher, "Enhanced mass transport in nanofluids," *Nano Letters*, vol. 6, no. 3, pp. 419–423, 2006.

[3] C. H. Chon and K. D. Kihm, "Thermal conductivity enhancement of nanofluids by Brownian motion," *Journal of Heat Transfer*, vol. 127, no. 8, p. 810, 2005.

[4] P. Bhattacharya, S. K. Saha, A. Yadav, P. E. Phelan, and R. S. Prasher, "Brownian dynamics simulation to determine the effective thermal conductivity of nanofluids," *Journal of Applied Physics*, vol. 95, no. 11, pp. 6492–6494, 2004.

[5] R. Prasher, P. Bhattacharya, and P. E. Phelan, "Thermal conductivity of nanoscale colloidal solutions (nanofluids)," *Physical Review Letters*, vol. 94, no. 2, Article ID 025901, 4 pages, 2005.

[6] S. P. Jang and S. U. S. Choi, "Role of Brownian motion in the enhanced thermal conductivity of nanofluids," *Applied Physics Letters*, vol. 84, no. 21, pp. 4316–4318, 2004.

[7] J. Koo and C. Kleinstreuer, "A new thermal conductivity model for nanofluids," *Journal of Nanoparticle Research*, vol. 6, no. 6, pp. 577–588, 2004.

[8] R. Prasher, P. Bhattacharya, and P. E. Phelan, "Brownian-motion-based convective-conductive model for the effective thermal conductivity of nanofluids," *Journal of Heat Transfer*, vol. 128, no. 6, pp. 588–595, 2006.

[9] K.-F. V. Wong and T. Kurma, "Transport properties of alumina nanofluids," *Nanotechnology*, vol. 19, no. 34, Article ID 345702, 8 pages, 2008.

[10] B.-X. Wang, L.-P. Zhou, and X.-F. Peng, "A fractal model for predicting the effective thermal conductivity of liquid with suspension of nanoparticles," *International Journal of Heat and Mass Transfer*, vol. 46, no. 14, pp. 2665–2672, 2003.

[11] K. S. Hong, T.-K. Hong, and H.-S. Yang, "Thermal conductivity of Fe nanofluids depending on the cluster size of nanoparticles," *Applied Physics Letters*, vol. 88, no. 3, Article ID 031901, 3 pages, 2006.

[12] W. Yu and S. Choi, "The role of interfacial layers in the enhanced thermal conductivity of nanofluids: a renovated Hamilton-Crosser model," *Journal of Nanoparticle Research*, vol. 6, no. 4, pp. 355–361, 2004.

[13] Y. Xuan, Q. Li, and W. Hu, "Aggregation structure and thermal conductivity of nanofluids," *AIChE Journal*, vol. 49, no. 4, pp. 1038–1043, 2003.

[14] D. Lee, J.-W. Kim, and B. G. Kim, "A new parameter to control heat transport in nanofluids: surface charge state of the particle in suspension," *Journal of Physical Chemistry B*, vol. 110, no. 9, pp. 4323–4328, 2006.

[15] R. Prasher, P. E. Phelan, and P. Bhattacharya, "Effect of aggregation kinetics on the thermal conductivity of nanoscale colloidal solutions (nanofluid)," *Nano Letters*, vol. 6, no. 7, pp. 1529–1534, 2006.

[16] S. Choi, Z. G. Zhang, W. Yu, F. E. Lockwood, and E. A. Grulke, "Anomalous thermal conductivity enhancement in nanotube suspensions," *Applied Physics Letters*, vol. 79, no. 14, pp. 2252–2254, 2001.

[17] R. Prasher, P. Bhattacharya, and P. E. Phelan, "Brownian-motion-based convective-conductive model for the effective thermal conductivity of nanofluids," *Journal of Heat Transfer*, vol. 128, no. 6, pp. 588–595, 2006.

[18] S. Das, S. Choi, W. Liu, and T. Pradeep, *Nanofluids: Science and Technology*, John Wiley & Sons, New York, NY, USA, 2007.

[19] H. Xie, J. Wang, T. Xi, Y. Liu, and F. Ai, "Dependence of the thermal conductivity on nanoparticle-fluid mixture on the base fluid," *Journal of Materials Science Letters*, vol. 21, no. 19, pp. 1469–1471, 2002.

[20] H. Xie, J. Wang, T. Xi, Y. Liu, F. Ai, and Q. Wu, "Thermal conductivity enhancement of suspensions containing nanosized alumina particles," *Journal of Applied Physics*, vol. 91, no. 7, p. 4568, 2002.

[21] J. A. Eastman, S. Choi, S. Li, W. Yu, and L. J. Thompson, "Anomalously increased effective thermal conductivities of ethylene glycol-based nanofluids containing copper nanoparticles," *Applied Physics Letters*, vol. 78, no. 6, pp. 718–720, 2001.

[22] R. L. Hamilton and O. K. Crosser, "Thermal conductivity of heterogeneous two-component systems," *Industrial and Engineering Chemistry Fundamentals*, vol. 1, no. 3, pp. 187–191, 1962.

[23] S. K. Das, N. Putra, P. Thiesen, and W. Roetzel, "Temperature dependence of thermal conductivity enhancement for nanofluids," *Journal of Heat Transfer*, vol. 125, no. 4, pp. 567–574, 2003.

[24] C. H. Chon, K. D. Kihm, S. P. Lee, and S. Choi, "Empirical correlation finding the role of temperature and particle size for nanofluid (Al_2O_3) thermal conductivity enhancement," *Applied Physics Letters*, vol. 87, no. 15, Article ID 153107, 3 pages, 2005.

[25] M. Chopkar, P. K. Das, and I. Manna, "Synthesis and characterization of nanofluid for advanced heat transfer applications," *Scripta Materialia*, vol. 55, no. 6, pp. 549–552, 2006.

[26] W. Evans, J. Fish, and P. Keblinski, "Role of Brownian motion hydrodynamics on nanofluid thermal conductivity," *Applied Physics Letters*, vol. 88, no. 9, Article ID 093116, 2006.

[27] M. Vladkov and J.-L. Barrat, "Modeling transient absorption and thermal conductivity in a simple nanofluid," *Nano Letters*, vol. 6, no. 6, pp. 1224–1229, 2006.

[28] P. Keblinski and J. Thomin, "Hydrodynamic field around a Brownian particle," *Physical Review E*, vol. 73, no. 1, Article ID 010502, 4 pages, 2006.

[29] W. C. Williams, I. C. Bang, E. Forrest, L. W. Hu, and J. Buongiorno, "Preparation and characterization of various nanofluids," in *Proceedings of the NSTI Nanotechnology Conference and Trade Show (Nanotech '06)*, vol. 2, pp. 408–411, Boston, Mass, USA, May 2006.

[30] V. Trisaksri and S. Wongwises, "Critical review of heat transfer characteristics of nanofluids," *Renewable and Sustainable Energy Reviews*, vol. 11, no. 3, pp. 512–523, 2007.

[31] K. Kwak and C. Kim, "Viscosity and thermal conductivity of copper oxide nanofluid dispersed in ethylene glycol," *Korea-Australia Rheology Journal*, vol. 17, no. 2, pp. 35–40, 2005.

[32] C. Y. Ho, J. Kestin, and W. A. WakeHam, *Transport Properties of Fluids: Thermal Conductivity, Viscosity, and Diffusion Coefficient*, Cindas Data Series on Material Properties, vol. I-1, Hemisphere, New York, NY, USA, 1988.

[33] M. P. Beck, T. Sun, and A. S. Teja, "The thermal conductivity of alumina nanoparticles dispersed in ethylene glycol," *Fluid Phase Equilibria*, vol. 260, no. 2, pp. 275–278, 2007.

[34] S. H. Kim, S. R. Choi, and D. Kim, "Thermal conductivity of metal-oxide nanofluids," *Journal of Heat Transfer*, vol. 129, no. 3, pp. 298–307, 2007.

[35] C. S. Jwo, T. P. Teng, C. J. Hung, and Y. T. Guo, "Research and development of measurement device for thermal conductivity of nanofluids," *Journal of Physics: Conference Series*, vol. 13, pp. 55–58, 2005.

[36] J. Holman, *Heat Transfer*, McGraw-Hill, New York, NY, USA, 9th edition, 2002.

[37] A. Wheeler and A. Ganji, *Introduction to Engineering Experimentation*, Prentice Hall, Upper Saddle River, NJ, USA, 1996.

[38] S. Lee, S. Choi, S. Li, and J. A. Eastman, "Measuring thermal conductivity of fluids containing oxide nanoparticles," *Journal of Heat Transfer*, vol. 121, no. 2, pp. 280–288, 1999.

[39] D. Yoo, K. S. Hong, and H.-S. Yang, "Study of thermal conductivity of nanofluids for the application of heat transfer fluids," *Thermochimica Acta*, vol. 455, no. 1-2, pp. 66–69, 2007.

[40] J. Ma, *Thermal conductivity of fluids containing nanometer sized particles*, M.S. thesis, Department of Mechanical Engineering, MIT, 2006.

[41] X. Wang, X. Xu, and S. Choi, "Thermal conductivity of nanoparticle-fluid mixture," *Journal of Thermophysics and Heat Transfer*, vol. 13, no. 4, pp. 474–480, 1999.

[42] E. V. Timofeeva, A. N. Gavrilov, J. M. McCloskey, et al., "Thermal conductivity and particle agglomeration in alumina nanofluids: experiment and theory," *Physical Review E*, vol. 76, no. 6, Article ID 061203, 2007.

[43] M. von Smoluchowski, "Versuch einer mathematischen theorie der koagulationskinetic kolloider losunger," *Zeitschrift für Physikalische Chemie*, vol. 92, p. 129, 1917.

Hindawi Publishing Corporation
Advances in Mechanical Engineering
Volume 2010, Article ID 795478, 9 pages
doi:10.1155/2010/795478

Review Article

Heat Transfer Mechanisms and Clustering in Nanofluids

Kaufui V. Wong and Michael J. Castillo

Department of Mechanical and Aerospace Engineering, University of Miami, Coral Gables, FL 33124, USA

Correspondence should be addressed to Kaufui V. Wong, kwong@miami.edu

Received 18 May 2009; Accepted 24 November 2009

Academic Editor: Yogesh Jaluria

This paper surveys heat transfer in nanofluids. It summarizes and analyzes the theories regarding heat transfer mechanisms in nanofluids, and it discusses the effects of clustering on thermal conductivity. The heat transfer associated with conduction is presented through various experiments followed by a discussion of the theories developed. Relationships between thermal conductivity and various factors such as temperature, concentration, and particle size are also displayed along with a discussion on clustering. There is a brief discussion on convection where the number of studies is limited. There is research currently being performed on the manipulation of the properties governing the thermal conductivity of nanofluids—the particle size, shape, and surface area. Other factors that affect heat transfer are the material of the nanoparticle, particle volume concentration, and the fluid used. Although the interest in this relatively new class of fluids has generated many experimental studies, there is still disagreement over several aspects of heat transfer in nanofluids, primarily concerning the mechanisms behind the increased thermal conductivity. Although nanoparticles have greatly decreased the risks, there is still evidence of unwanted agglomeration which causes erosion and affect the overall conductivity. Research is currently being conducted to determine how to minimize this unwanted clustering.

1. Introduction

The growth of technology found in high-tech industries, such as microelectronics, transportation, and manufacturing, has created a cornucopia of ideas that would have wide ranging effects on many obstacles facing today's scientific world including energy efficiency, pollution, and reusability. However, there are many factors hindering further development in these industries, one being the ability to rapidly cool the products being used. Cooling is necessary for maintaining the operational performance and reliability of new products, and as a result of increased heat loads and heat fluxes caused by the increase in power and decrease in feature sizes present in new products, the demand for a more efficient cooling process has increased dramatically in the last decade. Consequently, more companies are beginning to invest more capital into the research of more efficient heat transfer processes.

The conventional method for enhancing heat transfer in a thermal system consists of increasing the heat transfer surface area as well as the flow velocity of the working fluid [1]. The dispersion of solid nanoparticles in heat transfer fluids is a relatively new method. Extended surfaces such as fins and microchannels (width $<100\,\mu$m) have already been used to increase the heat transfer surface area. Their performance in effectively removing as much as $1000\,\text{W/cm}^2$ has shown a great improvement in the area of cooling. However, further development of this technology is at a standstill because it has already been pushed to its achievable limits. Thus, attention is now turning towards the dispersion of solid particles in fluids.

Since Maxwell's theories in 1873, scientists have attempted to increase the thermal conductivity of a fluid through the combination of solid particles and a heat transfer fluid. Although liquid cooling is prevalent today (i.e., in automobiles and in some microelectronics), it has been severely limited because of the inherent poor thermal conductivity of traditional heat transfer fluids. Efforts to increase this fundamental limit began with the dispersion of millimeter- or micrometer-sized particles in fluids. Although this action increased the thermal conductivity of the heat transfer fluid, it was not practical because the increase in

heat transfer required a large number of particles (>10% by volume). This often resulted in a significant pressure drop, thus requiring more pumping power. Furthermore, because of their size, these particles rapidly settled in the liquid, clogged microchannels, and caused wear in pipes, pumps, and bearings.

As technology turned to miniaturization and nanotechnology, the idea of nanofluids was developed at various institutions around the world (initial development was performed at Argonne National Laboratory, and much research is still carried out at this location). Coined by Stephen U. S. Choi in 1995, the term nanofluids (short for nanoparticle fluid suspension) is used to describe stable suspensions of nanoparticles (average size <100 nm) in traditional heat transfer fluids such as water, oil, or ethylene glycol [1]. Experimentation has shown significant improvement in the thermal conductivity of fluids containing oxide and metallic nanoparticles. With volume concentrations between 0.5% and 4%, nanofluids have shown an enhancement of 15%–40% of the thermal conductivity of the base fluid [2]. It has also been observed that nanoparticles stay suspended in the fluid longer than micrometer-sized particles, thus reducing the severity of the obstacles presented by the rapid settling of the particles (such as abrasion and clogging of pipes and microchannels).

Experiments, such as those found in references [3–10], are continuously being conducted to achieve a deeper understanding of the mechanisms behind the increase in thermal conductivity caused by these nanoparticle suspensions. In addition, the paper by Sandhu [11] declared the improved thermal conductivity of magnetic nanofluids. Philip et al. [12] showed that arranging the linear aggregation length from nano- to micron-scales, the thermal conductivity of the nanofluid was enhanced up to 216%, using 4.5 volume percentage of nanoparticles. Repeated magnetic cycling shows that the enhancement is reversible.

There has been a dramatic increase of interest in the field of nanofluids as shown by the exponential increase in the number of publications concerning the subject matter in the Science Citation Index (SCI) journals. Several businesses, corporations, and scientific institutions have begun research towards the common goal of achieving the highest possible thermal properties at the smallest possible concentration (preferably <1% by volume). Nanofluids have the potential of becoming compact, cost-effective liquid cooling systems in high-performance situations.

2. Conduction Heat Transfer in Nanofluids

Maxwell first proposed the idea of suspending metallic particles in conventional heat transfer fluids in 1873 [13]. He believed that the metallic particles (which have thermal conductivities that are significantly larger than that of liquids as shown in Figure 1) would increase the electrical and thermal conductivity of the fluids. This idea was carried on throughout the next century as scientists attempted to create a fluid with millimeter- and micrometer-sized particles that could be used for practical applications. However, even though their efforts showed that particles did increase the heat transfer properties of their base fluids, they could not overcome problems caused by the large size of the particles. It was not until the advent of nanotechnology that the thought of nanoparticles came about.

The idea of nanofluids created an influx of experimentation that has led to the knowledge that we have today. Though experiments have been carried out with nanoparticles formed from a wide array of materials including aluminum oxide (Al_2O_3), copper (Cu), copper oxide (CuO), gold (Au), silver (Ag), silicon carbide (SiC), titanium carbide (TiC), titanium oxide (TiO_2), and carbon nanotubes, the most common nanoparticles are Al_2O_3 and CuO [14]. The base fluids used most commonly are water, engine oil, and ethylene glycol. The nanofluids used in these experiments are created by mixing the base fluid and the nanoparticles together and then stabilizing the suspension.

Nanoparticles can be produced by either physical or chemical means. Current physical processes include mechanical grinding and the inert-gas-condensation technique pioneered by Granqvist and Buhrman. Presented in 1976, the latter technique involves evaporation in a temperature-regulated oven containing an inert gas [15]. Current chemical processes include chemical precipitation, chemical vapor deposition, microemulsions, spray pyrolisis, thermal spraying, and a sonochemical method for the production of iron nanoparticles [16]. The most common processes currently used in the production of metal nanoparticles include mechanical milling, inert-gas-condensation technique, chemical precipitation, spray pyrolisis, and thermal spraying [2]. Although nanoparticles are constantly being produced in small volumes for experimental needs, there is still research being conducted towards achieving more cost-efficient production processes in order to begin the move towards large-scale production.

There are currently two methods used to disperse nanoparticles in the base fluid: the two-step technique and the single-step technique. The *two-step method* involves making the nanoparticles first, by either physical or chemical means and then dispersing them into the base fluid. In combination with the inert-gas-condensation technique (which has been proven to be a viable process for producing bulk quantities of nanopowders), the two-step method can be used to initiate the move towards commercialization by facilitating the mass production of nanofluids [17]. The *single-step method* involves simultaneously making and dispersing nanoparticles into the base fluid [1]. This method is favorable when using metallic nanoparticles—since the nanoparticles are placed in the base fluid as they are produced, this process helps prevent oxidation of the particles.

Because of the attractive van der Waals forces between the particles, they tend to agglomerate before they are dispersed in the liquid (especially if nanopowders are used); therefore, a means of separating the particles is necessary. Groups of particles will settle out of the liquid and decrease the conductivity of the nanofluid. Only by fully separating all nanoparticle agglomerates into their individual particles in the host liquid will a well-dispersed, stable suspension exist, and only under this condition will the optimum thermal conductivity exist. Xuan and Li [19] proposed different

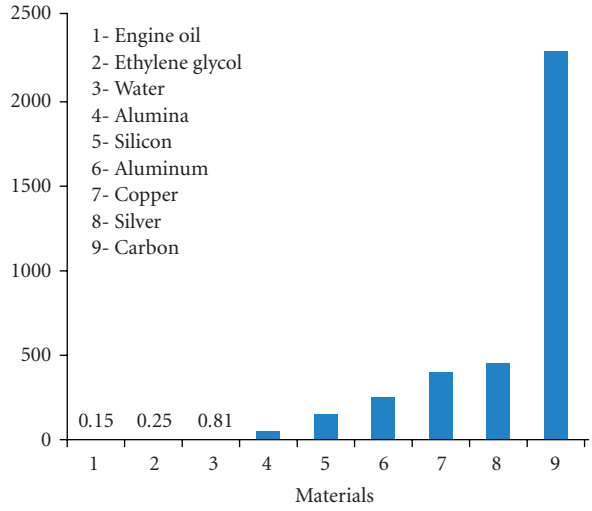

Figure 1: Thermal Conductivity of Typical Materials [18].

methods for the stabilization of the suspension including changing the pH value of the nanofluid, using dispersants, and using ultrasonic vibration. The most commonly used method is the ultrasonic vibration which has been relatively successful in eliminating agglomerated nanoparticles. There is certain hesitation when using dispersants because they can affect the chemical composition of the nanofluid and change the results. If dispersants are used, it cannot be clearly determined if the change in thermal conductivity was affected by the stabilizers placed in the fluid. This problem can be taken into account by comparing the nanofluid conductivity with that of the liquid with dispersant.

There are three methods commonly employed to measure the thermal conductivity of nanofluids: the transient hot wire method, temperature oscillation, and the steady-state parallel plate method [14]. The most commonly used method is the transient hot wire method which involves the use of small diameter wires that act as electrical resistance heaters and resistance thermometers [20]. The wire is heated by passing a current through it, and the rise in temperature over the time elapsed is measured. Since the wire is essentially wrapped in the liquid, the heat generated will be diffused into the liquid. The higher the thermal conductivity of the surrounding liquid, the lower the rise in temperature will be. To calculate the thermal conductivity of the surrounding liquid, a derivation of Fourier's law for radial transient heat conduction is used [1]. This differential equation for the conduction of heat is

$$\frac{\partial^2 T}{\partial x^2} + \frac{\partial^2 T}{\partial y^2} + \frac{\partial^2 T}{\partial z^2} = \frac{1}{\alpha} \cdot \frac{\partial T}{\partial t}. \quad (1)$$

Using a solution presented by Carslaw and Jaeger [21], the conductivity of a solution can be expressed as

$$\frac{q}{4\pi(T_2 - T_1)} \cdot \ln \frac{t_2}{t_1}, \quad (2)$$

where T_1 and T_2 represent the temperature of the heat source at times t_1 and t_2, respectively.

Many experiments have been performed using nanofluids, and although the results vary, they show an amplification of the thermal conductivity of the base fluid. Observations show four important characteristics of nanofluids:

(i) increased thermal conductivity at low nanoparticle concentrations,

(ii) linear relationship between thermal conductivity and concentration,

(iii) thermal conductivity being strongly dependent on temperature,

(iv) thermal conductivity being strongly dependent on the size of the particles used.

As a result of debates as to why these characteristics are present in nanofluids, various theories have been developed.

Lee et al. [22] measured the thermal conductivity of nanofluids using CuO and Al_2O_3 nanoparticles and water and ethylene glycol as the base fluids. Results showed an enhancement in the thermal conductivity of ethylene glycol of more than 20% at 4% volume fraction of CuO nanoparticles. Further experimentation revealed that the thermal conductivity increased as the volume concentration of nanoparticles was increased; thus, it was determined that the thermal conductivity of nanofluids was dependent on the thermal conductivity of both the particles and the base fluid in most ranges of k_p/k_0, where k_p is the conductivity of the particleand k_0 is the conductivity of the base fluid. For large values of k_p/k_0, the later statement may not be true. Although the thermal conductivity of the nanofluid is always greater than that of the base fluid without nanoparticles, this increase will be different for each base fluid.

Xie et al. [23] measured the thermal conductivity of nanofluids containing Al_2O_3 nanoparticles. They also investigated the effects of the pH value of the suspension and the specific surface area (SSA) of the dispersed particles. In accordance with the previous results, the thermal conductivity of the fluid was enhanced with the addition of the nanoparticles. However they also noted that the thermal conductivity increased as the difference between the pH value and the isoelectric point (pH value at which there is no electric charge) of Al_2O_3 increased and that the enhancements were highly dependent on the specific surface area of the nanoparticles. When compared to theoretical models, the measured thermal conductivity was much higher than the calculated values. A relationship between temperature and thermal conductivity was later presented by Das et al. [24]. In this study, not only it was determined that the thermal conductivity increased with an increase in temperature, but also it was shown that nanofluids composed of smaller particles experienced a greater enhancement than with larger particles. One possible explanation for this could be attributed to the Brownian motion of the particles in the fluid. Since temperature represents the overall kinetic energy of the particles, an increase in temperature will cause increased motion in the particles. It is easier for smaller particles to move; therefore, smaller particles will display a higher level of Brownian motion than larger particles. This

results in greater heat conduction among smaller particles as the temperature is increased.

Results from these various experiments may have varied, but they all showed that the thermal conductivity of a fluid containing nanoparticles was greater than that of a base fluid with no particle suspension. Moreover, it was shown that the thermal conductivity was affected by factors such as temperature, particle size, and pH level. Several theoretical models have been proposed to explain the behavior of nanoparticles. Many of these models can be categorized as either static or dynamic models [22]. Static models assume that the nanoparticles are stationary in the base fluid, forming a composite material. In these models, the thermal properties of nanofluids are predicted through conduction-based models such as that of Maxwell. One such model is the modified Maxwell theory of Hamilton and Crosser [25] which gives the enhancement of thermal conductivity as

$$k_{\text{eff}} = k_0 \cdot \frac{k_p + (n-1)k_0 - (n-1)\varepsilon\left(k_0 - k_p\right)}{k_p + (n-1)k_0 + \varepsilon\left(k_0 - k_p\right)}, \quad (3)$$

$$n = \frac{3}{\psi}, \quad (4)$$

where k_{eff} is the effective conductivity, k_p is the conductivity of the particle, k_0 is the conductivity of the base fluid, ε is the particle volume fraction, n is the particle shape factor, and ψ is the sphericity of the particles [1]. This model was in good agreement with experimental data obtained with the use of Al_2O_3 nanoparticles in a nanofluid, but it was not able to accurately predict the thermal conductivity of nanofluids containing CuO nanoparticles. It should be noted that in (3) the effective thermal conductivity is independent of the thermal conductivity of the particle as the ratio of k_p/k_0 becomes large.

Dynamic models assume that nanoparticles are in constant, random motion in the base fluid (i.e., Brownian motion), as shown in Figure 2.

In the dynamic models, it is believed that this random motion may be the main cause of the increased thermal properties associated with nanofluids. Taking Brownian motion to be a key mechanism in the thermal properties of nanofluids, Jang and Choi [26] developed a model that portrayed the relationship between conductivity, temperature, concentration, and particle size. However, there is disagreement with the assumption that random motion plays a key role in the transfer of heat in a nanofluid. Keblinski et al. [27] proposed an explanation of four possible factors for the heat transfer mechanism in nanofluids one of which was Brownian motion. However, the study concluded that the movement of nanoparticles due to Brownian motion was too slow in transporting heat through a fluid. To travel from one point to another, a particle moves a large distance over many different paths in order to reach a destination that may be a short distance from the starting point. Therefore, the random motion of particles, no matter how agitated or energetic they may be, cannot be a key factor in the improvement of heat transfer. Jang and Choi [26] also came to a similar conclusion. Here, it was determined that the collision between nanoparticles due to random motion was a very slow process and could, therefore, be neglected in the calculation of thermal conductivity.

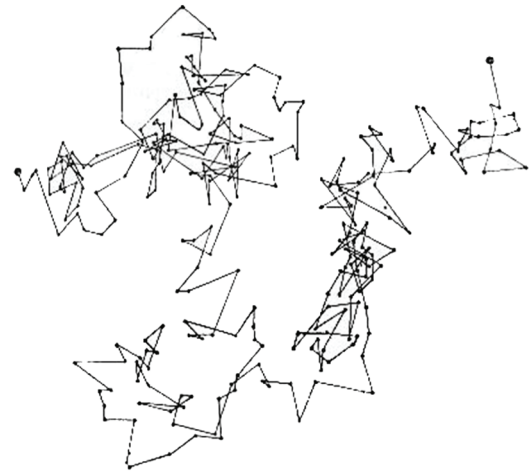

Figure 2: Interpretation of Brownian Motion [28].

Although they contributed to the idea that collisions resulting from Brownian motion did not contribute to the overall conduction of heat, Jang and Choi [26] were able to develop a dynamic model that takes into account convection heat transfer induced by Brownian nanoparticles. The general expression derived in this study introduced four modes of energy transport in nanofluids:

(i) collision between base fluid molecules (i.e., thermal conductivity of base fluid),

(ii) thermal diffusion in nanoparticles in fluids,

(iii) collision between nanoparticles due to Brownian motion (neglected because it is a very slow process),

(iv) thermal interactions of dynamic nanoparticles with base fluid molecules (once overlooked, this mode is now considered to be a key factor in the relationship between conductivity, temperature, and particle size).

The major aspect of this model was the introduction of the idea that nanoparticles can produce a convection-like effect in a fluid. The thermal conductivity for their model is given by

$$k_{\text{eff}} = k_{\text{Bf}}(1-f) + k_{\text{nano}} f + 3C_1 \frac{d_{\text{Bf}}}{d_{\text{nano}}} k_{\text{Bf}} \text{Re}_{d_{\text{nano}}}^2 \text{Pr} f, \quad (5)$$

where k_{eff} is the effective thermal conductivity of the nanofluid, k_{Bf} is the base fluid conductivity, f is the volume fraction of the nanoparticles, k_{nano} is the thermal conductivity of the nanoparticles, C_1 is an empirical constant, d_{Bf} is the diameter of the base fluid molecule, and d_{nano} is the diameter of a nanoparticle [1]. $\text{Re}_{d_{\text{nano}}}$ is the Reynolds number defined by

$$\text{Re}_{d_{\text{nano}}} = \frac{\overline{C}_{\text{R.M.}} d_{\text{nano}}}{\nu}, \quad (6)$$

where v is the dynamic viscosity of the base fluid, and $\overline{C}_{R.M.}$ is the random motion velocity of nanoparticles defined by

$$\overline{C}_{\text{R.M.}} = \frac{D_0}{I_{Bf}}, \tag{7}$$

where I_{Bf} is the mean-free path of a base fluid molecule. D_0 is the nanoparticle diffusion coefficient given by

$$D_0 = \frac{k_b T}{3\pi\mu d_{\text{nano}}}, \tag{8}$$

where μ is the viscosity of the base fluid, T is the temperature of the base fluid, and k_b is the Boltzmann constant. The predictions presented by this model are in excellent agreement with temperature-dependent conductivity data from experiments involving nanofluids containing Al_2O_3 nanoparticles. Models derived from Maxwell's equations fail to correlate with this type of experimental data.

Another model developed by Kumar et al. [29] involves the combination of the stationary particle model and the moving particle model. The stationary particle model looks at the increased surface area as the particle size decreases. By assuming two parallel paths of heat flow (one through base fluid molecules and the other through the nanoparticles), this model shows the linear dependence of thermal conductivity on particle concentration and the inverse dependence of thermal conductivity on the size of the particle. The moving particle model accounts for the temperature effect and is derived from the Stokes-Einstein formula. The effective thermal conductivity of the nanofluids, k_{eff}, for this model is given by

$$k_{\text{eff}} = k_m \left[1 + \frac{k_p \varepsilon r_m}{k_m (1-\varepsilon) r_p} \right], \tag{9}$$

where k_m is the base fluid conductivity, ε is the nanoparticle volume fraction, r_m is the radius of the base fluid molecules, and r_p is the radius of the nanoparticles. The nanoparticle's thermal conductivity, k_p, is defined as.

$$k_p = c\overline{u}_p. \tag{10}$$

The mean velocity of the nanoparticle $\overline{u}_p$ is derived from the Stokes-Einstein formula

$$\overline{u}_p = \frac{2k_b T}{\left(\pi \eta d_p^2\right)}, \tag{11}$$

where T is the fluid temperature, η is the dynamic viscosity of the fluid, and d_p is the diameter of the nanoparticle. The combination of the stationary particle model and the moving particle model shows the dependence of thermal conductivity on particle size, concentration, and temperature. Although this model correlates with the experimental data for nanofluids containing gold at small concentrations, there is a discrepancy in the stationary particle model. It has been pointed out that if the radius of the nanoparticles is larger than that of the liquid molecules, then the calculated thermal conductivity for the nanofluid will equal that of the base fluid, an unrealistic situation. Therefore, when using this model, an unphysical assumption that the mean-free path of a nanoparticle is on the order of 1 cm is made in the moving particle model [29]. There are still some issues over the benefits of this model, and as a result, it is the source of some debates today concerning the dynamic model.

The influence of particle anisotropy on the effective thermal conductivity of a suspension was experimentally studied by Cherkasova and Shan [30]. Suspensions of micron-sized, silicon-carbide particles with varying aspect-ratio distributions were prepared and measured. It was shown that the conductivity of the silicon-carbide suspensions can be quantitatively predicted by the effective medium theory presented by Nan et al. [31], as long as the volume-weighted aspect ratio of the particles is used.

The effect of Kapitza resistance between the particle and fluid can significantly impact the effective thermal conductivity of nanofluids. This effect was included into the model by Nan et al. [31], which predicted the experimental data of carbon nanotube suspensions reasonably well. Ju and Li [32] and Xue [33] also presented models for the effective thermal conductivities of carbon nanotube-based mixtures with an interfacial thermal resistance effect.

References [34, 35] discuss experiments where the interfacial layers of nanoparticles were examined. Document [36] discusses the relationship between temperature, particle size, and the thermal conductivity of the nanofluids examined. The survey done here does not include any work involving synthetic nanofluids, which form a class by themselves [37–39].

3. Convective Heat Transfer in Nanofluids

If nanofluids can improve the heat transfer coefficient of heat exchangers and energy systems, then they can aid in reducing the size of such systems while leading to increased energy and fuel efficiencies. Nanofluid convective heat transfer research may be classified by fluid conditions of laminar flow, turbulent flow, and pool boiling. The number of studies in these areas is limited, with the smallest number of studies having been reported in the last class of pool boiling.

Works in laminar flow include references [40–44]. Some of the works show heat transfer enhancements for laminar flow with different particle types (alumina and copper oxide) and sizes. Nanofluid heat transfer results for multiwalled carbon nanotubes (MWCNTs) show excellent heat transfer and thermal conductivity enhancement [42]. The results published by Yang et al. [44] displayed a heat transfer enhancement trend that is opposite to that for thermal conductivity—there is a drop in enhancement with increased temperature. But the temperature range studied is small, and the temperature dependency is not strong. More test data needs to be obtained before any definite conclusions can be drawn.

Heat transfer enhancements in turbulent flow of nanofluids include references [45–48]. The studies were performed on water-based nanofluids containing alumina, titanium oxide, copper particles, and amorphous carbonic nanoparticles. There seems to be a consensus that

the Reynolds number has little or no effect on the enhancement of heat transfer. Furthermore, the heat transfer improvement increased as the particle volume concentration was increased.

Putra et al. [49] investigated the convection of Al_2O_3 and CuO in water-based nanofluids. It was discovered that the natural convection of nanofluids was less intense than that of the base fluid. Moreover, it deteriorated as the particle density and concentration were increased. Smaller particles experienced even worse convective heat transfer because the particle density increases as the particle size decreases. However, Khanafer et al. [50] developed a model for the convective heat transfer of nanofluids that produced different results. With the assumption that the base fluid and the nanoparticles were in thermal equilibrium and flowed at the same velocity (i.e., nanofluid is in single phase), it was shown that the heat transfer rate increased as the particle volume fraction increased. Another model proposed by Kim et al. [51] introduced a factor f to include the effect of the thermal conductivity ratio between the nanoparticles and the base fluid, the shape factor and volume fraction of particles, and the ratio of density and heat capacity of nanoparticles to the base fluid. Results from this model showed that the amount of heat transfer in the nanofluid increased as the particle volume fraction was increased.

It is evident that the results of Kim and Khanafer contradict the results of Putra. Possible explanations for these differences could be dependent on the assumptions made in each model. Before nanofluids can be introduced to industrialized applications, there must be a better understanding of convection heat transfer and its effects on the overall thermal conductivity of the nanoparticle suspension.

4. Clustering in Nanofluids

One of the main obstacles encountered in microfluid experiments was the agglomeration of particles. Even though research, such as that documented in [22, 23], shows a substantial increase in the thermal conductivity of the base fluid with the addition of nanoparticles, the movement towards practical applications has been hampered by the rapid settling of the nanoparticles. The settling of particles not only decreased the overall heat transfer of the fluid (by decreasing the effective surface area used for heat transfer), but also led to the abrasion of surfaces, clogging of microchannels, and a decrease in pressure—which resulted in an increase in pumping power [14].

Although nanosized particles have greatly reduced the problem of agglomerated particles, it still occurs and can hinder the thermal conductivity of the nanofluid, especially at concentrations over 5%—agglomeration is more apparent when using oxide nanoparticles because they require a higher volume concentration compared to metallic nanoparticles in order to achieve the same thermal conductivity enhancement [2]. The tendency of particles to group together before they are dispersed in the fluid is due to the van der Waals forces. This is particularly seen in metallic particles since dipoles can occur easily in the molecules of these particles. The creation of dipoles prompts the attraction of other dipoles in the vicinity. The van der Waals forces stem from the attraction of these dipoles, which can be induced even in neutral particles. This attractive force is considered to be the main culprit behind the agglomeration of particles, especially in nanopowders.

To alleviate this problem, there have been various proposals for the manufacture and dispersion of nanoparticles in fluids. One proposal involves adding surface treatments to the nanoparticles. It was seen that when copper nanoparticles were coated with a 2–10 nm thick organic layer a stable suspension would be achieved in ethylene glycol [16]. There is research currently being conducted towards improving the two-step process to produce well-dispersed nanofluids. Moreover, there exist a few one-step processes that result in nanoparticles being uniformly dispersed and stably suspended in the base fluid. One such method involves condensing copper nanopowders directly from the vapor phase into flowing ethylene glycol in a vacuum chamber [52]. Documents [53–55] also show stable, well-dispersed suspensions in nanofluids containing TiO2, CuO, and Cu. In these experiments, a one-step process called submerged arc nanoparticle synthesis was used to create the nanoparticles.

Various techniques have been implemented to reduce the clustering of particles once they are in the fluid [56, 57]. Usually, they involve some sort of agitation within the nanofluid to separate the clusters into individual particles and keep them from settling. These methods include the use of dispersants, changing the pH value of the base fluid, and using ultrasonic vibration to excite the particles [6]. Among these methods, the most commonly used ones are ultrasonic vibration and the use of dispersants. Both techniques are relatively effective, but when using dispersants, the amount added to the fluid must be a very low percentage (usually 1% or less). This is done so as to minimize its effects on the thermal conductivity of the nanofluid.

However, it should be noted that loose particle chains may be responsible for some of the high thermal conductivities of nanofluids; see Prasher et al. [58].

The Argonne National Laboratory also developed the single-step and two-step processes for the dispersion of nanoparticles in a fluid [1]. The single-step process consists of simultaneously making and dispersing the particles in the fluid. The two-step method separates the manufacture and dispersion of particles into two steps (particles are manufactured first and then dispersed into the base fluid). The two-step process is the more commonly used method and is usually used in conjunction with ultrasonic vibration to reduce the amount of clustered particles in the fluid.

Analysis of the reviewed literature shows that there is still no conclusive theory concerning the prevention of clustering in the nanoparticle suspensions. Before using nanofluids in practical applications, the problem of clustering must be consistently kept to a minimum. When looking at long-term effects, clustering of the particles will eventually cause a decrease in the thermal conductivity of the nanofluid and may also cause wear in the pipes or pumps through which it is flowing. Therefore, nanofluids cannot be used in systems designed for long-term use until this problem

is solved. Otherwise, the use of nanofluids may decrease the life expectancy of a system, even if it improves the overall efficiency. In the mean time, an optimization and design problem persists when nanofluids are used in the field.

5. Conclusion

Even though nanofluids are still relatively new, they have caused a dramatic increase in the interest of ultra-high performance cooling. Experiments are continuously being conducted to achieve a deeper understanding of the mechanisms behind the increase in thermal conductivity caused by these nanoparticle suspensions. As a result, various conclusions have been drawn regarding the characteristics of nanofluids including the relationship between thermal conductivity, particle size, nanoparticle concentration, and temperature.

Heat can be transferred through conduction, convection, and radiation. There is a more thorough understanding of conduction in nanofluids than the other two, and various models have been formulated to predict the thermal behavior of nanofluids. Static models investigate the thermal conductivity of a nanofluid assuming a stationary suspension of particles in the base fluid. This allows for the use of derived forms of Maxwell's equation. Dynamic models assume that the particles are in constant, random motion while dispersed in the fluid. These models are the source of much debate today over the involvement of Brownian motion in the thermal conductivity of nanofluids. While some scientists believe that this random motion is the source of conduction in nanofluids, studies show that it is insignificant compared to other factors because the transfer of heat is a very slow process in Brownian motion. However, some researchers were able to develop a dynamic model that portrayed four modes of energy transport. The major aspect of this model was the convection heat-transfer induced by Brownian motion in particles. Results from this model correlated excellently with experimental data of nanofluids containing aluminum oxide particles.

Convection heat transfer is recognized within nanofluids, but there is not enough research results published to develop a model that fully explains this behavior in nanofluids. Furthermore, several of the research papers available seem to contradict each other as some data shows an increase in convection as the particle volume fraction is increased, while other data shows deterioration in convective heat transfer as the particle density and concentration were increased.

Clustering still poses a problem in nanofluids even though the occurrence of agglomeration has decreased from the previous micrometer-sized particles suspensions. Various methods are currently used to keep particles from clustering together, but in the long run, it is inevitable. Clustering is a problem that must be solved before nanofluids can be considered for long-term practical uses. Although the increase in thermal conductivity would increase the efficiency of the systems where nanofluids are used, the life of the system may be decreased over time if particles begin to form clusters.

Nanofluids have the potential to open the doors to major advancements in many high-tech industries where limits on cooling have posed limits on innovation. Since all other cooling options have been exhausted, nanofluids are the only option left with the possibility of increasing heat transfer capabilities of current systems. However, a full understanding of the mechanisms behind the enhancement of thermal conductivity in nanofluids has not been reached and there is still disagreement between some of the experimental results. This lack of agreement has led to the generation of various models. Once a general model that fully explains the behavior of nanoparticle suspensions has been developed, steps can be taken towards practical uses. Moreover, better techniques for the dispersion of particles in fluids must be created so as to minimize clustering. When these objectives have been reached, nanofluids will enter the practical arenas of science in a more meaningful way.

At the present time, there is quite an amount of work going on to create synthetic nanofluids for various applications. This is evidenced by the number of patented nanofluids. However, the literatures on these are not generally available.

References

[1] S. K. Das, S. U. S. Choi, W. Yu, and T. Pradeep, *Nanofluids: Science and Technology*, John Wiley & Sons, Hoboken, NJ, USA, 2008.

[2] W. Yu, D. M. France, J. L. Routbort, and S. U. S. Choi, "Review and comparison of nanofluid thermal conductivity and heat transfer enhancements," *Heat Transfer Engineering*, vol. 29, no. 5, pp. 432–460, 2008.

[3] D. J. Jeffrey, "Conduction through a random suspension of spheres," *Proceedings of the Royal Society of London. Series A*, vol. 335, pp. 355–367, 1973.

[4] J. Koo and C. Kleinstreuer, "A new thermal conductivity model for nanofluids," *Journal of Nanoparticle Research*, vol. 6, no. 6, pp. 577–588, 2004.

[5] B.-X. Wang, L.-P. Zhou, and X.-F. Peng, "A fractal model for predicting the effective thermal conductivity of liquid with suspension of nanoparticles," *International Journal of Heat and Mass Transfer*, vol. 46, no. 14, pp. 2665–2672, 2003.

[6] Y. Xuan and Q. Li, "Heat transfer enhancement of nanofluids," *International Journal of Heat and Fluid Flow*, vol. 21, no. 1, pp. 58–64, 2000.

[7] T.-K. Hong, H.-S. Yang, and C. J. Choi, "Study of the enhanced thermal conductivity of Fe nanofluids," *Journal of Applied Physics*, vol. 97, no. 6, Article ID 064311, 4 pages, 2005.

[8] S. A. Putnam, D. G. Cahill, P. V. Braun, Z. Ge, and R. G. Shimmin, "Thermal conductivity of nanoparticle suspensions," *Journal of Applied Physics*, vol. 99, no. 8, Article ID 084308, 6 pages, 2006.

[9] S. M. S. Murshed, K. C. Leong, and C. Yang, "Enhanced thermal conductivity of TiO_2—water based nanofluids," *International Journal of Thermal Sciences*, vol. 44, no. 4, pp. 367–373, 2005.

[10] S. M. S. Murshed, K. C. Leong, and C. Yang, "A combined model for the effective thermal conductivity of nanofluids," *Applied Thermal Engineering*, vol. 29, no. 11-12, pp. 2477–2483, 2009.

[11] A. Sandhu, "Magnetic nanofluids: chain reaction," *Nature Nanotechnology*. In press.

[12] J. Philip, P. D. Shima, and B. Raj, "Nanofluid with tunable thermal properties," *Applied Physics Letters*, vol. 92, no. 4, Article ID 043108, 2008.

[13] J. C. Maxwell, *Treatise on Electricity and Magnetism*, Clarendon Press, Oxford, UK, 1873.

[14] V. Trisaksri and S. Wongwises, "Critical review of heat transfer characteristics of nanofluids," National Research Council of Thailand (NRCT), 2006, http://www.energy-based.nrct.go.th/Article/Ts-3%20critical%20review%20of%20heat%20transfer%20characteristics%20of%20nanofluids.pdf.

[15] C. G. Granqvist and R. A. Burhman, "Ultrafine metal particles," *Journal of Applied Physics*, vol. 47, no. 5, pp. 2200–2219, 1976.

[16] K. S. Suslick, M. Fang, and T. Hyeon, "Sonochemical synthesis of iron colloids," *Journal of the American Chemical Society*, vol. 118, no. 47, pp. 11960–11961, 1996.

[17] J. M. Romano, J. C. Parker, and Q. B. Ford, "Application opportunities for nanoparticles made from the condensation of physical vapors," in *Proceedings of the International Conference on Powder Metallurgy and Particulate Materials*, vol. 2, pp. 12–13, Chicago, Ill, USA, June 1997.

[18] M. Kostic, "Nanofluids: Advanced Flow and Heat Transfer Fluids," Northern Illinois University, 2004, http://www.kostic.niu.edu/DRnanofluids.

[19] Y. Xuan and Q. Li, "Heat transfer enhancement of nanofluids," *International Journal of Heat and Fluid Flow*, vol. 21, no. 1, pp. 58–64, 2000.

[20] "Thermal Conductivity of Liquids and Gases," National Institute of Standards and Technology (NIST), http://fluidproperties.nist.gov/thermal.html.

[21] H. S. Carslaw and J. C. Jaeger, *Conduction of Heat in Solids*, Oxford University Press, New York, NY, USA, 1967.

[22] S. Lee, S. U.-S. Choi, S. Li, and J. A. Eastman, "Measuring thermal conductivity of fluids containing oxide nanoparticles," *Journal of Heat Transfer*, vol. 121, no. 2, pp. 280–289, 1999.

[23] H. Xie, J. Wang, T. Xi, Y. Liu, F. Ai, and Q. Wu, "Thermal conductivity enhancement of suspensions containing nanosized alumina particles," *Journal of Applied Physics*, vol. 91, no. 7, pp. 4568–4572, 2002.

[24] S. K. Das, N. Putra, P. Thiesen, and W. Roetzel, "Temperature dependence of thermal conductivity enhancement for nanofluids," *Journal of Heat Transfer*, vol. 125, no. 4, pp. 567–574, 2003.

[25] R. L. Hamilton and O. K. Crosser, "Thermal conductivity of heterogeneous two-component systems," *Industrial and Engineering Chemistry Fundamentals*, vol. 1, no. 3, pp. 187–191, 1962.

[26] S. P. Jang and S. U. S. Choi, "Role of Brownian motion in the enhanced thermal conductivity of nanofluids," *Applied Physics Letters*, vol. 84, no. 21, pp. 4316–4318, 2004.

[27] P. Keblinski, S. R. Phillpot, S. U. S. Choi, and J. A. Eastman, "Mechanics of heat flow in suspensions of nano-sized particles (nanofluids)," *International Journal of Heat and Mass Transfer*, vol. 307, pp. 313–317, 2003.

[28] K. Hoon and Y. K. Lee, "Brownian motion of a microscopic particle," http://www.hasdeu.bz.edu.ro/softuri/fizica/mariana/Termodinamica/Brownian_1/files/report.br1.

[29] D. H. Kumar, H. E. Patel, V. R. R. Kumar, T. Sundararajan, T. Pradeep, and S. K. Das, "Model for heat conduction in nanofluids," *Physical Review Letters*, vol. 93, no. 14, Article ID 144301, 2004.

[30] A. S. Cherkasova and J. W. Shan, "Particle aspect-ratio effects on the thermal conductivity of micro- and nanoparticle suspensions," *Journal of Heat Transfer*, vol. 130, no. 8, Article ID 082406, 7 pages, 2008.

[31] C.-W. Nan, R. Birringer, D. R. Clarke, and H. Gleiter, "Effective thermal conductivity of particulate composites with interfacial thermal resistance," *Journal of Applied Physics*, vol. 81, no. 10, pp. 6692–6699, 1997.

[32] S. Ju and Z. Y. Li, "Theory of thermal conductance in carbon nanotube composites," *Physics Letters A*, vol. 353, no. 2-3, pp. 194–197, 2006.

[33] Q. Z. Xue, "Model for the effective thermal conductivity of carbon nanotube composites," *Nanotechnology*, vol. 17, no. 6, pp. 1655–1660, 2006.

[34] W. Yu and S. U. S. Choi, "The role of interfacial layers in the enhanced thermal conductivity of nanofluids: a renovated Maxwell model," *Journal of Nanoparticle Research*, vol. 5, no. 1-2, pp. 167–171, 2003.

[35] W. Yu and S. U. S. Choi, "The role of interfacial layers in the enhanced thermal conductivity of nanofluids: a renovated Hamilton-Crosser model," *Journal of Nanoparticle Research*, vol. 6, no. 4, pp. 355–361, 2004.

[36] C. H. Chon, K. D. Kihm, S. P. Lee, and S. U. S. Choi, "Empirical correlation finding the role of temperature and particle size for nanofluid (Al_2O_3) thermal conductivity enhancement," *Applied Physics Letters*, vol. 87, no. 15, Article ID 153107, 3 pages, 2005.

[37] M.-S. Liu, M. C. C. Lin, I.-T. Huang, and C.-C. Wang, "Enhancement of thermal conductivity with carbon nanotube for nanofluids," *International Communications in Heat and Mass Transfer*, vol. 32, no. 9, pp. 1202–1210, 2005.

[38] F. D. S. Marquis and L. P. F. Chibante, "Improving the heat transfer of nanofluids and nanolubricants with carbon nanotubes," *JOM*, vol. 57, no. 12, pp. 32–43, 2005.

[39] L. Vekas and B. Doina, "Magnetic nanofluids, preparation, properties and some applications," in *Proceedings of the 1st Nanoforum Workshop*, Sinaia, Romania, October 2003.

[40] D. Wen and Y. Ding, "Experimental investigation into convective heat transfer of nanofluids at the entrance region under laminar flow conditions," *International Journal of Heat and Mass Transfer*, vol. 47, no. 24, pp. 5181–5188, 2004.

[41] S. Z. Heris, S. Gh. Etemad, and M. N. Esfahany, "Experimental investigation of oxide nanofluids laminar flow convective heat transfer," *International Communications in Heat and Mass Transfer*, vol. 33, no. 4, pp. 529–535, 2006.

[42] Y. Ding, H. Alias, D. Wen, and R. A. Williams, "Heat transfer of aqueous suspensions of carbon nanotubes (CNT nanofluids)," *International Journal of Heat and Mass Transfer*, vol. 49, no. 1-2, pp. 240–250, 2006.

[43] D. J. Faulkner, D. R. Rector, J. J. Davidson, and R. Shekarriz, "Enhanced heat transfer through the use of nanofluids in forced convection," in *Proceedings of the ASME International Mechanical Engineering Congress and Exposition (IMECE '04)*, pp. 219–224, Anaheim, Calif, USA, November 2004.

[44] Y. Yang, Z. G. Zhang, E. A. Grulke, W. B. Anderson, and G. Wu, "Heat transfer properties of nanoparticle-in-fluid dispersions (nanofluids) in laminar flow," *International Journal of Heat and Mass Transfer*, vol. 48, no. 6, pp. 1107–1116, 2005.

[45] B. C. Pak and Y. I. Cho, "Hydrodynamic and heat transfer study of dispersed fluids with submicron metallic oxide particles," *Experimental Heat Transfer*, vol. 11, no. 2, pp. 151–170, 1998.

[46] Y. Xuan and Q. Li, "Investigation on convective heat transfer and flow features of nanofluids," *Journal of Heat Transfer*, vol. 125, no. 1, pp. 151–155, 2003.

[47] D. Kim, Y. Kwon, Y. Cho, et al., "Convective heat transfer characteristics of nanofluids under laminar and turbulent flow conditions," *Current Applied Physics*, vol. 9, no. 2, supplement 1, pp. e119–e123, 2009.

[48] J. Buongiorno, "Convective transport in nanofluids," *Journal of Heat Transfer*, vol. 128, no. 3, pp. 240–250, 2006.
[49] N. Putra, W. Roetzel, and S. K. Das, "Natural convection of nano-fluids," *Heat and Mass Transfer*, vol. 39, no. 8-9, pp. 775–784, 2003.
[50] K. Khanafer, K. Vafai, and M. Lightstone, "Buoyancy-driven heat transfer enhancement in a two-dimensional enclosure utilizing nanofluids," *International Journal of Heat and Mass Transfer*, vol. 46, no. 19, pp. 3639–3653, 2003.
[51] J. Kim, Y. T. Kang, and C.-K. Choi, "Analysis of convective instability and heat transfer characteristics of nanofluids," *Physics of Fluids*, vol. 16, no. 7, pp. 2395–2401, 2004.
[52] J. A. Eastman, S. U. S. Choi, S. Li, W. Yu, and L. J. Thompson, "Anomalously increased effective thermal conductivities of ethylene glycol-based nanofluids containing copper nanoparticles," *Applied Physics Letters*, vol. 78, no. 6, pp. 718–720, 2001.
[53] H. Chang, T. T. Tsung, Y. C. Yang, et al., "Nanoparticle suspension preparation using the arc spray nanoparticle synthesis system combined with ultrasonic vibration and rotating electrode," *International Journal of Advanced Manufacturing Technology*, vol. 26, no. 5-6, pp. 552–558, 2005.
[54] C.-H. Lo, T.-T. Tsung, L.-C. Chen, C.-H. Su, and H.-M. Lin, "Fabrication of copper oxide nanofluid using submerged arc nanoparticle synthesis system (SANSS)," *Journal of Nanoparticle Research*, vol. 7, no. 2-3, pp. 313–320, 2005.
[55] C.-H. Lo, T.-T. Tsung, and L.-C. Chen, "Shape-controlled synthesis of Cu-based nanofluid using submerged arc nanoparticle synthesis system (SANSS)," *Journal of Crystal Growth*, vol. 277, no. 1–4, pp. 636–642, 2005.
[56] Q. Cao and J. Tavares, "Dual-Plasma Synthesis of Coated Nanoparticles and Nanofluids," November 2006, http://aiche.confex.com/aiche/2006/techprogram/P65561.HTM.
[57] S. M. S. Murshed, K. C. Leong, and C. Yang, "Thermophysical and electrokinetic properties of nanofluids—a critical review," *Applied Thermal Engineering*, vol. 28, no. 17-18, pp. 2109–2125, 2008.
[58] R. Prasher, P. Bhattacharya, and P. E. Phelan, "Brownian-motion-based convective-conductive model for the effective thermal conductivity of nanofluids," *Journal of Heat Transfer*, vol. 128, no. 6, pp. 588–595, 2006.

Hindawi Publishing Corporation
Advances in Mechanical Engineering
Volume 2010, Article ID 719406, 5 pages
doi:10.1155/2010/719406

Research Article

Is Classical Energy Equation Adequate for Convective Heat Transfer in Nanofluids?

Jing Fan and Liqiu Wang

Department of Mechanical Engineering, The University of Hong Kong, Pokfulam Road, Hong Kong

Correspondence should be addressed to Liqiu Wang, lqwang@hku.hk

Received 20 August 2009; Accepted 17 September 2009

Academic Editor: Oronzio Manca

To address whether the heat transfer in nanofluids still satisfies the classical energy equation, we theoretically examine the macroscale manifestation of the microscale physics in nanofluids. The microscale interaction between nanoparticles and base fluids manifests itself as thermal waves/resonance at the macroscale. The energy equation that governs the heat transfer in nanofluids is of a dual-phase-lagging type instead of the *postulated* and *commonly-used* classical energy equation. The interplays among diffusion, convection, and thermal waves/resonance enrich the heat transfer in nanofluids considerably.

1. Introduction

Choi coined the term "nanofluids" for the fluids with nanoelements (nanoparticles, nanotubes, or nanofibers) suspended in them [1]. Recent experiments on nanofluids have shown, for example, twofold increases in thermal conductivity [2], strong temperature dependence of thermal conductivity [3], substantial increases in convective heat transfer coefficient [4, 5], and threefold increases in critical heat flux (CHF) in boiling heat transfer [2, 3, 6]. State-of-the-art expositions of major advances on the synthesis, characterization, and application of nanofluids are available, for example, in [2, 3, 6–12]. These characteristics make them very attractive for a large number of industries such as transportation, electronics, defense, space, nuclear systems cooling, and biomedicine.

The study of nanofluids is still in its infancy [2, 3, 6–12]. The precise nature and mechanism of the significant improvement of thermal performance are still not known. There is also a lack of agreement between experimental results and between theoretical models. The fact that the enhancement in thermal properties comes from the presence of nanoparticles has directed research efforts nearly exclusively towards thermal transport at nanoscale. The classical conservation equations including the energy equation have been postulated as the macroscale model of nanofluid convective heat transfer but without adequate justification. Thermal conductivity and convective heat transfer coefficient are a macroscale phenomenological characterization of heat transfer and their measurements are not performed at the nanoscale, but rather at the macroscale. Therefore, interest should focus not only on what happens at the nanoscale but also on how the presence of nanoelements affects the heat transport at macroscale.

We attempt to examine whether the classical energy equation is adequate for describing convective heat transfer in nanofluids at macroscale based on a macroscale heat transfer model in nanofluids, which is rigorously developed by scaling-up the microscale model for the heat transfer in the nanoparticles and in the base fluids. The approach for scaling-up is the volume averaging [13–15] with help of multiscale theorems [15].

2. Macroscale Energy Equation

The microscale model for heat transfer in nanofluids is well known. It consists of the field equation and the constitutive equation. The field equation comes from the conservation laws of mass, momentum, and energy. The commonly-used

constitutive equation includes the Newton law of viscosity and the Fourier law of heat conduction [16].

For transport in nanofluids, the macroscale is a phenomenological scale that is much larger than the microscale and much smaller than the system length scale. Interest in the macroscale rather than the microscale comes from the fact that a prediction at the microscale is complicated due to the complex microscale structure of nanofluids, and also because we are usually more interested in large scales of transport for practical applications. Existence of such a macroscale description equivalent to the microscale behavior requires a good separation of length scales and has been well discussed in [15, 17].

To develop a macroscale model of heat transfer in nanofluids, the method of volume averaging starts with a microscale description. Both conservation and constitutive equations are introduced at the microscale. The resulting microscale field equations are then averaged over a representative elementary volume (REV), the smallest differential volume resulting in statistically meaningful local averaging properties, to obtain the macroscale field equations. In the process of averaging, the *multiscale theorems* [15] are used to convert integrals of gradient, divergence, curl, and partial time derivatives of a function into some combination of gradient, divergence, curl, and partial time derivatives of integrals of the function and integrals over the boundary of the REV.

Consider heat transfer in nanofluids with the continuous base fluid and the dispersed nanoparticle denoted by c- and d-phases, respectively. Note that the dispersed nanoparticles can be liquid droplets for general nanofluids [10, 12]. As a two-component mixture (base fluid + nanoparticles), its microscale model can be written as [18]

$$
\begin{aligned}
&\nabla \cdot \mathbf{v}_c = 0, \quad \text{in the } c\text{-phase},\\
&\rho_c \frac{\partial \mathbf{v}_c}{\partial t} + \rho_c \mathbf{v}_c \cdot \nabla \mathbf{v}_c\\
&\quad = -\nabla p_c + \rho_c \mathbf{g} + \mu_c \nabla^2 \mathbf{v}_c, \quad \text{in the } c\text{-phase},\\
&\left(\rho c_p\right)_c \frac{\partial T_c}{\partial t} + \left(\rho c_p\right)_c \mathbf{v}_c \cdot \nabla T_c\\
&\quad = \nabla \cdot (k_c \nabla T_c), \quad \text{in the } c\text{-phase},\\
&\nabla \cdot \mathbf{v}_d = 0, \quad \text{in the } d\text{-phase},\\
&\rho_d \frac{\partial \mathbf{v}_d}{\partial t} + \rho_d \mathbf{v}_d \cdot \nabla \mathbf{v}_d\\
&\quad = -\nabla p_d + \rho_d \mathbf{g} + \mu_d \nabla^2 \mathbf{v}_d, \quad \text{in the } d\text{-phase},\\
&\left(\rho c_p\right)_d \frac{\partial T_d}{\partial t} + \left(\rho c_p\right)_d \mathbf{v}_d \cdot \nabla T_d\\
&\quad = \nabla \cdot (k_d \nabla T_d), \quad \text{in the } d\text{-phase},\\
&\mathbf{v}_c = \mathbf{v}_d, \quad \text{at } A_{cd},\\
&T_c = T_d, \quad \text{at } A_{cd},\\
&\mathbf{n}_{dc} \cdot k_c \nabla T_c = \mathbf{n}_{dc} \cdot k_d \nabla \mathrm{T}_d, \quad \text{at } A_{cd}.
\end{aligned}
\tag{1}
$$

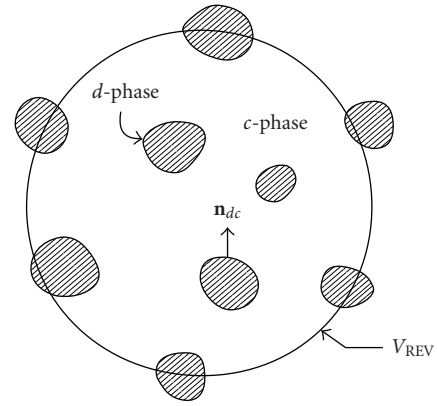

Figure 1: Representative elementary volume (REV).

Here $\mathbf{v}$ and T are the velocity and the temperature, respectively. ρ, c_p, k, p, μ, and $\mathbf{g}$ are the density, specific heat, thermal conductivity, pressure, viscosity, and gravitational acceleration, respectively. Subscripts c and d refer to the c- and d-phases, respectively. A_{cd} represents the area of the c-d interface contained in the REV, and $\mathbf{n}_{dc}$ is the outward-directed surface normal from the d-phase toward the c-phase, (Figure 1). To be thorough, we must also specify the initial conditions and the boundary conditions at the entrances and exits of the REV; however, we need not do so for our discussion.

Applying the volume averaging and multiscale theorems to scale-up the microscale model yields a macroscale model [12, 19], where the energy equation reads

$$
\begin{aligned}
&\varepsilon_c \left(\rho c_p\right)_c \frac{\partial \langle T_c \rangle^c}{\partial t} + \varepsilon_c \left(\rho c_p\right)_c \langle \mathbf{v}_c \rangle^c \cdot \nabla \langle T_c \rangle^c - \mathbf{u}_{cc} \cdot \nabla \langle T_c \rangle^c\\
&\quad - \mathbf{u}_{cd} \cdot \nabla \langle T_d \rangle^d\\
&\quad = \nabla \cdot \left(\mathbf{K}_{cc} \cdot \nabla \langle T_c \rangle^c + \mathbf{K}_{cd} \cdot \nabla \langle T_d \rangle^d\right)\\
&\quad - a_v h \left(\langle T_c \rangle^c - \langle T_d \rangle^d\right),\\
&\varepsilon_d \left(\rho c_p\right)_d \frac{\partial \langle T_d \rangle^d}{\partial t} + \varepsilon_d \left(\rho c_p\right)_d \langle \mathbf{v}_d \rangle^d \cdot \nabla \langle T_d \rangle^d - \mathbf{u}_{dc} \cdot \nabla \langle T_c \rangle^c\\
&\quad - \mathbf{u}_{dd} \nabla \langle T_d \rangle^d\\
&\quad = \nabla \cdot \left(\mathbf{K}_{dc} \cdot \nabla \langle T_c \rangle^c + \mathbf{K}_{dd} \cdot \nabla \langle T_d \rangle^d\right)\\
&\quad - a_v h \left(\langle T_d \rangle^d - \langle T_c \rangle^c\right).
\end{aligned}
\tag{2}
$$

Here ε_i is the volume fraction of the i-phase (the index i can take c or d), with V_i and V_{REV} as the volume of the i-phase in REV, and the volume of the REV respectively:

$$
\varepsilon_i = \frac{V_i}{V_{\mathrm{REV}}}. \tag{3}
$$

The *intrinsic average* is defined by

$$\langle \Psi_i \rangle^i = \frac{1}{V_i} \int_{V_i} \Psi_i dV. \tag{4}$$

$\mathbf{K}_{cc}$, $\mathbf{K}_{cd}$, $\mathbf{K}_{dc}$, $\mathbf{K}_{dd}$, $\mathbf{u}_{cc}$, $\mathbf{u}_{cd}$, $\mathbf{u}_{dc}$, $\mathbf{u}_{dd}$, and $a_v h$ represent the effects of microscale physics on the macroscale heat transfer. The readers are referred to [12, 19, 20] for their governing equations and numerical computations.

3. Results and Discussion

Rewrite (2) in their operator form:

$$\begin{bmatrix} \mathcal{A} & \mathcal{B} \\ \mathcal{C} & \mathcal{D} \end{bmatrix} \begin{bmatrix} \langle T_c \rangle^c \\ \langle T_d \rangle^d \end{bmatrix} = 0. \tag{5}$$

where $\mathcal{A} = \gamma_c(\partial/\partial t) + \gamma_c \langle \mathbf{v}_c \rangle^c \cdot \nabla - \mathbf{u}_{cc} \cdot \nabla - \nabla \cdot (\mathbf{K}_{cc} \cdot \nabla) + a_v h$, $\mathcal{B} = -\mathbf{u}_{cd} \cdot \nabla - \nabla \cdot (\mathbf{K}_{cd} \cdot \nabla) - a_v h$, $\mathcal{C} = -\mathbf{u}_{dc} \cdot \nabla - \nabla \cdot (\mathbf{K}_{dc} \cdot \nabla) - a_v h$, and $\mathcal{D} = \gamma_d(\partial/\partial t) + \gamma_d \langle \mathbf{v}_d \rangle^d \cdot \nabla - \mathbf{u}_{dd} \cdot \nabla - \nabla \cdot (\mathbf{K}_{dd} \cdot \nabla)$. We then obtain an uncoupled form by evaluating the operator determinant such that

$$\begin{aligned} &\left[\left(\gamma_c \frac{\partial}{\partial t} + \gamma_c \langle \mathbf{v}_c \rangle^c \cdot \nabla - \mathbf{u}_{cc} \cdot \nabla - \nabla \cdot (\mathbf{K}_{cc} \cdot \nabla) \quad + a_v h \right) \right. \\ &\times \left(\gamma_d \frac{\partial}{\partial t} + \gamma_d \langle \mathbf{v}_d \rangle^d \cdot \nabla - \mathbf{u}_{dd} \cdot \nabla - \nabla \cdot (\mathbf{K}_{dd} \cdot \nabla) + a_v h \right) \\ &- (\mathbf{u}_{cd} \cdot \nabla + \nabla \cdot (\mathbf{K}_{cd} \cdot \nabla) + a_v h) \\ &\left. \times (\mathbf{u}_{dc} \cdot \nabla + \nabla \cdot (\mathbf{K}_{dc} \cdot \nabla) + a_v h) \right] \langle T_i \rangle^i = 0, \end{aligned} \tag{6}$$

where the index i can take c or d. $\gamma_c = \varepsilon_c (\rho c)_c$ and $\gamma_d = \varepsilon_d (\rho c)_d$ are the c-phase and d-phase effective thermal capacities, respectively. Its explicit form reads, after dividing by $a_v h(\gamma_c + \gamma_d)$,

$$\begin{aligned} &\frac{\partial \langle T_i \rangle^i}{\partial t} + \frac{\gamma_c \gamma_d}{a_v h(\gamma_c + \gamma_d)} \frac{\partial^2 \langle T_i \rangle^i}{\partial t^2} + \frac{1}{(\gamma_c + \gamma_d)} \\ &\quad \times \left(\gamma_c \langle \mathbf{v}_c \rangle^c + \gamma_d \langle \mathbf{v}_d \rangle^d \right) \cdot \nabla \langle T_i \rangle^i \\ &= \frac{1}{\gamma_c + \gamma_d} [\nabla \cdot (\mathbf{K}_{cc} \cdot \nabla) + \nabla \cdot (\mathbf{K}_{cd} \cdot \nabla) + \nabla \cdot (\mathbf{K}_{dc} \cdot \nabla) \\ &\qquad + \nabla \cdot (\mathbf{K}_{dd} \cdot \nabla)] \langle T_i \rangle^i \\ &\quad + \frac{1}{a_v h(\gamma_c + \gamma_d)} \\ &\quad \times \left\{ \gamma_c \frac{\partial}{\partial t} [\nabla \cdot (\mathbf{K}_{dd} \cdot \nabla)] + \gamma_d \frac{\partial}{\partial t} [\nabla \cdot (\mathbf{K}_{cc} \cdot \nabla)] \right. \\ &\qquad \left. - \gamma_c \gamma_d \frac{\partial}{\partial t} \left[\left(\langle \mathbf{v}_c \rangle^c + \langle \mathbf{v}_d \rangle^d \right) \cdot \nabla \right] \right\} \langle T_i \rangle^i \\ &\quad + \frac{1}{a_v h(\gamma_c + \gamma_d)} \\ &\quad \times \left\{ \left\{ [\nabla \cdot (\mathbf{K}_{cd} \cdot \nabla)][\nabla \cdot (\mathbf{K}_{dc} \cdot \nabla)] \right. \right. \\ &\qquad \left. - [\nabla \cdot (\mathbf{K}_{cc} \cdot \nabla)][\nabla \cdot (\mathbf{K}_{dd} \cdot \nabla)] \right\} \langle T_i \rangle^i \\ &\qquad + \left[\gamma_c \frac{\partial}{\partial t} \left(\mathbf{u}_{dd} \cdot \nabla \langle T_i \rangle^i \right) + \gamma_d \frac{\partial}{\partial t} \left(\mathbf{u}_{cc} \cdot \nabla \langle T_i \rangle^i \right) \right] \\ &\qquad - \left\{ (\mathbf{u}_{cc} \cdot \nabla)[\nabla \cdot (\mathbf{K}_{dd} \cdot \nabla)] \right. \\ &\qquad + (\mathbf{u}_{dd} \cdot \nabla)[\nabla \cdot (\mathbf{K}_{cc} \cdot \nabla)] \\ &\qquad - (\mathbf{u}_{cd} \cdot \nabla)[\nabla \cdot (\mathbf{K}_{dc} \cdot \nabla)] \\ &\qquad - (\mathbf{u}_{dc} \cdot \nabla)[\nabla \cdot (\mathbf{K}_{cd} \cdot \nabla)] \\ &\qquad - \gamma_c (\langle \mathbf{v}_c \rangle^c \cdot \nabla)[\mathbf{u}_{dd} \cdot \nabla + \nabla \cdot (\mathbf{K}_{dd} \cdot \nabla)] \\ &\qquad \left. - \gamma_d \left(\langle \mathbf{v}_d \rangle^d \cdot \nabla \right) [\mathbf{u}_{cc} \cdot \nabla + \nabla \cdot (\mathbf{K}_{cc} \cdot \nabla)] \right\} \langle T_i \rangle^i \\ &\quad - \left[(\mathbf{u}_{cc} \cdot \nabla)(\mathbf{u}_{dd} \cdot \nabla) - (\mathbf{u}_{cd} \cdot \nabla)(\mathbf{u}_{dc} \cdot \nabla) \right. \\ &\qquad \left. + \gamma_c \gamma_d (\langle \mathbf{v}_c \rangle^c \cdot \nabla) \left(\langle \mathbf{v}_d \rangle^d \cdot \nabla \right) \right] \langle T_i \rangle^i \Big\}. \end{aligned} \tag{7}$$

When the system is isotropic and the physical properties of the two phases are constant, it reduces to

$$\begin{aligned} &\frac{\partial \langle T_i \rangle^i}{\partial t} + \tau_q \frac{\partial^2 \langle T_i \rangle^i}{\partial t^2} + \langle \mathbf{v}_{cd} \rangle^{cd} \cdot \nabla \langle T_i \rangle^i \\ &\quad = \alpha \ \Delta \ \langle T_i \rangle^i + \alpha \tau_T \frac{\partial}{\partial t} \left(\Delta \ \langle T_i \rangle^i \right) \\ &\qquad + \frac{\alpha}{k} \left[F(\mathbf{r}, t) + \tau_q \frac{\partial F(\mathbf{r}, t)}{\partial t} \right], \end{aligned} \tag{8}$$

where

$$\begin{aligned} \langle \mathbf{v}_{cd} \rangle^{cd} &= \frac{1}{(\gamma_c + \gamma_d)} \left(\gamma_c \langle \mathbf{v}_c \rangle^c + \gamma_d \langle \mathbf{v}_d \rangle^d \right), \\ \tau_q &= \frac{\gamma_c \gamma_d}{a_v h(\gamma_c + \gamma_d)}, \\ \tau_T &= \frac{\gamma_c k_{dd} + \gamma_d k_{cc}}{a_v h(k_{cc} + k_{cd} + k_{dc} + k_{dd})}, \\ k &= k_{cc} + k_{cd} + k_{dc} + k_{dd}, \\ \alpha &= \frac{k_{cc} + k_{cd} + k_{dc} + k_{dd}}{\gamma_c + \gamma_d}, \end{aligned} \tag{9}$$

$$
\begin{aligned}
&F(\mathbf{r},\ t)+\tau_q\frac{\partial F(\mathbf{r},\ t)}{\partial t}\\
&=\frac{1}{a_v h}\Big\{(k_{cd}k_{dc}-k_{cc}k_{dd})\Delta^2\langle T_i\rangle^i\\
&\quad+\Big[\gamma_c\frac{\partial}{\partial t}\Big(\mathbf{u}_{dd}\cdot\nabla\langle T_i\rangle^i\Big)+\gamma_d\frac{\partial}{\partial t}\Big(\mathbf{u}_{cc}\cdot\nabla\langle T_i\rangle^i\Big)\\
&\quad-\gamma_c\gamma_d\frac{\partial}{\partial t}\Big(\langle\mathbf{v}_c\rangle^c+\langle\mathbf{v}_d\rangle^d\Big)\cdot\nabla\langle T_i\rangle^i\Big]\\
&\quad-\Big\{k_{dd}\Delta[(\mathbf{u}_{cc}+\gamma_c\langle\mathbf{v}_c\rangle^c)\cdot\nabla]\\
&\quad+k_{cc}\Delta\Big[\Big(\mathbf{u}_{dd}+\gamma_d\langle\mathbf{v}_d\rangle^d\Big)\cdot\nabla\Big]\\
&\quad-k_{dc}\Delta(\mathbf{u}_{cd}\cdot\nabla)-k_{cd}\Delta(\mathbf{u}_{dc}\cdot\nabla)\Big\}\langle T_i\rangle^i\\
&\quad-\Big\{[(\mathbf{u}_{cc}+\gamma_c\langle\mathbf{v}_c\rangle^c)\cdot\nabla](\mathbf{u}_{dd}\cdot\nabla)\\
&\quad-\Big[\Big(\mathbf{u}_{dd}+\gamma_d\langle\mathbf{v}_d\rangle^d\Big)\cdot\nabla\Big](\mathbf{u}_{cc}\cdot\nabla)\\
&\quad-[(\mathbf{u}_{cd}+\gamma_c\langle\mathbf{v}_c\rangle^c)\cdot\nabla]\\
&\quad\times\Big[\Big(\mathbf{u}_{dc}+\gamma_d\langle\mathbf{v}_d\rangle^d\Big)\cdot\nabla\Big]\Big\}\langle T_i\rangle^i\Big\}.
\end{aligned}
\tag{10}
$$

This is a dual-phase-lagging heat-conduction equation with τ_q and τ_T as the phase lags of the heat flux and the temperature gradient, respectively [15, 21, 22]. Here, $F(\mathbf{r},t)$ is the volumetric heat source. k, ρc, α, and $\langle\mathbf{v}_{cd}\rangle^{cd}$ are the effective thermal conductivity, capacity, diffusivity, and velocity of nanofluids, respectively. Therefore, the presence of nanoparticles shifts the classical energy equation for the heat transfer in the base fluid into the dual-phase-lagging energy equation in nanofluids at the macroscale. This is significant because all results regarding dual-phase-lagging heat transfer can thus be applied to study heat transfer in nanofluids [21, 22]. For the case of heat conduction in nanofluids, the inclusion of the solid-fluid interface heat transfer also leads to dual-phase-lagging heat-conduction equation, which resolves the conflict between experimental data of nanofluid thermal conductivity and classical theories of effective thermal conductivity of suspensions [23].

It is interesting to note that there are nontraditional convective terms $-\mathbf{u}_{cc}\cdot\nabla\langle T_c\rangle^c-\mathbf{u}_{cd}\cdot\nabla\langle T_d\rangle^d$ and $-\mathbf{u}_{dc}\cdot\nabla\langle T_c\rangle^c-\mathbf{u}_{dd}\cdot\nabla\langle\mathbf{T}_d\rangle^d$ in (2). In (8), however, such terms disappear because of the constraint from the mass conservation. Therefore, the microscale physics does not manifest itself as the macroscale convection. The velocity-like terms appear only in the source term in (8).

The presence of nanoparticles gives rise to variations of thermal capacity, conductivity, and diffusivity, which are given by, in terms of ratios over those of the base fluid,

$$
\begin{aligned}
\frac{\rho c}{(\rho c)_c}&=(1-\varepsilon_d)+\varepsilon_d\frac{(\rho c)_d}{(\rho c)_c},\\
\frac{k}{k_c}&=\frac{k_{cc}+k_{cd}+k_{dc}+k_{dd}}{k_c},\\
\frac{\alpha}{\alpha_c}&=\frac{k}{k_c}\frac{(\rho c)_c}{\rho c}.
\end{aligned}
\tag{11}
$$

Therefore, $\rho c/(\rho c)_c$ depends *only* on the volume fraction of nanoparticles and the nanoparticle-fluid capacity ratio. However, both k/k_c and α/α_c are affected by the geometry, property and dynamic process of nanoparticle-fluid interfaces.

Consider

$$
\frac{\tau_T}{\tau_q}=1+\frac{\gamma_c^2k_{dd}+\gamma_d^2k_{cc}-\gamma_c\gamma_d(k_{cd}+k_{dc})}{\gamma_c\gamma_d(k_{cc}+k_{cd}+k_{dc}+k_{dd})}.
\tag{12}
$$

It can be larger, equal, or smaller than 1 depending on the sign of $\gamma_c^2k_{dd}+\gamma_d^2k_{cc}-\gamma_c\gamma_d(k_{cd}+k_{dc})$. Therefore, by the condition for the existence of thermal waves that requires $\tau_T/\tau_q<1$[22, 24], we may have thermal waves in nanofluid heat transfer when

$$
\begin{aligned}
&\gamma_c^2k_{dd}+\gamma_d^2k_{cc}-\gamma_c\gamma_d(k_{cd}+k_{dc})\\
&=\Big(\gamma_c\sqrt{k_{dd}}-\gamma_d\sqrt{k_{cc}}\Big)^2+\gamma_c\gamma_d\Big(2\sqrt{k_{cc}k_{dd}}-k_{cd}-k_{dc}\Big)<0.
\end{aligned}
\tag{13}
$$

A necessary (but not sufficient) condition for (13) is $k_{cd}+k_{dc}>2\sqrt{k_{cc}k_{dd}}$. Note also that for heat transfer in nanofluids the microscale physics yields a time-dependent source term $F(\mathbf{r},t)$ in the dual-phase-lagging energy equation ((8) and (10)). Therefore, the resonance can also occur. These thermal waves and possibly resonance are believed to be the driving force for the enhancement of heat transfer. When $k_{cd}+k_{dc}=0$ so that τ_T/τ_q is always larger than 1, thermal waves and resonance would not appear. The sum $k_{cd}+k_{dc}$ is thus responsible for thermal waves and resonance in nanofluid heat transfer. It is also interesting to note that although each τ_q and τ_T is a_vh-dependent, the ratio $\tau_T/\tau_q$is not. Therefore the evaluation of τ_T/τ_q will be much simpler than τ_q or τ_T.

Therefore, the molecular physics and the microscale physics (interactions between nanoparticles and base fluids at the microscale in particular) manifest themselves as heat diffusion and thermal waves/resonance at the macroscale, respectively. Their overall macroscopic manifestation shifts the classical energy equation for the heat transfer in the base fluid into the dual-phase-lagging energy equation in nanofluids. When $\tau_T/\tau_q<1$, thermal waves dominate and (8) is of a hyperbolic type [22]. When $\tau_T/\tau_q\geq1$, however, heat diffusion dominates and (8) is parabolic [22]. Depending on factors like material properties of nanoparticles and base fluids, nanoparticles' geometrical structure and their distribution in the base fluids, and interfacial properties and dynamic processes on particle-fluid interfaces, the heat diffusion, thermal waves/resonance, and convection may either enhance or counteract each other. Consequently, the heat transfer in nanofluids is endowed with much richer features than that in the base fluid.

4. Concluding Remarks

In an attempt to determine how the presence of nanoparticles affects the heat transfer at the macroscale and isolates the mechanism responsible for the reported variation of thermal properties, a macroscale energy equation is developed and

examined analytically for nanofluid heat transfer. The model is obtained by scaling-up the microscale model for the heat transfer in the nanoparticles and in the base fluids. The approach for scaling-up is the volume averaging with help of multiscale theorems. The result shows that the presence of nanoparticles leads to a dual-phase-lagging energy equation in nanofluids at the macroscale. Therefore, the molecular physics and the microscale physics manifest themselves as heat diffusion and thermal waves at the macroscale, respectively. Depending on factors like material properties of nanoparticles and base fluids, nanoparticles' geometrical structure and their distribution in the base fluids, and interfacial properties and dynamic processes on particle-fluid interfaces, the heat diffusion, convection, and thermal waves may either enhance or counteract each other, which will enrich heat-transfer performance significantly.

Acknowledgment

The financial support from the Research Grants Council of Hong Kong (GRF718009 and GRF717508) is gratefully acknowledged.

References

[1] S. U. S. Choi, "Enhancing thermal conductivity of fluids with nanoparticles," in *Developments and Applications of Non-Newtonian Flows*, D. A. Singer and H. P. Wang, Eds., vol. 231 of *FED*, pp. 99–105, ASME, New York, NY, USA, 1995.

[2] G. P. Peterson and C. H. Li, "Heat and mass transfer in fluids with nanoparticle suspensions," *Advances in Heat Transfer*, vol. 39, pp. 257–376, 2006.

[3] S. K. Das, S. U. S. Choi, W. H. Yu, and T. Pradeep, *Nanofluids: Science and Technology*, John Wiley & Sons, Hoboken, NJ, USA, 2008.

[4] D. Wen, Y. Ding, and R. Williams, "Nanofluids turn up the heat," *The Chemical Engineer*, no. 771, pp. 32–34, 2005.

[5] D. Y. Tzou, "Thermal instability of nanofluids in natural convection," *International Journal of Heat and Mass Transfer*, vol. 51, no. 11-12, pp. 2967–2979, 2008.

[6] S. U. S. Choi, Z. G. Zhang, and P. Keblinski, "Nanofluids," in *Encyclopedia of Nanoscience and Nanotechnology*, H. S. Nalwa, Ed., vol. 6, pp. 757–773, American Scientific Publishers, New York, NY, USA, 2004.

[7] J. A. Eastman, S. R. Phillpot, S. U. S. Choi, and P. Keblinski, "Thermal transport in nanofluids," *Annual Review of Materials Research*, vol. 34, pp. 219–246, 2004.

[8] P. E. Phelan, P. Bhattacharya, and R. S. Prasher, "Nanofluids for heat transfer applications," *Annual Reviews of Heat Transfer*, vol. 14, pp. 255–275, 2005.

[9] C. B. Sobhan and G. P. Peterson, *Microscale and Nanoscale Heat Transfer: Fundamentals and Engineering Applications*, CRC Press, Boca Raton, Fla, USA, 2008.

[10] L. Q. Wang and X. H. Wei, "Nanofluids: synthesis, heat conduction, and extension," *Journal of Heat Transfer*, vol. 131, no. 3, Article ID 033102, 7 pages, 2009.

[11] S. U. S. Choi, "Nanofluids: from vision to reality through research," *Journal of Heat Transfer*, vol. 131, Article ID 033106, 9 pages, 2009.

[12] L. Q. Wang and M. Quintard, "Nanofluids of the future," in *Advances in Transport Phenomena*, pp. 179–243, Springer, Heidelberg, Germany, 2009.

[13] S. Whitaker, *The Method of Volume Averaging*, Kluwer Academic Publishers, Dordrecht, The Netherlands, 1999.

[14] L. Q. Wang, "Flows through porous media: a theoretical development at macroscale," *Transport in Porous Media*, vol. 39, no. 1, pp. 1–24, 2000.

[15] L. Q. Wang, M. T. Xu, and X. H. Wei, "Multiscale theorems," *Advances in Chemical Engineering*, vol. 34, pp. 175–468, 2008.

[16] L. Q. Wang, "A general theory of diffusion," *Progress of Theoretical Physics*, vol. 101, no. 3, pp. 541–557, 1999.

[17] J. L. Auriault, "Heterogeneous medium: is an equivalent macroscopic description possible?" *International Journal of Engineering Science*, vol. 29, no. 7, pp. 785–795, 1991.

[18] R. B. Bird, W. E. Stewart, and E. N. Lightfoot, *Transport Phenomena*, John Wiley & Sons, New York, NY, USA, 3rd edition, 2007.

[19] M. Quintard and S. Whitaker, "Theoretical analysis of transport in porous media," in *Handbook of Heat Transfer in Porous Media*, K. Vafai, Ed., pp. 1–52, Marcel Dekker, New York, NY, USA, 2000.

[20] J. Fan and L. Q. Wang, "Microstructural effects on macroscale thermal properties in nanofluids," *NANO*, (in press).

[21] D. Y. Tzou, *Macro-to Microscale Heat Transfer: The Lagging Behavior*, Taylor & Francis, London, UK, 1997.

[22] L. Q. Wang, X. S. Zhou, and X. H. Wei, *Heat Conduction: Mathematical Models and Analytical Solutions*, Springer, Berlin, Germany, 2008.

[23] P. Vadasz, "Heat conduction in nanofluid suspensions," *Journal of Heat Transfer*, vol. 128, no. 5, pp. 465–477, 2006.

[24] M. T. Xu and L. Q. Wang, "Thermal oscillation and resonance in dual-phase-lagging heat conduction," *International Journal of Heat and Mass Transfer*, vol. 45, no. 5, pp. 1055–1061, 2002.

Hindawi Publishing Corporation
Advances in Mechanical Engineering
Volume 2010, Article ID 742739, 10 pages
doi:10.1155/2010/742739

Research Article

Experimental Studies of Natural Convection Heat Transfer of Al_2O_3/DI Water Nanoparticle Suspensions (Nanofluids)

Calvin H. Li[1] and G. P. Peterson[2]

[1] *Department of Mechanical, Industrial, and Manufacturing Engineering, University of Toledo, Toledo, OH 43606, USA*
[2] *Woodruff School of Mechanical Engineering, Georgia Institute of Technology, Atlanta, GA 30332-0325, USA*

Correspondence should be addressed to Calvin H. Li, calvin.li@utoledo.edu

Received 5 May 2009; Accepted 4 June 2009

Academic Editor: Oronzio Manca

The natural convection heat transfer characteristics of Al_2O_3/water nanofluids comprised of 47 nm, Al_2O_3 and water, with volume fractions ranging from 0.5% through 6%, has been investigated through a set of experimental measurements. The temperature of the heated surface and the Nusselt number of different volume fractions of Al_2O_3/water nanofluids natural convection tests clearly demonstrated a deviation from that of pure base fluids (distilled water). In the investigation, a deterioration of the natural convection heat transfer coefficient was observed with increases of the volume fraction of the nanoparticles in the nanofluids. The deterioration phenomenon was further investigated through a visualization study on a 850 nm diameter polystyrene particle/water suspension in a bottom heating rectangular enclosure. The influence of particle movements on the heat transfer and natural flow of the polystyrene particle/DI water suspension were filmed, and the temperature changes on the heating and cooling surfaces were recorded. The results were analyzed in an effort to explain the causes of the natural convection heat transfer deterioration of the 47 nm Al_2O_3/water nanofluids observed in the experiments. The visualization results confirmed the natural convective heat transfer deterioration, and further explained the causes of the deterioration of the nanofluids natural convective heat transfer.

1. Introduction

There is increasing evidence that nanoparticles dispersed in liquid base fluids can have a significant impact on the effective thermal conductivity of nanoparticle/liquid suspensions (nanofluids) [1–18]. For example, nanofluids consisting of 10 nm Cu nanoparticles suspended in ethylene glycol with a volume fraction of 0.3%, have shown a 40% enhancement in the effective thermal conductivity, when compared to that of the base fluid (ethylene glycol) [15]. In addition, 36 nm CuO nanoparticles in distilled water with a volume fraction of 5% have exhibited as much as a 60% increase in the effective thermal conductivity over that of the base fluid (distilled water) at room temperature [16], and 33 nm Al_2O_3 nanoparticles in distilled water have exhibited a 30% enhancement in the effective thermal conductivity [16]. Moreover, the enhancement of the effective thermal conductivity of these metal oxide nanoparticle nanofluids has been shown to increase with increases in temperature [17].

Recent experiments indicated that water-based nanofluids of 29 nm CuO and 36 nm Al_2O_3 nanoparticles resulted in a range of effective thermal conductivity enhancements from 30% to 52% for CuO/Distilled water nanofluids, and 8% to 30% for Al_2O_3/Distilled water nanofluids, at volume fractions of 6% and 10%, respectively, and at a bulk temperatures ranging from 27.5°C to 34.7°C [18].

Several mechanisms have been proposed to explain the enhancements described above. Of the two most likely, the first attributed the effective thermal conductivity enhancement to the increased thermal conductivity of the nanoparticles and agglomerations. The second focused on the contribution of the Brownian motion of the nanoparticles. The significance of these two mechanisms are both closely related to the bulk temperature of the nanoparticle suspension, the mean size of the nanoparticles, the volume fraction of

nanoparticle in the nanofluids, and the physical properties of base fluid materials.

The increased thermal conductivity of nanoparticle suspensions has been well documented and can be estimated using Maxwell's equation [19] or the Hamilton and Crosser equation [20]. The Brownian motion mechanism and contribution of the nanoparticles in the base fluid has received a significant amount of attention more recently, and has been extensively explored and/or explained [13, 21–24].

Other heat transfer modes of nanofluids, such as natural and forced convection and boiling heat transfer, have also been investigated by a number of researchers [25–34]. Like the study on the effective thermal conductivity of these nanofluids, several mechanisms and explanations have been proposed. For the natural convection heat transfer of nanofluids, Okada et al. [28, 29] experimentally measured the change of layering and concentration of large soda glass particle/water suspensions in a rectangular cross-section cell, which had a bottom heating surface and five other isothermal walls. The same group of researchers also measured the natural convection heat transfer of 2.97 micron SiO_2/water suspension in a rectangular cross-section vessel, which was heated and cooled from two opposing vertical walls and had other four adiabatic walls. Khanafer et al. [30] and Jou and Tzeng [31] conducted numerical studies of the natural convection heat transfer of nanofluids in a two-dimensional enclosure.

Based on the assumptions used in these simulations, such as the thermal and flow equilibrium between the fluid phase and nanoparticles, the uniform shape and size for nanoparticles, and most importantly, the enhancement in the effective thermal conductivity of the nanofluids due to the thermal dispersion, the two numerical investigations resulted in the same conclusion, that the natural convection heat transfer of nanofluids had been greatly increased at various flow parameters. Putra et al. [32] experimentally evaluated Al_2O_3 and CuO nanoparticle/water nanofluids in a horizontal cylindrical unit, heated on one vertical side and cooled on the other vertical side in a horizontal direction. It was found that a systematic and definite deterioration in natural convection heat transfer had occurred in both of these types of nanofluids. Similar natural convection heat transfer deterioration results were also reported in the investigation at various volume fractions of TiO_2/water nanofluids [33]. Discussion of those two reports focused on several possible parameters, which could lead to this deterioration, such as the thermophysical properties, particle concentration, the pH value, and the particle/water surface interaction.

To determine the effect of nanoparticle concentration, a visualization study of the natural convection of 57 micron diameter glass particle suspensions under intermittent heating was conducted [34]. A transient change of flow patterns was observed and a particle-free layer at the top of convection cell was observed. When compared to tests on pure liquid, a peculiar sedimentation driven two-layer convection was found.

Based on the previous studies of the effective thermal conductivity and the viscosity of Al_2O_3/distilled water nanofluids, the current investigation was focused on the experimental measurement of natural convection heat transfer of Al_2O_3 nanofluids. The particle movement influences on the natural convection heat transfer deterioration was also analyzed by visually studying the heat transfer process of an 850 nm polystyrene particle/DI water suspension in a rectangular enclosure. The two components were integrated in an effort to explain the causes of the new phenomena of nanofluids natural convective heat transfer deterioration. In Al_2O_3 nanofluids test, there is no surfactant involved to avoid the hydrophobic to hydrophilic aqueous interfaces effect introduced by surfactants [35, 36], rather the samples were kept in original pH value around 7 and ultrasonic bath was used to make sure a good dispersion in a reasonably time period of 24 hours. As pointed by [37], the tested effective thermal conductivities of the nanoparticle suspensions were repeatable with negligible changes in this time period.

2. Experimental Test Facility and Results

2.1. The Experimental Measurement of Natural Convection Heat Transfer of Al_2O_3 Nanofluids. In the current investigation, the natural convection heat transfer of Al_2O_3 nanofluids was studied using the test facility shown in Figure 1. This system was thermally insulated and consisted of a support rig, two copper bars, one rubber o-ring and the thermal insulation materials. The copper bars have a diameter of 25.4 mm (1 inch), and a length of 254 mm (10 inches). The o-ring had a diameter of 2.5 mm and formed a circle with 25.4 mm outer diameter, which was used to form a test cell along with the two 25.4 mm diameter cross-section copper bars. Starting at the surfaces, eighteen k-type thermocouples (Omega, USA) were inserted at the center of both copper bars 25.4 mm apart along the axis. Temperatures at each insertion point were measured simultaneously using a 40-channel thermocouple amplifier HP 34970A data acquisition system at a DAQ rate of 100 fps. The heat flux was determined through a one-dimensional conduction equation. The lower copper bar was connected to a heater to heat up the bottom of test cell, and the upper copper bar was connected to a heat pipe heat dissipater, which rejected heat to the environment. The whole system was calibrated with pure water and the uncertain was estimated to be less than 5%.

The Al_2O_3 nanofluids were produced by dispersing Al_2O_3 nanoparticles into the base fluid, distilled water (DI water). The Al_2O_3 nanoparticles were purchased from Nanophase Technologies Corporation, USA, and had a spherical shape with a mean diameter of 47 nm as shown in Figure 2. Prior to each test, the Al_2O_3 nanofluids were processed in an ultrasonic bath for 90 minutes to break any possible aggregations of Al_2O_3 nanoparticles and to keep the nanofluids uniformly dispersed. The dispersing method could ensure that the nanofluids were stable for more than 24 hours without any visible sedimentations and agglomerations. After the Al_2O_3 nanofluid samples were prepared, they were charged into the test cell for the natural convection heat transfer tests.

The heat flux in the copper bars was determined by measuring the temperatures at different locations inside

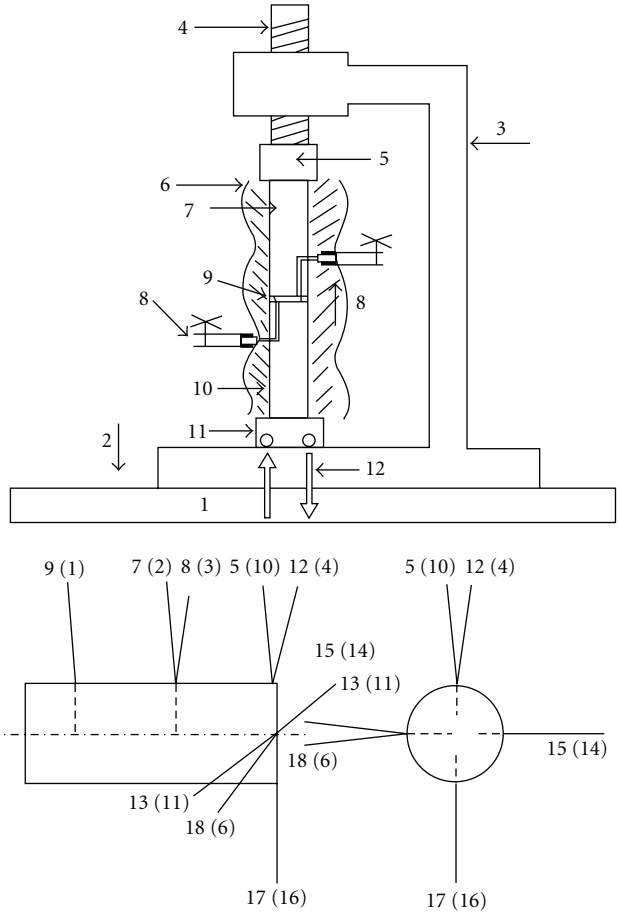

Figure 1: Experimental test facility: (Left) 1: horizontal plane table; 2: base plate; 3: vertical support; 4: load screw; 5: heat dissipater; 6: thermal insulation wrapper; 7: upper copper bar; 8: sample charge tubes; 9: o-ring; 10: lower copper bar; 11: heat sink; 12: coolant inlet and outlet; (Right) the thermocouple distribution on both copper bars [18].

the upper and lower copper bars to obtain temperature profiles and was then computed with one-dimensional heat conduction equation as follows:

$$\frac{\partial^2 T}{\partial t^2} = \frac{1}{\alpha}\frac{\partial T}{\partial t}, \tag{1}$$

$$q = k_{\text{copper}} A_{\text{bar}} \left.\frac{\partial T}{\partial x}\right|_{x=\text{surface}}. \tag{2}$$

After the heat flux was obtained, the heat transfer coefficient, h, was calculated by

$$h = \frac{q}{A_{\text{bar}}}\left(T_{\text{lower}} - T_{\text{upper}}\right). \tag{3}$$

The Nusselt number (Nu) and the Rayleigh number (Ra) were calculated based on the temperature difference between the upper and bottom surfaces and heat transfer coefficient, as shown in (4). The effective thermal conductivity and viscosity of Al_2O_3 nanofluids were obtained from the previous work [18, 38]. The mean heat flux of this experiment was found to be 120 W/m^2, and the distance between two surfaces of the test cell was 2.5 mm:

$$\begin{aligned} \text{Nu} &= h * \frac{d}{k}, \\ \text{Ra} &= \frac{g\beta\Delta T d^3}{(\nu\alpha)}, \\ \text{Nu} &= c * \text{Ra}^n. \end{aligned} \tag{4}$$

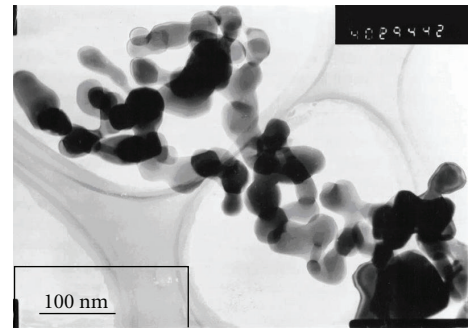

Figure 2: TEM picture of Al_2O_3 nanoparticles.

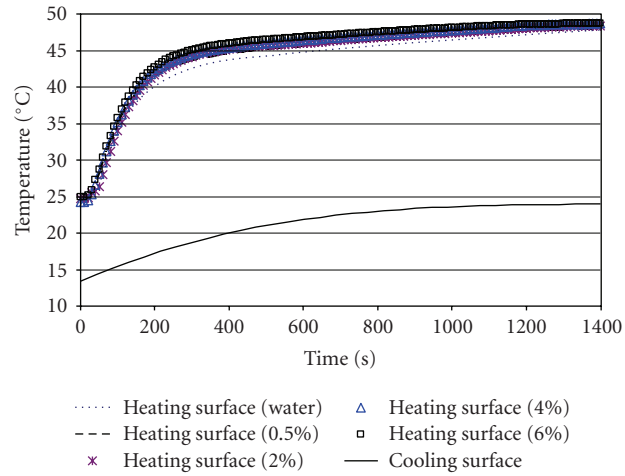

Figure 3: The temporal change in temperature of the heated and cooled surfaces for different Al_2O_3/DI water nanoparticle suspension samples tested.

2.2. Experimental Results of Natural Convection Heat Transfer of Al_2O_3/DI Water Nanofluids. For the experimental measurements of natural convective heat transfer, temperature changes against time were recorded and are presented in Figures 3 and 4. As indicated, the temperature differences between each pair of different volume fraction nanofluids were approximately 1°C. The highest heating surface temperature occurred at the 6% volume fraction nanofluid, and the lowest heating surface temperature occurred for pure water. The cooling surface temperatures of different volume fraction Al_2O_3/DI water nanofluids had virtually no difference due to the excellent heat transfer performance of heat pipe heat dissipater.

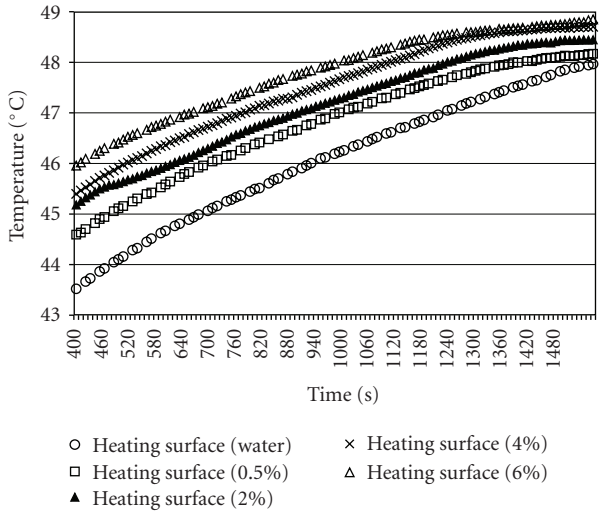

Figure 4: Temperature change of the heated surface as a function of time after 400 seconds of Al_2O_3/DI water nanoparticle suspension samples.

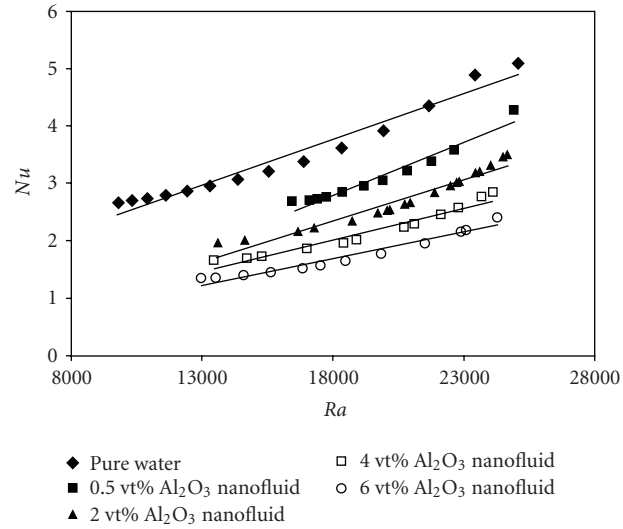

Figure 5: The Nu number of natural convection versus the Ra number of Al_2O_3/DI water nanoparticle suspension samples.

It was interesting to note that, within the first 200 seconds, the heating surface temperatures of Al_2O_3/DI water nanofluids at all volume fractions underwent an evolving process whereby the heating surface temperature of 6% volume fraction nanofluid moved up to be the highest and the heating surface temperature of pure water changed to be the lowest among all the heating surface temperatures, which originally were at the same value. After the first 200 seconds, the temperature of the heating surface for the pure water case was still the lowest, with the next lowest being the 0.5% volume fraction nanofluid, followed by the 2% volume fraction nanofluid, the 4% volume fraction nanofluid, and finally the highest heating surface temperature occurred for the 6% volume fraction nanofluid. After the first 400 seconds, the heating surface temperature differences of all the different volume fraction tests were reduced but still had the same order that heating surface of the 6% volume fraction had the highest value, followed by the 4% volume fraction, and next by 2% volume fraction, then by 0.5% volume fraction, and finally by pure water, as shown in Figure 4.

The relationships between the Nu and Ra numbers for each volume fraction of the Al_2O_3/DI water nanofluid and pure water are presented in Figure 5, which demonstrates that the pure water had the highest Nu number at a given Ra number, followed by the 0.5% volume fraction Al_2O_3/DI water nanofluid, 2% volume fraction Al_2O_3/DI water nanofluid, 4% volume fraction Al_2O_3/DI water nanofluid, and finally the 6% volume fraction Al_2O_3/DI water nanofluid. This decreasing trend of Nu number with the increase of volume fraction has also been previously reported by other investigators [32, 33], which clearly illustrated a deterioration of natural convection heat transfer against the increase of volume fraction of Al_2O_3/DI water nanofluids with the experimental data of pure water and Al_2O_3/DI water nanofluids.

This deterioration of natural convection heat transfer against the increase of volume fraction of Al_2O_3/DI water nanofluids is directly opposite to the enhanced effective thermal conductivity of Al_2O_3/DI water nanofluids with the increase of volume fraction, which is shown in Figure 6(a). This can be partially explained by the enhanced viscosity of the Al_2O_3/DI water nanofluids as shown in Figure 6(b), which matched the prediction of Einstein's equation of $\mu = \mu_{BF} * (1 - \phi)^{-2.5}$ [39] as demonstrated in Figure 7. However, many experimental and theoretical studies on the forced convection heat transfer of nanofluids demonstrated that the forced convection heat transfer would be enhanced by the nanofluids compared to that of pure base fluid under the same enhanced viscosity conditions [21, 40–43]. Henceforth, the increase of viscosity could not explain the deterioration of natural convection heat transfer of nanofluids alone. It was proposed that the kinetics of particles in flowing were the reason for the change of heat transport in laminar flow of polystyrene suspensions by [44, 45] and the double-layering of particle concentration for the natural convection of 57 micron diameter glass particle suspensions by [34]. Therefore, visualization investigations on particle kinetics, more specifically, the bulk migrating movement of Al_2O_3 nanoparticles in the nanofluids and the rotational and translational Brownian movements of individual Al_2O_3 nanoparticles, are very necessary. Currently, the experimental observation methods of the nanometer scale particle movements are very limited. In order to conduct the nanoparticle kinetics observation investigation, a 850 nm polystyrene particle/DI water suspension has been employed for the visualization study under the optical microscope.

2.3. Visual Study of Submicron Particle Suspension Transient Natural Convection. To complement the experimental measurements of natural convection heat transfer of Al_2O_3/DI

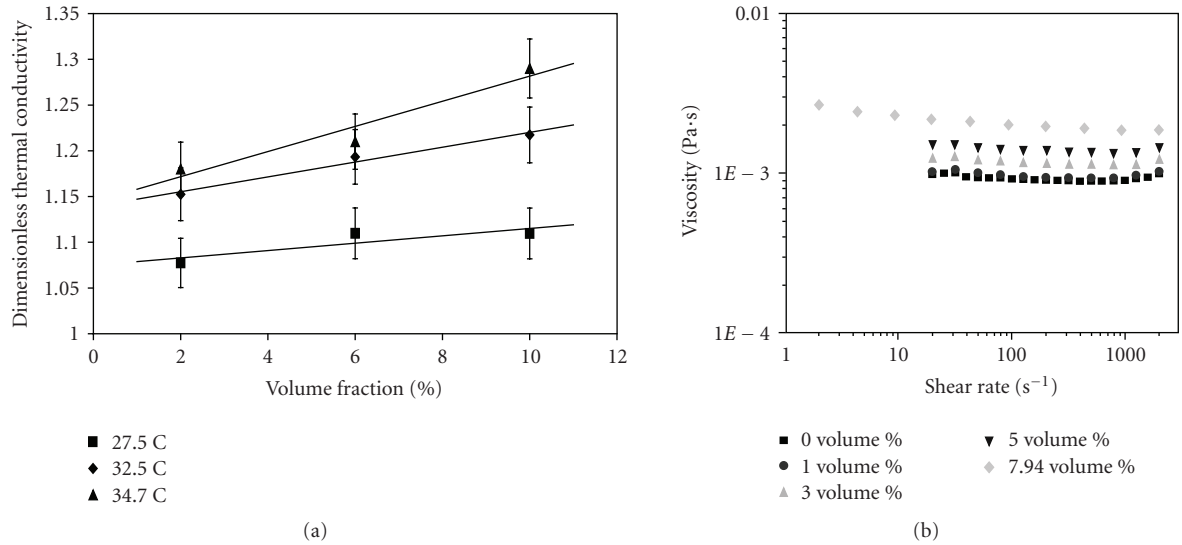

Figure 6: The normalized effective thermal conductivity (multivolume fraction and temperature) and viscosity (room temperature) of Al_2O_3/DI water nanoparticle suspensions [18, 38].

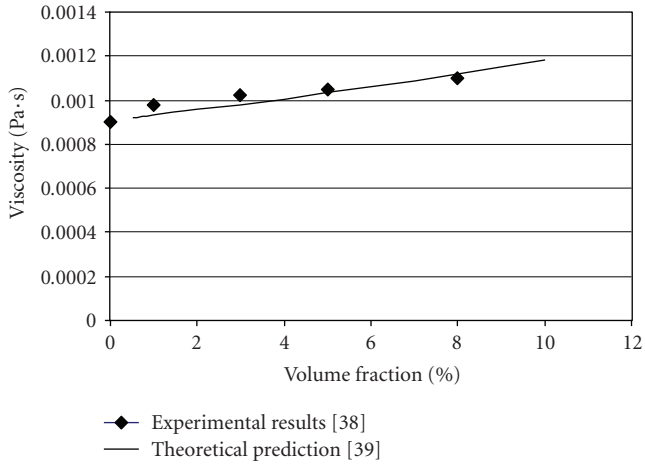

Figure 7: Comparison of the experimental results of Al_2O_3/DI water nanoparticle suspensions [38] and theoretical predictions [39].

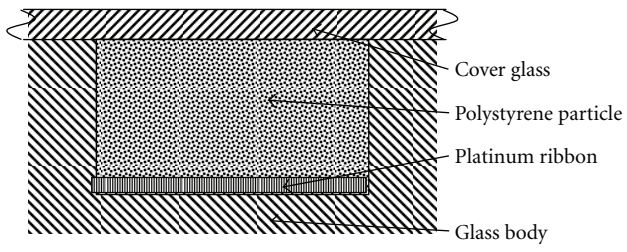

Figure 8: Cross-section view of the testing closure cells with platinum ribbon as bottom heating surface.

water nanofluids and to study the influences of local and bulk nanoparticles movements in the natural convection heat transfer of Al_2O_3/DI water nanofluids, a series of visualization investigations of the natural convection heat transfer of 850 nm polystyrene/DI water suspensions were conducted to analyze and predict the relationship between the movement of the particles and flow pattern and the resulting heat transfer coefficient deterioration found in the foregoing experiments on Al_2O_3/DI water nanofluids.

A rectangular enclosure was fabricated to provide a bottom heating geometry as illustrated in Figure 8, and a diluted 850 nm diameter polystyrene/DI water suspension was charged into the rectangular enclosure. A platinum ribbon was placed on the bottom of the rectangular enclosure to provide the heating surface for the visualization experiments. The original 2.5% volume fraction suspension was purchased from Seradyn, Inc., and the platinum ribbon (99.9% pure) was obtained from Scientific Instrument Services, Inc.

The platinum ribbon heater was first calibrated under the range of temperatures in the natural convection heat transfer measurements of nanofluids, and the relationship between temperature and platinum ribbon electric resistance was obtained. The repeatability and stability of the relationship were verified by a number of repeats of the calibration tests. The relationship between the temperature and the platinum electric resistance at the corresponding temperature is

$$R = R_0[1 + \alpha_e(T - T_0)]. \quad (5)$$

The coefficient α_e was obtained in the calibration setup in which the platinum ribbon was sandwiched between two thick layers of insulation material and was attached with three evenly placed thermocouples along its length. The entire calibration system was covered with a flexible insulation material in an environmental chamber. By carefully adjusting the temperature of the environmental chamber, the temperature differences between the three thermal couples were observed to be $\pm 0.1^\circ$C at a steady-state, and the electrical resistance and temperature were simultaneously

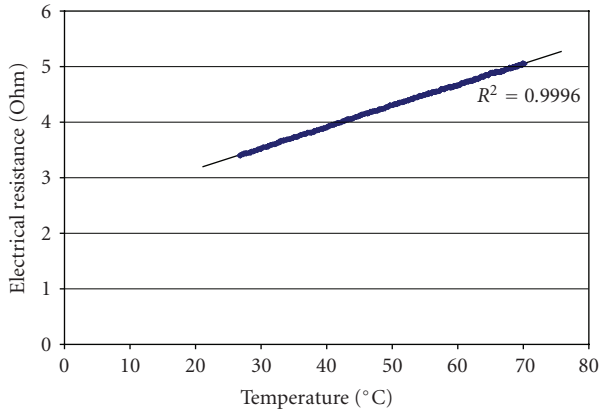

Figure 9: Calibration results for the 2.5 mm width platinum ribbon.

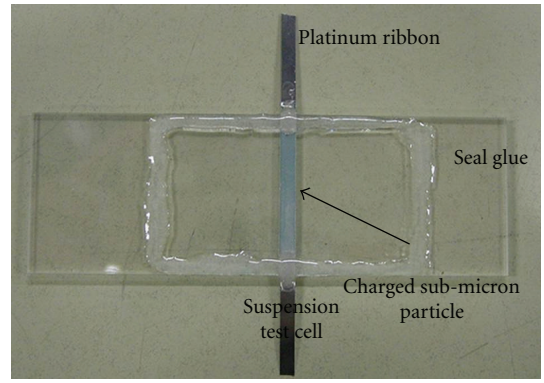

Figure 10: The test unit for the bottom heating visualization of the 850 nm polystyrene particle/DI water suspension.

recorded by a digital data logger. A linear curve fit was obtained from the data recorded, and the coefficient α_e was identified as shown in Figure 9. The electric resistance and temperature relationship for the 2.5 mm width platinum ribbon is shown as follows:

$$R = 0.0379 * t + 2.3981. \quad (6)$$

This relationship can be expressed in the form of (1) as

$$R = 3.398 * [1 + 0.00752 * (T - 278.2)]. \quad (7)$$

In this expression, the coefficient, α_e, is approximately equal to 0.00752 for the 2.5 mm width platinum ribbon.

This bottom heating rectangular enclosure unit was first fabricated on a glass slide using a Microelectromechanical System (MEMS) technique to create a 2.5 mm wide, 0.5 mm deep rectangular channel. And a 0.05 mm thick, 2.5 mm wide platinum ribbon was placed on the bottom of the channel. Then a 0.1 mm thick glass slide was used to cover the channel and to finish the enclosure. Inside the rectangular enclosure test unit, it was charged with the 0.1% volume fraction 850 nm diameter polystyrene/water suspension diluted from the original 2.5% volume fraction suspension.

The sample charged test unit for the bottom heating natural convection visualization is shown in Figure 10. The electric power, electric resistance measurement device and thermocouples were all connected to the test unit under the optical microscope as represented in Figure 11. The temperature of the upper surface of the test cell was measured directly with thermocouples and the bottom heating surface temperature was calculated through the relationship between the temperature and electrical resistance as described in (7). Both surface temperatures were used later to calculate the Ra number of the 0.1% volume fraction 850 nm diameter polystyrene/water suspensions.

The simultaneous temperature and electric resistance data collection was started when a heating power of 2.7 W was applied to the platinum ribbon. During the entire bottom heating natural convection heat transfer visualization process, the particle movements were filmed using an optical microscope mounted with a high speed visualization system. The optical microscope was equipped with a 50X objective lens. The mounted charge-coupled device (CCD) imaging system had a maximum magnification of 500 frames per second (fps) rate and a maximum recording rate of 2000 fps with a reduced magnification. The movements of the 850 nm diameter polystyrene particles were synchronized with the temperature data recorded through the HP 34970A data logger to explore the effects of particle movements on the natural convection heat transfer in the bottom heating rectangular enclosure.

2.4. Results of Visualization Study on 850 nm Diameter Polystyrene/Water Suspensions. The visualization results of both bulk movement and individual particle movement of the 850 nm polystyrene particles were quite interesting. As shown in Figure 12 the individual particle movements, the rotational and translational Brownian motions of the particles, were found to be quite strong all the time. Before power was applied to the platinum ribbon heater, the individual particle Brownian motion was the only phenomena that were observed, as shown in Figure 12(a). Particles were moving in random patterns around each original position in the suspension. Immediately following the initiation of power to the platinum ribbon heater, in addition to Brownian motions, the particles began to slowly migrate from the bottom to the top. More interestingly, the random Brownian motion and the migrating movement appear independent to each other. More often than not, the displacement Brownian motion of particles will move in the direction against the bulk migrating movement. This stage of particle movements was captured in Figure 12(b). In a relatively long time period after the heating was turned on, the migrating movements of particles maintained roughly at the same order of magnitude as the displacement Brownian motion had, and the Brownian motions of particles were still very distinguishable, as shown in Figure 12(c). At the moment approximately 210 seconds after the platinum ribbon heating power was turned on, Strong bulk migrating movement was observed, which was several orders greater than that of the individual particles Brownian motions. The Brownian

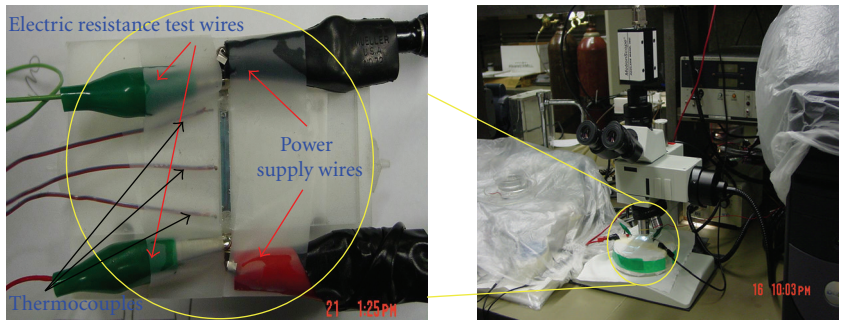

Figure 11: The test facility for the bottom heating test cell of the 850 nm polystyrene particle/DI water suspension (right) and observation facility (left).

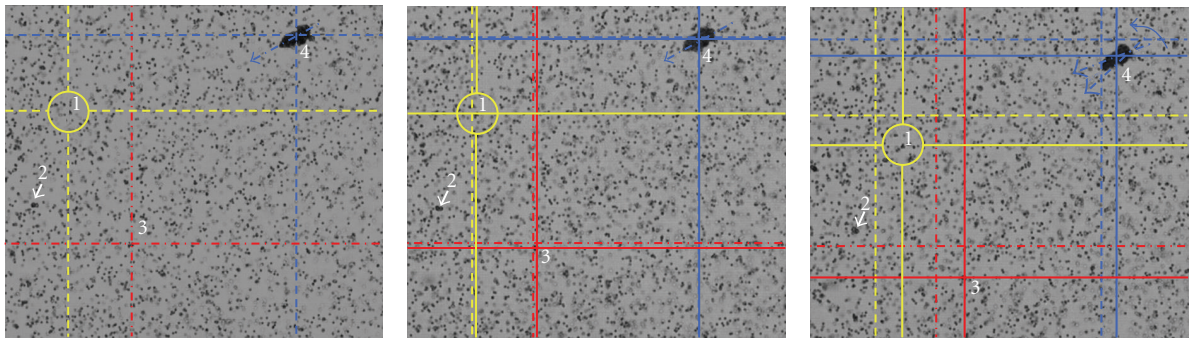

0 (0 s) 239 (0.956 s) 1588 (6.352 s)

(a) (b) (c)

Figure 12: The zoom-in observation of Brownian motions and bulk migrating (thermophoresis) movement of particles before the onset of natural convection. (Particle 1 is doing translational Brownian motion, particle 2 is doing rotational Brownian motion, and particle 3 is doing both Brownian motions with and without the bulk migrating movement. Particle agglomeration 4 is doing bulk migrating movement only).

motions were not to be distinguished any more. From then on, the 850 nm diameter polystyrene/water suspension experienced a natural convection inside the rectangular enclosure. As demonstrated in Figure 13, a vertical layer of concentrated particles was visualized in the middle region of the enclosure and was represented by the red arrows in Figure 13(a). This phenomenon is similar to what was previously reported by [20] except that it was believed that, in the current experiment, the concentration layer was caused by natural convection cycles rather than the double diffusive convection resulting from temperature and concentration gradients in [20]. Figure 13(b) presented one recorded image of particle bulk movement at the top of the middle region in the enclosure. The temperatures of both the bottom heating surface and the upper cooling surface were recorded simultaneously with the images as shown in Figure 14. In the time period right after the heating power was turned on, the temperature of the bottom heating surface increased relatively sharply first. Then the bottom heating surface temperature increase became more gradually. At the moment of around 207 seconds after the heating power on the platinum ribbon was turned on, the bottom heating surface temperature dropped around 5°C abruptly and then climbed back to the previous value in a time period of several tens seconds. This sudden drop of bottom heating surface temperature corresponded to the visualization of a sudden augmentation of bulk migrating movement at the same time. After this period of temperature recovering, the bottom heating surface temperature kept at relatively stable value with a minor increase comparing to the temperature changing manner prior to the moment of the sudden drop. With the temperature information of both surfaces, it was found out that the Ra number was greater than the critical Ra number of 1708 for the onset of natural convection in an enclosure [46]. It implied that the onset of internal natural convection of 850 nm diameter polystyrene/water suspension was delayed, with the evidence of a larger critical Ra number.

3. Discussions and Conclusions

From the experimental measurements of Al_2O_3/DI water nanoparticle suspension natural convection heat transfer, the natural convective heat transfer of 47 nm Al_2O_3/DI water nanofluids demonstrated a deterioration with the increase of volume fraction of Al_2O_3 nanoparticle, as reported in previous experiments [27, 33]. The experimental results were directly against the simulation results that the nanofluids could enhance the heat transfer coefficient in natural convection heat transfer by [30, 31].

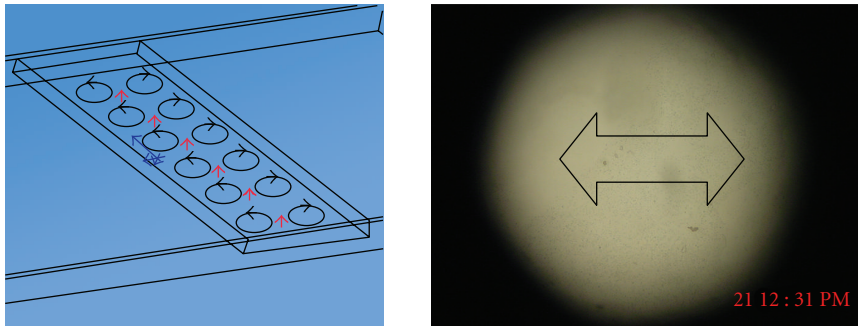

(a) (b)

Figure 13: Bottom heating natural convection of submicron particle suspension ((a) the natural convection in the cell; (b) zoom-out top view of massive submicron particle drift pattern), and the arrows are the moving directions.

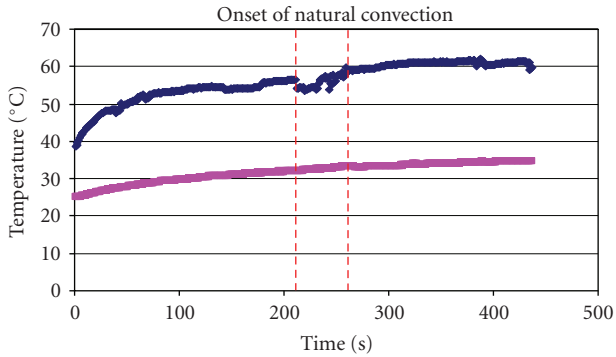

Figure 14: Temperature change of bottom heating surface (upper line) and upper cool surface (lower line) of submicron particle suspension.

For visualization experiments on the 850 nm diameter polystyrene/water suspension, the results indicated that the Brownian motions and thermophoresis movements were the key reasons for the heat transfer before the onset of natural convection heat transfer. Those particle movements delayed the onset of the natural convection heat transfer and might still play a role in the heat transfer deterioration after the onset. The Brownian motions and bulk migrating (thermophoresis) movement were not proposed in the previous experimental nanofluids natural convection heat transfer study [32, 33]. More recently, the combined influence of the Brownian motions and thermophoresis movement on the natural convection heat transfer found in current research echoes a recent theoretical study on nanofluids natural convection heat transfer by [47], which theoretically confirmed the influence from Brownian motions and thermophoresis movement of nanoparticles to the nanofluid natural convection heat transfer. However, its conclusion of the nanoparticle movement effect supported the previous simulation results that nanofluids would have a higher natural convective heat transfer coefficient of nanofluids than that of pure water [30, 31].

Based on the observations of the 850 nm diameter polystyrene/water suspension natural convection heat transfer and the previous reports, it is reasonable to anticipate that nanometer size particles will have an even stronger Brownian motions and thermophoresis movement, which will greatly influence the nanofluids natural convection heat transfer process by delaying the onset of natural convective flow and heat transfer. This delayed onset of natural convection heat transfer may be directly caused by the enhanced effective thermal conductivity and enhanced effective viscosity of the nanofluids as the results of the mixing and stirring effects of the nanoparticle Brownian motions, as shown in Figure 6. This mixing and stirring effect was extensively demonstrated by [13]. It is believed that the enhanced effective thermal conductivity will reduce the temperature gradient and the enhanced effective viscosity will damp out the hydrodynamic perturbation, and in turn, will delay the onset of natural convection heat transfer. After the natural convection heat transfer is developed, both enhanced effective thermal conductivity and effective viscosity will still play a role in slowing down the bulk movement of the nanofluids in natural convection by reducing the temperature gradient and advection momentum. If taking into account the size effect, it should be reasonable to expect that the nanoscale particle should have stronger Brownian motion and thermophoresis activities, and the natural convection onset should be even further slowed down.

In summary, a combined experimental investigation of natural convection heat transfer characteristics of 47 nm Al_2O_3 nanofluids at various volumetric fractions and a 850 nm diameter polystyrene/water suspension has been conducted. The visual observation study on the 850 nm diameter polystyrene/water suspension served as a virtual reference to interpret the deterioration of nanofluids natural convection heat transfer. The results of current investigation were compared with the previously reported results to offer new experimental evidence for the unclarified phenomena. The controversy resulted from simulation study and experimental study is still not clear, but it might be caused by the simulation assumption of uniform nanoparticle size distribution, constant properties, lack of gravity effect on nanoparticles, and the interaction among nanoparticles. To nail down the exact reasons, an extensive comparison study on the results with different assumption in simulation is needed.

The reasons drawn in current study for the natural convection heat transfer deterioration are summarized as follows:

(1) the higher viscosity of the nanofluids,

(2) the temperature gradient smoothing and perturbation damping effects in the body of nanofluids by the mixing and stirring effect of the Brownian motions, which might cause the delayed onset of natural convection,

(3) the influence on the flow field and temperature field from the Brownian motions and thermophoresis movements after the natural convection was developed.

Although care has been taken to eliminate other influences from the nanofluid and polystyrene/water suspension samples, it is still possible that other factors might have played a role, such as the slow aggregation of individual particles, the sedimentation of the particles and/or aggregations, and the influence of the nonuniform size of the particles.

Nomenclature

A_{bar}: Cross-sectional area of the copper bar
A_{cell}: Cross-sectional area of the test cell
$A_{o\text{-}ring}$: o-ring contact area with the copper bar surface
c: Constant
d: Distance of gap
h: Heat transfer coefficient
k_{eff}: Effective thermal conductivity of the fluid suspension
$k_{o\text{-}ring}$: Thermal conductivity of the rubber o-ring
k_{copper}: Thermal conductivity of the copper bar
k_f: Thermal conductivity of the base fluid
n: Constant
q: Heat flux
R: Resistance of platinum ribbon at temperature T
R_o: Resistance of platinum ribbon at the reference temperature T_o
∇T_{cell}: Temperature difference between surface of the upper and lower copper bars
∇T_{bar}: Temperature difference between two adjacent thermocouples along the axis of the copper bars
x: The coordinate on the axis of copper bars
∇Z_{bar}: The distance between two adjacent thermocouples along the axis of the copper bars
∇Z_{cell}: Thickness of the test cell
T: Absolute temperature
α: Thermal diffusivity of fluid/ratio of the nanoparticle and base fluid thermal conductivity
α_e: Electric resistance-temperature coefficient of the platinum ribbon
β: Volume expansion coefficient of the fluid
ϕ: Volume fraction of the nanoparticle suspension
μ_{BF}: The viscosity of the base fluid
μ: Viscosity
ν: Kinematic viscosity of the fluid.

Acknowledgments

The authors would like to acknowledge the support of the Office of Naval Research through Grant ONR N000140010454, the National Science Foundation through grant CTS-0312848, and The University of Toledo through the startup grant.

References

[1] S. U. S. Choi, "Enhancing thermal conductivity of fluids with nanoparticles," in *Developments and Applications of Non-Newtonian Flows*, D. A. Siginer and H. P. Wang, Eds., ASME, New York, NY, USA, 1995.

[2] J. A. Eastman, S. U. S. Choi, S. Li, L. J. Thompson, and S. Lee, "Enhanced thermal conductivity through the development of nanofluids," in *Proceedings of the Symposium on Nanophase and Nanocomposite Materials II*, S. Komarneni, J. C. Parker, and H. J. Wollenberger, Eds., vol. 457 of *Materials Research Society Symposium Proceedings*, pp. 3–11, Warrendale, Pa, USA, 1997.

[3] B. Wang, H. Li, and X. Peng, "Effect of surface adsorption on heat transfer enhancement for liquid with nano-particle suspensions," *Journal of Engineering Thermophysics*, vol. 24, no. 4, pp. 465–470, 2000.

[4] B. Wang, H. Li, and X. Peng, "Research on the heat-conduction enhancement for liquid with nano-particle suspensions," *Journal of Thermal Science*, vol. 11, no. 3, pp. 193–288, 2002.

[5] Y. Xuan and Q. Li, "Heat transfer enhancement of nanofluids," *International Journal of Heat and Fluid Flow*, vol. 21, no. 1, pp. 58–64, 2000.

[6] H. Xie, J. Wang, T. Xi, Y. Liu, and F. Ai, "Dependence of the thermal conductivity on nanoparticle-fluid mixture on the base fluid," *Journal of Materials Science Letters*, vol. 21, no. 19, pp. 1469–1471, 2002.

[7] H. Xie, J. Wang, T. Xi, Y. Liu, F. Ai, and Q. Wu, "Thermal conductivity enhancement of suspensions containing nanosized alumina particles," *Journal of Applied Physics*, vol. 91, no. 7, pp. 4568–4572, 2002.

[8] X. Wang, X. Xu, and S. U. S. Choi, "Thermal conductivity of nanoparticle-fluid mixture," *Journal of Thermophysics and Heat Transfer*, vol. 13, no. 4, pp. 474–480, 1999.

[9] B. X. Wang, H. Li, and X. F. Peng, "Research on the effective thermal conductivity of nano-particle colloids," in *Proceedings of the 6th ASME-JSME Thermal Engineering Joint Conference*, Hawaii Island, Hawaii, USA, March 2003, [CD-ROM].

[10] Q.-Z. Xue, "Model for effective thermal conductivity of nanofluids," *Physics Letters A*, vol. 307, no. 5-6, pp. 313–317, 2003.

[11] B. X. Wang, L.-P. Zhou, and X.-F. Peng, "A fractal model for predicting the effective thermal conductivity of liquid with suspension of nanoparticles," *International Journal of Heat and Mass Transfer*, vol. 46, no. 14, pp. 2665–2672, 2003.

[12] S. P. Lee and S. U. S. Choi, "Application of metallic nanoparticle suspensions in advanced cooling systems," in *Recent Advances in Solids/Structures and Application of Metallic Materials*, Y. Kwon, D. Davis, and H. Chung, Eds., PVP vol. 342, MD vol. 72, pp. 227–234, The American Society of Mechanical Engineers, New York, NY, USA, 1996.

[13] C. H. Li and G. P. Peterson, "Mixing effect on the enhancement of the effective thermal conductivity of nanoparticle suspensions (nanofluids)," *International Journal of Heat and Mass Transfer*, vol. 50, no. 23-24, pp. 4668–4677, 2007.

[14] P. Keblinski, S. R. Phillpot, S. U. S. Choi, and J. A. Eastman, "Mechanisms of heat flow in suspensions of nano-sized particles (nanofluids)," *International Journal of Heat and Mass Transfer*, vol. 45, no. 4, pp. 855–863, 2002.

[15] J. A. Eastman, S. U. S. Choi, S. Li, W. Yu, and L. J. Thompson, "Anomalously increased effective thermal conductivities of ethylene glycol-based nanofluids containing copper nanoparticles," *Applied Physics Letters*, vol. 78, no. 6, pp. 718–720, 2001.

[16] S. Lee, S. U. S. Choi, S. Li, and J. A. Eastman, "Measuring thermal conductivity of fluids containing oxide nanoparticles," *Journal of Heat Transfer*, vol. 121, no. 2, pp. 280–288, 1999.

[17] S. K. Das, N. Putra, P. Thiesen, and W. Roetzel, "Temperature dependence of thermal conductivity enhancement for nanofluids," *Journal of Heat Transfer*, vol. 125, no. 4, pp. 567–574, 2003.

[18] C. H. Li and G. P. Peterson, "Experimental investigation of temperature and volume fraction variations on the effective thermal conductivity of nanoparticle suspensions (nanofluids)," *Journal of Applied Physics*, vol. 99, no. 8, Article ID 084314, 2006.

[19] J. C. Maxwell, *A Treatise on Electricity and Magnetism*, vol. 1, Oxford University, New York, NY, USA, 3rd edition, 1892.

[20] R. L. Hamilton and O. K. Crosser, "Thermal conductivity of heterogeneous two-component systems," *Industrial and Engineering Chemistry Fundamentals*, vol. 1, no. 3, pp. 187–191, 1962.

[21] G. P. Peterson and C. H. Li, in *Advances in Heat Transfer*, J. P. Hartnett and T. F. Irvine, Eds., vol. 39, pp. 261–392, Pergamon, New York, NY, USA, 2006.

[22] C. H. Li and G. P. Peterson, "Dual role of nanoparticles in the thermal conductivity enhancement of nanoparticle suspensions," in *Proceedings of the ASME International Mechanical Engineering Congress and Exposition*, vol. 376, pp. 745–750, Orlando, Fla, USA, 2005, [CD-ROM].

[23] S. P. Jang and S. U. S. Choi, "Role of Brownian motion in the enhanced thermal conductivity of nanofluids," *Applied Physics Letters*, vol. 84, no. 21, pp. 4316–4318, 2004.

[24] R. Prasher, P. Bhattacharya, and P. E. Phelan, "Thermal conductivity of nanoscale colloidal solutions (nanofluids)," *Physical Review Letters*, vol. 94, no. 2, Article ID 025901, pp. 1–4, 2005.

[25] Y. Xuan and Q. Li, "Investigation on convective heat transfer and flow features of nanofluids," *Journal of Heat Transfer*, vol. 125, no. 1, pp. 151–155, 2003.

[26] S. M. You, J. H. Kim, and K. H. Kim, "Effect of nanoparticles on critical heat flux of water in pool boiling heat transfer," *Applied Physics Letters*, vol. 83, no. 16, pp. 3374–3376, 2003.

[27] S. K. Das, N. Putra, and W. Roetzel, "Pool boiling characteristics of nano-fluids," *International Journal of Heat and Mass Transfer*, vol. 46, no. 5, pp. 851–862, 2003.

[28] M. Okada and T. Suzuki, "Natural convection of water—fine particle suspension in a rectangular cell," *International Journal of Heat and Mass Transfer*, vol. 40, no. 13, pp. 3201–3208, 1997.

[29] C. Kang, M. Okada, A. Hattori, and K. Oyama, "Natural convection of water-fine particle suspension in a rectangular vessel heated and cooled from opposing vertical walls (classification of the natural convection in the case of suspension with a narrow-size distribution)," *International Journal of Heat and Mass Transfer*, vol. 44, no. 15, pp. 2973–2982, 2001.

[30] K. Khanafer, K. Vafai, and M. Lightstone, "Buoyancy-driven heat transfer enhancement in a two-dimensional enclosure utilizing nanofluids," *International Journal of Heat and Mass Transfer*, vol. 46, no. 19, pp. 3639–3653, 2003.

[31] R.-Y. Jou and S.-C. Tzeng, "Numerical research of nature convective heat transfer enhancement filled with nanofluids in rectangular enclosures," *International Communications in Heat and Mass Transfer*, vol. 33, no. 6, pp. 727–736, 2006.

[32] N. Putra, W. Roetzel, and S. K. Das, "Natural convection of nano-fluids," *Heat and Mass Transfer*, vol. 39, no. 8-9, pp. 775–784, 2003.

[33] D. Wen and Y. Ding, "Formulation of nanofluids for natural convective heat transfer applications," *International Journal of Heat and Fluid Flow*, vol. 26, no. 6, pp. 855–864, 2005.

[34] B. Chen, F. Mikami, and N. Nishikawa, "Experimental studies on transient features of natural convection in particles suspensions," *International Journal of Heat and Mass Transfer*, vol. 48, no. 14, pp. 2933–2942, 2005.

[35] N. Shenogina, R. Godawat, P. Keblinski, and S. Garde, "How wetting and adhesion affect thermal conductance of a range of hydrophobic to hydrophilic aqueous interfaces," *Physical Review Letters*, vol. 102, Article ID 156101, 2009.

[36] X. F. Li, D. S. Zhu, X. J. Wang, N. Wang, J. W. Gao, and H. Li, "Thermal conductivity enhancement dependent pH and chemical surfactant for Cu-H_2O nanofluids," *Thermochimica Acta*, vol. 469, no. 1-2, pp. 98–103, 2008.

[37] C. H. Li and G. P. Peterson, "Development in the effective thermal conductivity research of nanoparticle suspensions (nanofluids)," in *Nanoparticles: New Research*, S. L. Lombardi, Ed., Nova Science, 2008.

[38] J. B. Gordon, "Nanofluids: Rheology and its Implication on Heat Transfer," private seminar, MIT, Boston, Mass, USA, April 2006.

[39] H. C. Brinkman, "The viscosity of concentrated suspensions and solutions," *The Journal of Chemical Physics*, vol. 20, no. 4, pp. 571–581, 1952.

[40] B. C. Pak and Y. I. Cho, "Hydrodynamic and heat transfer study of dispersed fluids with submicron metallic oxide particles," *Experimental Heat Transfer*, vol. 11, no. 2, pp. 151–170, 1998.

[41] Y. Xuan and W. Roetzel, "Conceptions for heat transfer correlation of nanofluids," *International Journal of Heat and Mass Transfer*, vol. 43, no. 19, pp. 3701–3707, 2000.

[42] Y. Xuan and Q. Li, "Investigation on convective heat transfer and flow features of nanofluids," *Journal of Heat Transfer*, vol. 125, no. 1, pp. 151–155, 2003.

[43] J. Eastman, S. R. Phillpot, S. U. S. Choi, and P. Keblinski, "Thermal transport in nanolfuids," *Annual Review of Material Research*, vol. 34, pp. 219–246, 2004.

[44] A. S. Ahuja, "Augmentation of heat transport in laminar flow of polystyrene suspensions. I. Experiments and results," *Journal of Applied Physics*, vol. 46, no. 8, pp. 3408–3416, 1975.

[45] A. S. Ahuja, "Augmentation of heat transport in laminar flow of polystyrene suspensions. II. Analysis of the data," *Journal of Applied Physics*, vol. 46, no. 8, pp. 3417–3425, 1975.

[46] B. Gebhart, Y. Jaluria, R. L. Mahajan, and B. Sammakia, *Buoyancy-Induced Flows and Transport*, Hemisphere, Washingtong, DC, USA, 1988.

[47] D. Y. Tzou, "Thermal instability of nanofluids in natural convection," *International Journal of Heat and Mass Transfer*, vol. 51, no. 11-12, pp. 2967–2979, 2008.

Hindawi Publishing Corporation
Advances in Mechanical Engineering
Volume 2010, Article ID 976254, 10 pages
doi:10.1155/2010/976254

Research Article

Numerical Simulation of Water/Al_2O_3 Nanofluid Turbulent Convection

Vincenzo Bianco, Oronzio Manca, and Sergio Nardini

Dipartimento di Ingegneria Aerospaziale e Meccanica, Seconda Università degli Studi di Napoli, Via Roma 29, 81031 Aversa, Italy

Correspondence should be addressed to Vincenzo Bianco, vbianco@libero.it

Received 30 July 2009; Revised 15 April 2010; Accepted 19 April 2010

Academic Editor: Yogesh Jaluria

Turbulent forced convection flow of a water-Al_2O_3 nanofluid in a circular tube subjected to a constant and uniform temperature at the wall is numerically analyzed. The two-phase mixture model is employed to simulate the nanofluid convection, taking into account appropriate thermophysical properties. Particles are assumed spherical with a diameter equal to 38 nm. It is found that convective heat transfer coefficient for nanofluids is greater than that of the base liquid. Heat transfer enhancement is increasing with the particle volume concentration and Reynolds number. Comparisons with correlations present in the literature are accomplished and a very good agreement is found with Pak and Cho (1998). As for the friction factor, it shows a good agreement with the classical correlation used for normal fluid, such as Blasius formula.

1. Introduction

In a thermal system, convective heat transfer rate can be enhanced passively by changing flow geometry, boundary conditions, or by improving thermophysical properties, for example, enhancing fluid thermal conductivity. Suspending small solid particles in a fluid represents an innovative way to improve its thermal conductivity.

First studies on possibility of increasing thermal conductivity of a solid-liquid mixture by adding more volume fraction of solid particles were in Maxwell [1, 2]. Several investigations revealed that the thermal conductivity of the nanoparticles suspension could be increased by more than 20% for the case of very low nanoparticles concentrations [3–10].

Different concepts and models have been proposed to explain the enhancement in heat transfer [8, 11–14]. Theoretical and experimental investigations have been accomplished to estimate the effective thermal conductivity of nanofluids. Some experimental studies [15, 16] show that the measured thermal conductivity of nanofluids is much larger than the classical theoretical predictions [17]. Other experimental investigations [18, 19] found that the thermal conductivity has not shown any anomalous enhancement, and for lower volume fractions the results agree well with the classical equations [17, 20]. Many attempts have been made to formulate efficient theoretical models for the prediction of the effective thermal conductivity, but there is still a lack on this topic [21–23].

Relatively few theoretical and experimental investigations have been reported on convective heat transfer in confined flows, as also reviewed in [7–9, 24]. Experimental results are provided for convective heat transfer of nanofluids laminar and turbulent flow inside a tube in [11, 25–30].

Furthermore, a number of numerical studies dealt with laminar and turbulent convection. Basically there are two approaches to simulate nanofluids convection, the first approach consists of the single-phase model where the fluid with the suspended nanoparticles is assumed to be continuous, while the second approach uses a two-phase model in order to get a better description of the mixture taking into account the interactions between the liquid and the nanoparticles. The single-phase model with physical and thermal properties-all assumed to be constant with

temperature was, employed in [31–34]. It represents the simplest way to treat numerically the nanofluids, anyway this method was successfully validated with experimental data.

A numerical study on fully developed laminar mixed convection of a nanofluid consisting of water and Al_2O_3 in a horizontal curved tube was carried out in [35]. Three-dimensional elliptic-governing equations were used and the single phase model was employed. It was found that the nanoparticles volume fraction does not have a direct effect on the secondary flow, axial velocity, or the skin friction coefficient. For a given Reynolds number, a negative effect of buoyancy force on the Nusselt number was obtained while the nanoparticles concentration had a positive effect on the heat transfer enhancement and also on the skin friction reduction. The two-phase approach seems a better model to describe the nanofluid flow. In fact, the slip velocity between the fluid and particles may not be zero [11] due to several factors such as gravity, friction between the fluid and solid particles and Brownian forces, and the phenomena of Brownian diffusion, sedimentation, and dispersion. The two-phase approach provides a field description of the dynamics of each phase or, alternatively, the Lagrangian trajectories of individual particles coupled with the Eulerian description of the fluid flow field [36, 37]. Recently, a single- and two-phase model was employed with either constant or temperature-dependent properties [38]. The results for the two-models were quite similar, so the simpler model may be employed. Quite recently, a two phase mixture model was applied to study the turbulent forced convection flow of a nanofluid in a uniformly heated tube [39]. The comparison of calculated results with experimental values shows that the mixture model is more accurate than the single-phase model.

In the present paper, developing turbulent forced convection flow of Al_2O_3/water nanofluid in circular tube is numerically investigated. Steady state of a two-dimensional axial symmetric flow is considered and the channel is heated at uniform wall temperature. Alumina particles have a spherical size of 38 nm diameter.

The finite volume method is employed to solve the problem and the two phase approach is used to evaluate the developing forced convection flow. The obtained results are presented in terms of temperature distributions, local and average heat, mass transfer coefficients, and Nusselt number profiles.

2. Mathematical Modelling

Figure 1 shows the considered geometrical configuration. It consists of a tube with length (L) of 1.0 m and circular section with the diameter (D) equal to 0.01 m.

The considered nanofluid is a mixture composed of water and particles of Al_2O_3, with a diameter of 38 nm. The fluid enters with uniform temperature, $T_0 = 293$ K, and velocity profiles at the inlet section and the tube length is appropriate in order to obtain fully developed profiles (of velocity and temperature) at the outlet section. The condition of uniform wall temperature is considered and the flow and the thermal field are assumed to be symmetrical with respect to the vertical plane passing through the tube main axis, so half tube is considered, in order to save computational time without loosing in accuracy.

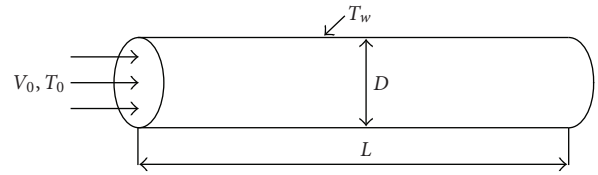

Figure 1: Schemae of the configuration under investigation.

2.1. Governing Equations. The two-phase mixture model is employed to analyze the thermal and fluid dynamic behavior of the considered nanofluid.

In the mixture model the fluid is considered to be a single fluid with two phases and the coupling between them is strong [39]. But each phase has its own velocity vector and within a given control volume there is a certain fraction of each phase.

One of the major issues in these simulations is found to be the evaluation of nanofluid thermophysical properties in general and viscosity and thermal conductivity in particular, because the use of classical models is questionable for nanofluids. On the other hand, too few experimental data on nanofluids are available to build new models.

The following formulation represents the mathematical description of the mixture model governing equations [39, 40].

Conservation of mass:

$$\nabla \cdot \left(\rho_m \vec{V}_m\right) = 0. \tag{1}$$

Conservation of momentum:

$$\nabla \cdot \left(\rho_m \vec{V}_m \vec{V}_m\right) = -\nabla P_m + \nabla \cdot (\tau - \tau_t) + \nabla \cdot \left(\sum_{k=1}^{n} \varphi_k \rho_k \vec{V}_{dr,k} \vec{V}_{dr,k}\right), \tag{2}$$

where $\vec{V}_{dr,k}$ is the drift velocity of the kth phase.

Volume fraction:

$$\nabla \cdot \left(\phi_p \rho_p \vec{V}_m\right) = -\nabla \cdot \left(\phi_p \rho_p \vec{V}_{dr,p}\right). \tag{3}$$

Conservation of energy:

$$\nabla \cdot \left(\sum_{k=1}^{n} \varphi_k \vec{V}_k (\rho_k H_k + P)\right) = \nabla \cdot \left(\lambda \nabla T - C_p \rho_m \overline{vt}\right). \tag{4}$$

Compression work and the viscous dissipation are assumed negligible in the energy equation (4).

In the equation of the conservation of momentum, (2), $\vec{V}_{dr,k}$ is the drift velocity for secondary phase k (i.e., the nanoparticles in the present study), defined as

$$\vec{V}_{dr,k} = \vec{V}_k - \vec{V}_m,$$
$$\tau = \mu_m \nabla \vec{V}_m, \tag{5}$$
$$\tau_t = \sum_{k=1}^{n} \varphi_k \rho_k \overline{v_k v_k}.$$

The slip velocity (relative velocity) is defined as the velocity of secondary phase (p) relative to the velocity of the primary phase (f)

$$\vec{V}_{pf} = \vec{V}_p - \vec{V}_f. \tag{6}$$

The drift velocity is related to the relative velocity

$$\vec{V}_{dr,p} = \vec{V}_{pf} - \sum_{k=1}^{n} \frac{\varphi_k \rho_k}{\rho_m} \vec{V}_{fk}. \tag{7}$$

The relative velocity, determined from (5) proposed by Manninen et al. [41] while from (6) by Schiller and Naumann [42] is used to calculate the drag function f_{drag}

$$\vec{V}_{pf} = \frac{\rho_p d_p^2}{18 \mu_f f_{\text{drag}}} \frac{\left(\rho_p - \rho_m\right)}{\rho_p} a, \tag{8}$$

$$f_{\text{drag}} = \begin{cases} 1 + 0.15\,\text{Re}_p^{0.687} & \text{Re}_p \le 1000 \\ 0.0183\,\text{Re}_p & \text{Re}_p > 1000. \end{cases} \tag{9}$$

The acceleration in (8) is

$$a = g - \left(\vec{V}_m \cdot \nabla\right) \vec{V}_m. \tag{10}$$

2.2. Turbulence Modeling. To close the governing equations of the thermofluid dynamics field. Experimental data or approximate models are necessary to close the governing equations of thermofluid dynamics fields in turbulence phenomena.

In the present work, the k-ε model proposed by Launder and Spalding [43] is considered. The k-ε model introduces two new equations, one for the turbulent kinetic energy and the other for the rate of dissipation. The two equations can be expressed in the following form:

$$\nabla \cdot \left(\rho_m \vec{V}_m k\right) = \nabla \cdot \left(\frac{\mu_{t,m}}{\sigma_k} \nabla k\right) + G_{k,m} - \rho_m \varepsilon, \tag{11}$$

$$\nabla \cdot \left(\rho_m \vec{V}_m \varepsilon\right) = \nabla \cdot \left(\frac{\mu_{t,m}}{\sigma_k} \nabla \varepsilon\right) + \frac{\varepsilon}{\kappa} \left(C_1 G_{k,m} - C_2 \rho_m \varepsilon\right), \tag{12}$$

where

$$\mu_{t,m} = \rho_m C_\mu \frac{k^2}{\varepsilon}, \tag{13}$$

$$G_{k,m} = \mu_{t,m} \left(\nabla \vec{V}_m + \left(\nabla \vec{V}_m\right)^T\right) \tag{14}$$

with $C_1 = 1.44$, $C_2 = 1.92$, $C_\mu = 0.09$, $\sigma_k = 1$, $\sigma_\varepsilon = 1.3$.

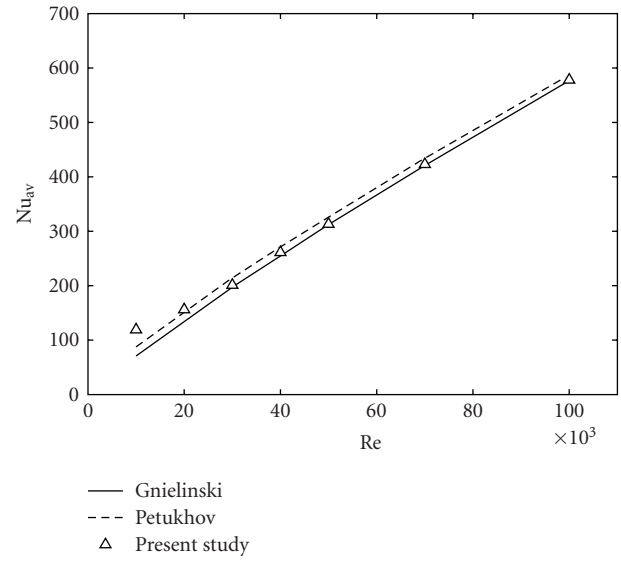

Figure 2: Grid validation by means of correlations suggested by Gnielinski [44] and Petukhov [45].

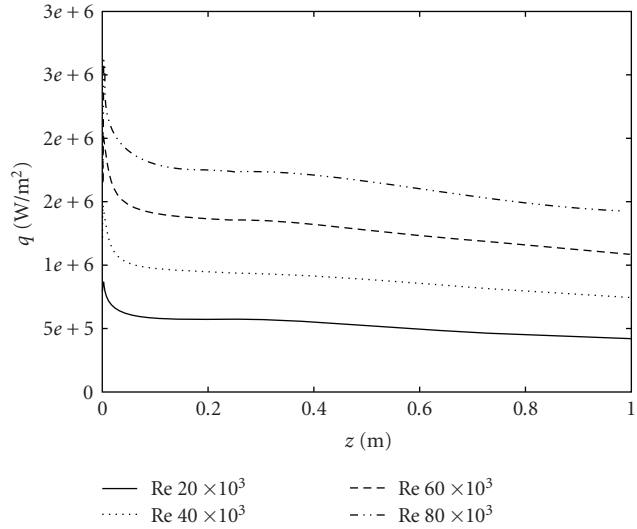

Figure 3: Heat flux for $\varphi = 4\%$ and several Reynolds numbers.

2.3. Boundary Conditions. At the channel inlet profiles, uniform axial velocity V_0 and temperature $T_0 = 293\,\text{K}$ are assumed. Moreover, a constant intensity turbulence, equal to 1%, is imposed. At the channel exit section, the fully developed conditions are considered, that is to say that all axial derivatives are zero. On the channel wall, the non-slip conditions and a uniform temperature of 350 K are imposed, while both turbulent kinetic energy and dissipation of turbulent kinetic energy are equal to zero. Moreover, flow and thermal fields are assumed symmetrical with respect to the axial plane.

2.4. Nanofluids Physical Properties. The most difficult problem in nanofluids simulation is represented by the evaluation of thermophysical properties, particularly viscosity

and thermal conductivity, because it is not clear if classical equations give reliable results. But on the other hand, too few experimental data are available to build new models [40].

In the present paper, the following equations are considered to evaluate Al_2O_3/water nanofluid thermophysical properties:

$$\rho_{nf} = (1-\varphi)\rho_{bf} + \varphi\rho_p, \tag{15}$$

$$Cp_{nf} = (1-\varphi)Cp_{bf} + \varphi Cp_p, \tag{16}$$

$$\mu_r = \frac{\mu_{nf}}{\mu_{bf}} = 123\varphi^2 + 7.3\varphi + 1, \tag{17}$$

$$\lambda_r = \frac{\lambda_{nf}}{\lambda_{bf}} = 4.97\varphi^2 + 2.72\varphi + 1. \tag{18}$$

Equations (15) and (16) are based on the classical theory of two-phase mixture and given in [25, 31–33, 39, 40]. Equation (16) was first employed in [25] and then utilized in many different papers [31–33, 38, 40]. Another formulation of specific heat, based on heat capacity concept, is present in literature, see for example [46]. The two formulations may, of course, provide some differences for specific heat values, but due to the lack of data both formulations can be considered equivalent, as observed in [47]. Equation (17) was proposed in [31–33, 48] and obtained as a result of a least square curve fitting of available experimental data [14, 49, 50] for the considered mixture. As for thermal conductivity, (18) was obtained in [31–33] using the well-known model proposed by Hamilton and Crosser [17], assuming spherical particles. Such a model, which was first developed on data from several mixtures containing relatively large particles, that is, millimeter and micrometer size particles, is believed to be acceptable for use with nanofluids, although it may give underestimated values of thermal conductivity. The equations employed to evaluate thermophysical properties are also appropriate for turbulence flow without any modification [39, 51].

In the present paper the thermo-physical properties considered for Al_2O_3 are [48]

$$\rho_p = 3880\,\frac{\text{kg}}{\text{m}^3}; \quad Cp_p = 773\,\frac{\text{J}}{\text{kgK}}; \quad \lambda_p = 36\,\frac{\text{W}}{\text{mK}}, \tag{19}$$

and those of base fluid are

$$\rho_{bf} = 998.2\,\frac{\text{kg}}{\text{m}^3}, \quad Cp_{bf} = 4182\,\frac{\text{J}}{\text{kgK}}, \quad \lambda_{bf} = 0.597\,\frac{\text{W}}{\text{mK}},$$
$$\mu_{bf} = 9.93\times10^{-4}\,\frac{\text{kg}}{\text{ms}}. \tag{20}$$

It should be underlined that the assumption of thermophysical properties constant with temperature may determine some error in the numerical results, mainly with respect to the viscosity. In fact, it changes by a factor of 2 from 293 K to 350 K.

2.5. Numerical Method and Validation. The computational fluid dynamic code FLUENT [52] was employed to solve the present problem. The governing equations (1)–(4) were solved by control volume approach. This method is based on the spatial integration of the conservation equations over finite control volumes, converting the governing equations to a set of algebraic equations. The algebraic "discretized equations" resulting from this spatial integration process were sequentially solved throughout the physical domain considered. FLUENT [52] solves the systems resulting from discretization schemes using a numerical method. The residuals resulting from the integration of the governing equations (1)–(4) are considered as convergence indicators.

In order to ensure the accuracy as well as the consistency of numerical results, several nonuniform grids have been

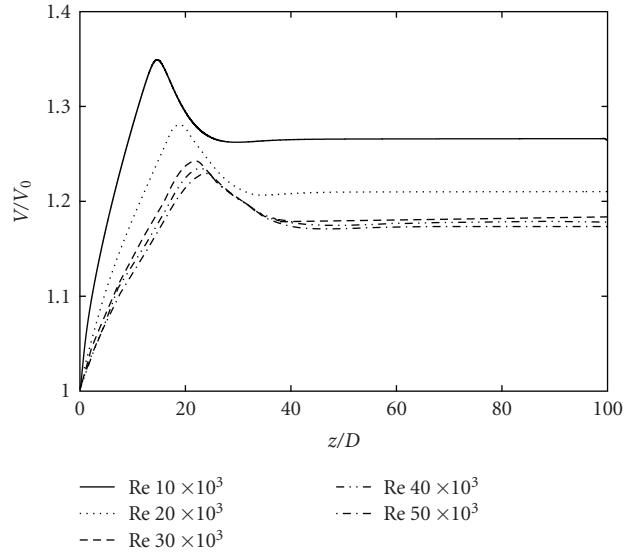

Figure 4: Axial profiles of centreline velocity referred to the average velocity for $\varphi = 4\%$ and different Re values.

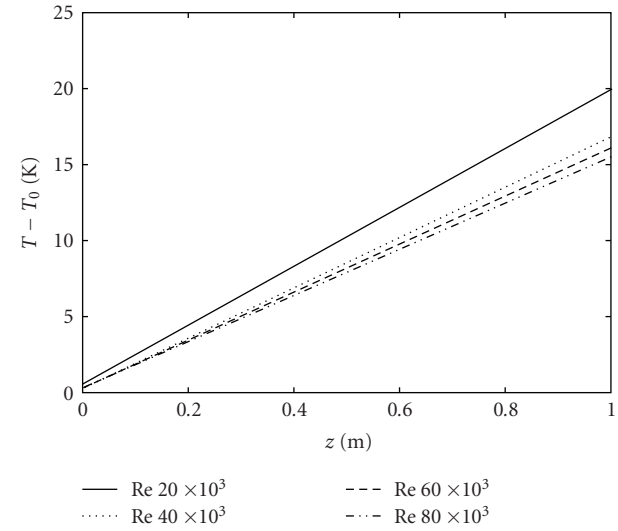

Figure 5: Profiles of bulk temperature along tube axis for Re = 4.0 × 10^4 and several concentrations.

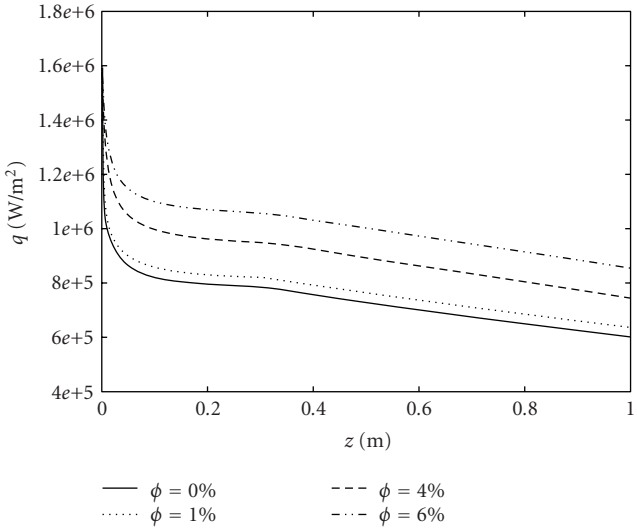

Figure 6: Heat flux for Re = 4.0×10^4 and several concentrations.

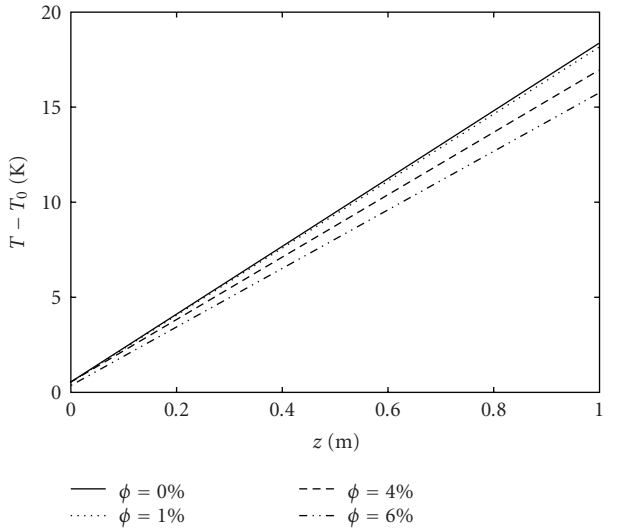

Figure 7: Profiles of bulk temperature along tube axis for Re = 4.0 $\times 10^4$ and several concentrations.

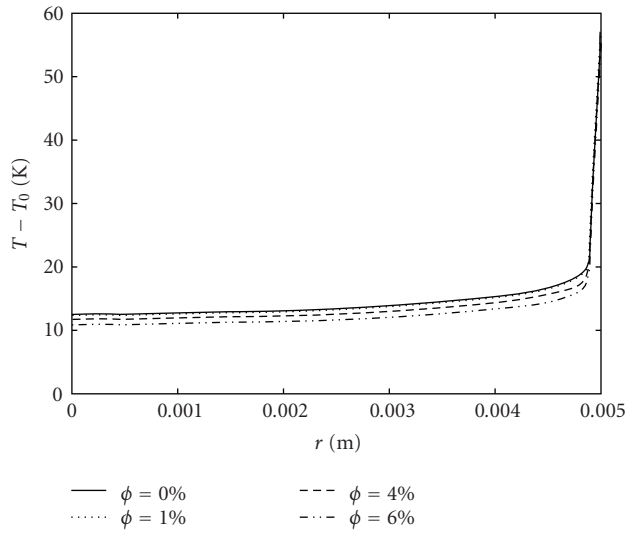

Figure 8: Profiles of temperature along tube radius at $z/L = 1$ for Re = 4.0×10^4 and several concentrations.

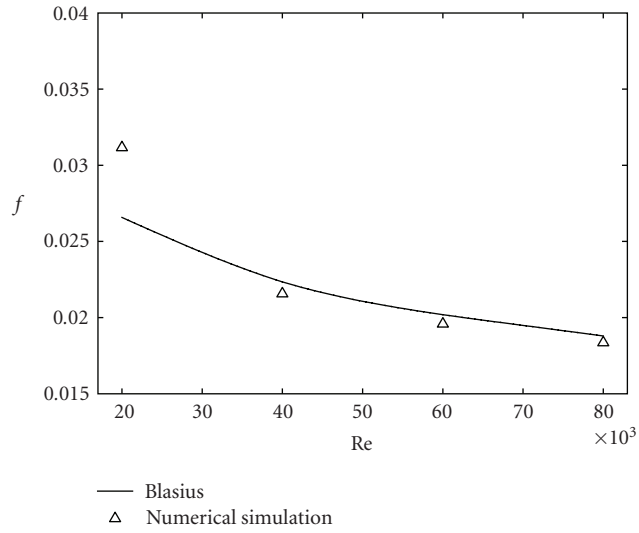

Figure 9: Friction factor as a function of Reynolds number for φ = 4%.

submitted to an extensive testing procedure for each of the cases considered.

Preliminary tests were carried out to test the accuracy of the numerical solution. To this scope four different grids were compared in terms of Nusselt number and the relative errors are reported in Table 1.

Results have shown that, for the problem under consideration, the $20 \times 24 \times 400$ non-uniform grid "3" appears to be satisfactory to ensure the precision of numerical results as well as their independency with respect to the number of nodes used. Such grid has, respectively, 20, 24, and 400 nodes along the radial, tangential, and axial directions, with highly packed grid points in the vicinity of the tube wall and especially at the entrance region.

The computer model has been successfully validated with correlation reported in [44, 45] for thermally and hydraulically developing flow with uniform heat flux on the wall, showing an average error of 3%, as reported in Figure 2.

3. Results

Investigations were carried out employing the two-phase mixture model, for concentration φ = 0%, 1%, 4%, and 6% and an imposed uniform wall temperature T_w = 350 K.

Heat flux profiles on tube wall are reported in Figure 3 for φ = 4% and several values of Reynolds number, Re = 2.0×10^4, 4.0×10^4, 6.0×10^4, and 8.0×10^4. Heat flux profiles are decreasing due to the heating of the fluid along the tube and their slope are nearly independent on the Reynolds number. The increase of local heat flux with respect to an increase of the Reynolds number is almost linear.

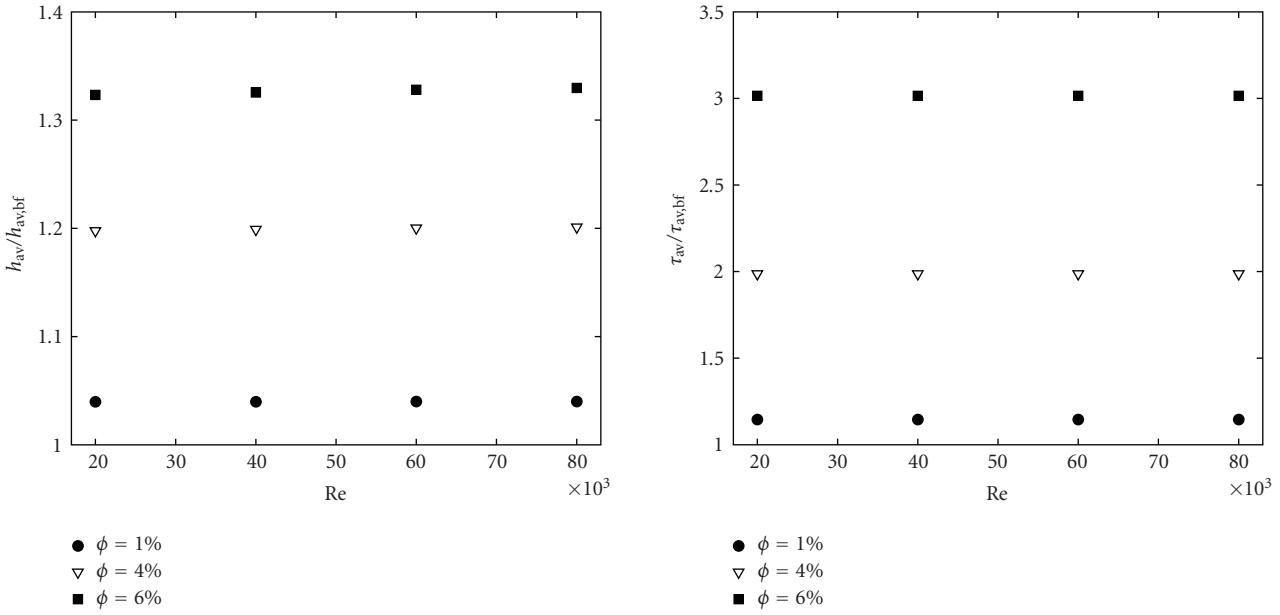

Figure 10: (a) Average heat transfer coefficient ratio; (b) average shear stress coefficient ratio.

Table 1: Differences in terms of Nusselt number among the different tested grids. Grid "1" has 5×6×200 elements, respectively on the radius, circumference, and longitudinal axis, grid "2" 10×12×400 elements, grid "3" 20×24×400 elements, and grid "4" 20×24×800 elements.

z/D	$\Delta Nu_{2,1}$	$\Delta Nu_{3,2}$	$\Delta Nu_{4,3}$
1	9.66%	2.53%	0.97%
10	−1.76%	8.35%	−0.02%
50	−0.39%	8.82%	0.00%
70	−0.41%	8.87%	0.00%
99	−0.24%	8.85%	0.02%

The development of the axial velocity along the tube centreline for φ = 4% and Re from 1.0×10^4 to 5.0×10^4 is shown in Figure 4. The results suggest the existence of a fully developed region for z/D = 30, for Re equals to $1.0 \cdot 10^4$, and $2.0 \cdot 10^4$, whereas in the other cases the developing length is equal to about z/D = 40. It is noted that, immediately after the tube inlet, the boundary layer growth pushes the fluid towards the centreline region, causing an increase of the centreline velocity in accordance with [39]. As the Reynolds number increases, the velocity maximum point moves further downstream, because the increase of axial momentum transports the generated turbulence in the flow direction. After the maximum point, the velocity at the centreline decreases in order to satisfy the continuity equation. Moreover, it is interesting to note that the maximum and fully developed values of the nondimensional centreline velocity decrease as Reynolds number increases. This effect is due to the fact that the corresponding velocity profiles become more uniform as Re increases.

Figure 5 presents bulk temperature along tube axis for φ = 4% and several values of Reynolds number. The profiles are linear and their slopes depend on Reynolds number value. The effect of Reynolds number is strong passing from Re = 2.0×10^4 to Re = 4.0×10^4 and becomes weaker for higher values.

The dependence of particle volume concentration on wall heat flux is reported in Figure 6 for Re = 4.0×10^4. It is very clear that the beneficial effect due to nanoparticles presence is due to the improvement of thermal proprieties of the mixture, whereas the additional effects such as gravity, drag on the particles, diffusion, and Brownian forces can be negligible in turbulent flows. Wall heat fluxes at z/L = 1 for φ = 1%, 4%, and 6% are higher than that for the base fluid of 4%, 24%, and 41%, respectively.

As a consequence of the heat transfer enhancement, bulk temperature decreases with particle volume concentration, as shown in Figure 7, passing at z/L = 1 section from 311 K for φ = 0% to 309 K for φ = 6%.

In Figure 8 radial temperature profiles at z/L = 1 for Re = 4.0×10^4 are reported for the investigated particle volume concentrations. For all concentration values, temperature is slightly dependent on position except when close to the tube wall. When concentration increases, temperature decreases. Furthermore, the difference between temperature values for base fluid and nanofluids increases as r increases, indicating again an augmentation in heat transfer.

The increase of the total heat transfer rates with the use of suspended nanoparticles is accompanied by an increment of the corresponding wall shear stress. A comparison between the friction factor determined from the Blasius relation

$$f = 0.316\,\mathrm{Re}^{-025} \tag{21}$$

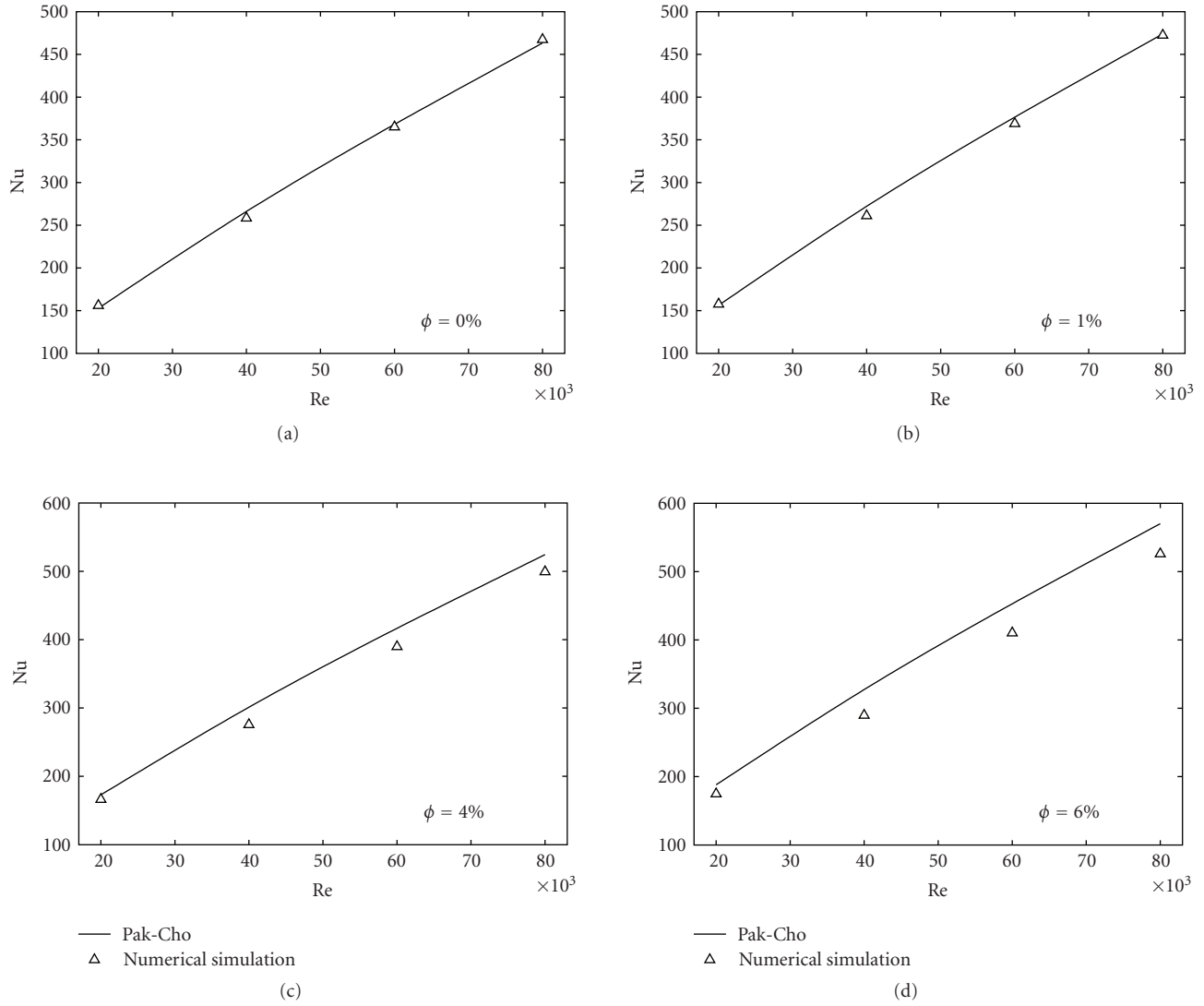

Figure 11: Average Nusselt number as a function of the Reynolds number for: (a) base fluid ($\varphi = 0\%$); (b) $\varphi = 1\%$; (c) $\varphi = 4\%$; (d) $\varphi = 6\%$.

and that calculated from present numerical investigation results is presented in Figure 9 for $\varphi = 4\%$. Data are in good agreement particularly for high Reynolds number values. The discrepancy at lower Re values could be due to the assumption of constant properties in the numerical simulations. It should be underlined that f is not dependent on φ value.

In Figure 10 the ratios between the nanofluids and basic fluid average heat transfer coefficients and shear stresses are reported for all the Reynolds numbers and concentrations investigated. Heat transfer coefficient ratios (Figure 10(a)) and shear stresses ratios (Figure 10(b)) are almost constant for each concentration value, so the percent increase is independent on Reynolds number. As the concentration increases, in an increment of the heat transfer coefficient, respect to the basic fluid of about 5%, 20% and 30% for particles concentrations of 1%, 4% and 6% respectively is detected. The corresponding increase in the shear stress ratios is significant, in fact there is an increase of 10%, 200%, and 300% for particles concentration of 1%, 4%, and 6%, respectively.

In Figure 11 average Nusselt numbers are reported together with those from correlation by Pak and Cho [25]. It is clear the strong agreement particularly for low Reynolds number values. In fact, the average error is less than 5% for particles concentration of 1% and 4%, while for a concentration of 6% (Figure 11(d)) the maximum error is 8%.

4. Conclusions

The present paper dealt with the stationary turbulent convection of water-Al_2O_3 nanofluid inside a circular tube, that was numerically investigated by means of finite volume method. The two-phase mixture model was employed to simulate the nanofluid convection, taking into account appropriate thermo-physical properties.

The results showed that heat transfer increased according to the particles volume concentration, but it was accompanied by increasing wall-shear stress values.

The highest heat transfer rates were detected, for each concentration, in correspondence to the highest Reynolds number; moreover a good agreement is found among the results of this study and the experimental correlation proposed by Pack and Cho [25]. This allows us to confirm that the mixture model approach for the simulation of nanofluid is satisfactory, as sustained also in [39, 40]. However, it seems that the accuracy of the model could be improved by using a better description of nanofluid thermophysical properties taking into account also the temperature dependence. Moreover, the need to investigate the effect of nanoparticle diameter is recognized as an important topic for future studies.

Nomenclature

a: Acceleration, m/s^2
Cp: Specific heat of the fluid, J/kgK
D: Hydraulic diameter, m
d: Particles diameter, m
f_{drag}: Drag function
g: Gravity acceleration, m/s^2
h: Heat transfer coefficient, W/m^{2}K
H: Hentalpy, J/kg
L: Channel length, m
Nu: Nusselt number, $\text{Nu} = \text{hD}_h/\text{k}_0$
k: Turbulent kinetic energy, m^2/s^2
P: Pressure, Pascal
q: Wall heat flux, W/m^2
Re: Reynolds number, $\text{Re} = \text{V}_0\text{D}_h/\mu$
T, t: Time-mean and fluctuating temperature, K
V,v: Time-mean and fluctuating velocity, m/s
z: Axial coordinate, m.

Greek Letters

ε: Dissipation of turbulent kinetic energy, m^2/s^3
φ: Particle volume concentration
λ: Thermal conductivity of the fluid, W/mK
μ: Fluid dynamic viscosity, kg/ms
ρ: Fluid density, kg/m^3
τ: Wall shear stress, Pa.

Subscripts

av: Average value
b: Bulk value
dr: Drif
m: Mixture
bf: Refers to base-fluid
nf: Refers to nanofluid property
f: Primary phase
p: Refers to particle property
r: Refers to "nanofluid/base-fluid" ratio
w: Value at wall channel
0: Refers to the reference (inlet) condition
k: The kth phase
t: Turbulent.

Acknowledgments

The authors would like to thank the anonymous reviewers for very helpful comments useful in improving the quality of the present paper. This work was supported by MIUR with Articolo 12 D. M. 593/2000 Grandi Laboratori "EliosLab."

References

[1] J. C. Maxwell, *Electricity and Magnetism*, Clarendon Press, Oxford, UK, 1873.
[2] J. C. Maxwell, *A Treatise on Electricity and Magnetism*, Oxford University Press, Cambridge, UK, 2nd edition, 1881.
[3] Y. Xuan and Q. Li, "Heat transfer enhancement of nanofluids," *International Journal of Heat and Fluid Flow*, vol. 21, no. 1, pp. 58–64, 2000.
[4] S. M. S. Murshed, K. C. Leong, and C. Yang, "Enhanced thermal conductivity of TiO_2—water based nanofluids," *International Journal of Thermal Sciences*, vol. 44, no. 4, pp. 367–373, 2005.
[5] K. Khanafer, K. Vafai, and M. Lightstone, "Buoyancy-driven heat transfer enhancement in a two-dimensional enclosure utilizing nanofluids," *International Journal of Heat and Mass Transfer*, vol. 46, no. 19, pp. 3639–3653, 2003.
[6] A.-R. A. Khaled and K. Vafai, "Heat transfer enhancement through control of thermal dispersion effects," *International Journal of Heat and Mass Transfer*, vol. 48, no. 11, pp. 2172–2185, 2005.
[7] R. Chein and J. Chuang, "Experimental microchannel heat sink performance studies using nanofluids," *International Journal of Thermal Sciences*, vol. 46, no. 1, pp. 57–66, 2007.
[8] G. Polidori, S. Fohanno, and C. T. Nguyen, "A note on heat transfer modelling of Newtonian nanofluids in laminar free convection," *International Journal of Thermal Sciences*, vol. 46, no. 8, pp. 739–744, 2007.
[9] X.-Q. Wang and A. S. Mujumdar, "Heat transfer characteristics of nanofluids: a review," *International Journal of Thermal Sciences*, vol. 46, no. 1, pp. 1–19, 2007.
[10] J. A. Eastman, U. S. Choi, S. Li, G. Soyez, L. J. Thompson, and R. J. DiMelfi, "Novel thermal properties of nanostructured materials," *Materials Science Forum*, vol. 312–314, pp. 629–634, 1999.
[11] Y. Xuan and Q. Li, "Heat transfer enhancement of nanofluids," *International Journal of Heat and Fluid Flow*, vol. 21, no. 1, pp. 58–64, 2000.
[12] Y. Xuan and W. Roetzel, "Conceptions for heat transfer correlation of nanofluids," *International Journal of Heat and Mass Transfer*, vol. 43, no. 19, pp. 3701–3707, 2000.
[13] P. Keblinski, S. R. Phillpot, S. U. S. Choi, and J. A. Eastman, "Mechanisms of heat flow in suspensions of nano-sized particles (nanofluids)," *International Journal of Heat and Mass Transfer*, vol. 45, no. 4, pp. 855–863, 2002.
[14] X. Wang, X. Xu, and S. U. S. Choi, "Thermal conductivity of nanoparticle-fluid mixture," *Journal of Thermophysics and Heat Transfer*, vol. 13, no. 4, pp. 474–480, 1999.
[15] S. U. S. Choi, Z. G. Zhang, W. Yu, F. E. Lockwood, and E. A. Grulke, "Anomalous thermal conductivity enhancement in nanotube suspensions," *Applied Physics Letters*, vol. 79, no. 14, pp. 2252–2254, 2001.

[16] D.-H. Yoo, K. S. Hong, and H.-S. Yang, "Study of thermal conductivity of nanofluids for the application of heat transfer fluids," *Thermochimica Acta*, vol. 455, no. 1-2, pp. 66–69, 2007.

[17] R. L. Hamilton and O. K. Crosser, "Thermal conductivity of heterogeneous two-component systems," *Industrial and Engineering Chemistry Fundamentals*, vol. 1, no. 3, pp. 187–191, 1962.

[18] S. A. Putnam, D. G. Cahill, P. V. Braun, Z. Ge, and R. G. Shimmin, "Thermal conductivity of nanoparticle suspensions," *Journal of Applied Physics*, vol. 99, no. 8, Article ID 084308, 2006.

[19] X. Zhang, H. Gu, and M. Fuj II, "Effective thermal conductivity and thermal diffusivity of nanofluids containing spherical and cylindrical nanoparticles," *Experimental Thermal and Fluid Science*, vol. 31, no. 6, pp. 593–599, 2007.

[20] S. M. S. Murshed, K. C. Leong, and C. Yang, "Investigations of thermal conductivity and viscosity of nanofluids," *International Journal of Thermal Sciences*, vol. 47, no. 5, pp. 560–568, 2008.

[21] Q.-Z. Xue, "Model for effective thermal conductivity of nanofluids," *Physics Letters A*, vol. 307, no. 5-6, pp. 313–317, 2003.

[22] Y. Xuan, Q. Li, and W. Hu, "Aggregation structure and thermal conductivity of nanofluids," *AIChE Journal*, vol. 49, no. 4, pp. 1038–1043, 2004.

[23] C. H. Chon, K. D. Kihm, S. P. Lee, and S. U. S. Choi, "Empirical correlation finding the role of temperature and particle size for nanofluid (Al_2O_3) thermal conductivity enhancement," *Applied Physics Letters*, vol. 87, no. 15, Article ID 153107, 3 pages, 2005.

[24] W. Daungthongsuk and S. Wongwises, "A critical review of convective heat transfer of nanofluids," *Renewable and Sustainable Energy Reviews*, vol. 11, no. 5, pp. 797–817, 2007.

[25] B. C. Pak and Y. I. Cho, "Hydrodynamic and heat transfer study of dispersed fluids with submicron metallic oxide particles," *Experimental Heat Transfer*, vol. 11, no. 2, pp. 151–170, 1998.

[26] Y. Xuan and Q. Li, "Investigation on convective heat transfer and flow features of nanofluids," *Journal of Heat Transfer*, vol. 125, no. 1, pp. 151–155, 2003.

[27] D. Wen and Y. Ding, "Experimental investigation into convective heat transfer of nanofluids at the entrance region under laminar flow conditions," *International Journal of Heat and Mass Transfer*, vol. 47, no. 24, pp. 5181–5188, 2004.

[28] Y. Ding, H. Alias, D. Wen, and R. A. Williams, "Heat transfer of aqueous suspensions of carbon nanotubes (CNT nanofluids)," *International Journal of Heat and Mass Transfer*, vol. 49, no. 1-2, pp. 240–250, 2006.

[29] Y. He, Y. Jin, H. Chen, Y. Ding, D. Cang, and H. Lu, "Heat transfer and flow behaviour of aqueous suspensions of TiO_2 nanoparticles (nanofluids) flowing upward through a vertical pipe," *International Journal of Heat and Mass Transfer*, vol. 50, no. 11-12, pp. 2272–2281, 2007.

[30] W. Williams, J. Buogiorno, and L.-W. Hu, "Experimental investigation of turbulent convective heat transfer and pressure loss of alumina/water and zirconia/water nanoparticle colloids (nanofluids) in horizontal tubes," *Journal of Heat Transfer*, vol. 130, no. 4, pp. 1–7, 2008.

[31] S. E. B. Maïga, C. T. Nguyen, N. Galanis, and G. Roy, "Heat transfer behaviours of nanofluids in a uniformly heated tube," *Superlattices and Microstructures*, vol. 35, no. 3–6, pp. 543–557, 2004.

[32] S. E. B. Maïga, S. J. Palm, C. T. Nguyen, G. Roy, and N. Galanis, "Heat transfer enhancement by using nanofluids in forced convection flows," *International Journal of Heat and Fluid Flow*, vol. 26, no. 4, pp. 530–546, 2005.

[33] S. E. B. Maïga, C. T. Nguyen, N. Galanis, G. Roy, T. Maré, and M. Coqueux, "Heat transfer enhancement in turbulent tube flow using Al_2O_3 nanoparticle suspension," *International Journal of Numerical Methods for Heat and Fluid Flow*, vol. 16, no. 3, pp. 275–292, 2006.

[34] A. K. Santra, S. Sen, and N. Chakraborty, "Study of heat transfer augmentation in a differentially heated square cavity using copper-water nanofluid," *International Journal of Thermal Sciences*, vol. 47, no. 9, pp. 1113–1122, 2008.

[35] A. Akbarinia and A. Behzadmehr, "Numerical study of laminar mixed convection of a nanofluid in horizontal curved tubes," *Applied Thermal Engineering*, vol. 27, no. 8-9, pp. 1327–1337, 2007.

[36] D. Gidaspow, *Multiphase Flow and Fluidization*, Academic Press, 1994.

[37] L. S. Fan and C. Zhu, *Principle of Gas-Solid Flows*, Cambridge University Press, Cambridge, UK, 1998.

[38] V. Bianco, F. Chiacchio, O. Manca, and S. Nardini, "Numerical investigation of nanofluids forced convection in circular tubes," *Applied Thermal Engineering*, vol. 29, no. 17-18, pp. 3632–3642, 2009.

[39] A. Behzadmehr, M. Saffar-Avval, and N. Galanis, "Prediction of turbulent forced convection of a nanofluid in a tube with uniform heat flux using a two phase approach," *International Journal of Heat and Fluid Flow*, vol. 28, no. 2, pp. 211–219, 2007.

[40] S. K. Das, S. U. S. Choi, W. Yu, and T. Pradeep, *Nanofluids Science and Technology*, John Wiley & Sons, Hoboken, NJ, USA, 2008.

[41] M. Manninen, V. Taivassalo, and S. Kallio, "On the mixture model for multiphase flow," Tech. Rep. 288, VTT Technical Research Centre of Finland, 1996.

[42] L. Schiller and A. Naumann, "A drag coefficient correlation," *Zeitschrift des Vereins Deutscher Ingenieure*, vol. 77, pp. 318–320, 1935.

[43] B. E. Lauder and D. B. Spalding, *Lectures in Mathematical Models of Turbulence*, Academic Press, London, UK, 1972.

[44] V. Gnielinski, "New equations for heat and mass transfer in turbulent pipe and channel flow," *International Chemical Engineering*, vol. 16, pp. 359–368, 1976.

[45] B. S. Petukhov, "Heat transfer and friction in turbulent pipe flow with variable physical properties," in *Advances in Heat Transfer*, J. P. Hartnett and T. F. Irvine, Eds., pp. 504–564, Academic Press, New York, NY, USA, 1970.

[46] R. B. Mansour, N. Galanis, and C. T. Nguyen, "Effect of uncertainties in physical properties on forced convection heat transfer with nanofluids," *Applied Thermal Engineering*, vol. 27, no. 1, pp. 240–249, 2007.

[47] S. Mirmasoumi and A. Behzadmehr, "Numerical study of laminar mixed convection of a nanofluid in a horizontal tube using two-phase mixture model," *Applied Thermal Engineering*, vol. 28, no. 7, pp. 717–727, 2008.

[48] H. Masuda, A. Ebata, K. Teramae, and N. Hishinuma, "Alteration of thermal conductivity and viscosity of liquid by dispersing ultra-fine particles (dispersion of Al_2O_3, SiO_2 and TiO_2 ultra-fine particles)," *Netsu Bussei*, vol. 4, no. 4, pp. 227–233, 1993 (Japanese).

[49] R. Lotfi, Y. Saboohi, and A. M. Rashidi, "Numerical study of forced convective heat transfer of nanofluids: comparison of different approaches," *International Communications in Heat and Mass Transfer*, vol. 37, no. 1, pp. 74–78, 2010.

[50] S. Lee, S. U. S. Choi, S. Li, and J. A. Eastman, "Measuring thermal conductivity of fluids containing oxide nanoparticles," *Journal of Heat Transfer*, vol. 121, no. 2, pp. 280–289, 1999.

[51] R. B. Mansour, N. Galanis, and C. T. Nguyen, "Effect of uncertainties in physical properties on forced convection heat transfer with nanofluids," *Applied Thermal Engineering*, vol. 27, no. 1, pp. 240–249, 2007.

[52] Fluent Incorporated, "Fluent 6.2 User Manual," 2006.